3.0 PROBABILISTIC SEISMIC HAZARD ANALYSIS

Spectral acceleration values for SONGS were obtained from the PSHA using the seismic sources discussed in Section 2.0. This SONGS 2010 PSHA followed the methods of the 1995 PSHA (SCE, 1995) and the 2001 PSHA (SCE, 2001). The 2001 PSHA results included both response spectral values and time histories, reflecting the effects of near-fault directivity and fling step. Unlike the 2001 PSHA results, the PSHA results reported here focus mainly on high frequency spectral accelerations and do not reflect the effects of near-fault directivity or fling step, which were found to be insignificant for SONGS. Based on the 2001 PSHA, the near-fault directivity and the fling steps only affect the low frequency range below about 1.5 Hertz (Hz), which is outside the frequencies of interest for structures and components at SONGS.

3.1 PSHA Methodology

3.1.1 General

The basic result of PSHA is a relationship between a ground motion parameter "*Z*" (peak ground acceleration [PGA] and spectral acceleration herein) and the mean number of seismic events per year in which "*Z*" at the site exceeds a specified value "*z*". This relationship is called a "hazard curve." The mean number of seismic events per year is referred to as "annual frequency of exceedance" and designated "$\nu(Z \geq z)$". The inverse of this number is called the "return period" (RP) and is expressed in years. Once the relationships between appropriate parameters and annual frequency of exceedance are obtained, various probabilistic calculations can be made assuming a Poisson process. Details of PSHA are available elsewhere (e.g., SSHAC, 1997: http://www.ce.memphis.edu/7137/). Apart from the general discussions below, only the key pertinent topics will be discussed here with some further details presented in Appendix B.

The five major components in PSHA consist of the following:

- Characterization of Seismogenic Sources. The location, geometry, and characteristics of seismic sources (or earthquake generating faults) relative to the site are evaluated and specified. This component is addressed in Section 2.0

- Specification of Recurrence Relationship. In the PSHA, one of the most important characteristics of a seismic source is its recurrence relationship or the relationship showing the annual recurrence of earthquakes of various magnitudes up to the "maximum" magnitude. The recurrence relationship is used to provide the mean number of earthquakes per year having a particular magnitude "m_j" on a given seismic source, "$\dot{N}_s(m_j)$". Two types of recurrence relationships were used: the characteristic and the truncated exponential (Youngs and Coppersmith, 1985). These two recurrence models were selected to be consistent with the UCERF 2 (WGCEP, 2008).

- Evaluation of Probability of Distance to Rupture. Assuming that the typical earthquake generating fault rupture can occur anywhere along the plane of an active fault with an equal probability, the conditional probability is computed so that the rupture plane is at a specified distance, r_k, from the site for the given m_j. This probability is evaluated by considering the rupture plane's dimensions and the distance definition used in the particular attenuation relationship being used.

- Calculation of Exceedance Using Attenuation Equation. The conditional probability that the ground motion parameter "*Z*" from the earthquake of a certain magnitude "m_j" occurring at a certain distance "r_k" on a particular seismic source fault will exceed a specified level "*z*" at the site is calculated based on the median and standard deviation of the ground motion given by the attenuation relationship.

- Calculation of Probabilistic Seismic Hazard. By combining the rate of occurrence of earthquakes of a given magnitude with the two conditional probability functions associated with steps 2 through 4 above, for each seismic source fault, the mean number of events per year (annual frequency of exceedance) resulting in "*Z*" being greater than "*z*" ($\nu(Z \geq z)$) at the site is computed for that particular seismic source fault. This process was repeated for each seismic source fault, and the contributions are added to obtain the total seismic hazard at the site for a given *z*. The complete hazard curve is obtained by repeating these computations for several levels of ground motion parameter *z.*

Once this mean number of events per year (annual frequency of exceedance) $\nu(Z \geq z)$ has been determined, the probability of the level of the seismic ground motion parameter being exceeded over a specified time period, t, is calculated by the following equation assuming the Poisson model for the earthquake occurrence:

$$Pr(Z \geq z) = 1 - \exp[-\nu(Z \geq z) \cdot t] \qquad \textbf{(3-1)}$$

The results of the SONGS 2010 PSHA are presented here in terms of the mean number of events per year or annual frequency of exceedance, $\nu(Z \geq z)$. The results are presented from an annual frequency of exceedance of 10^{-2} to 10^{-4} corresponding to a RP of 100 to 10,000 years. The computer program Haz4.2 developed by Abrahamson (2010, PC) was used in completing this PSHA. The results of quality assurance/quality control (QA/QC) work performed on the program are summarized in Appendix B.

3.1.2 Attenuation Relationships

The attenuation relationships from the NGA project, which are now called GMPEs, were used in this PSHA and are listed in Table 3-1 along with key parameter values. These attenuation relationships are referred to herein as the "NGA relationships" and consist of the following:

- Abrahamson and Silva (2008)
- Boore and Atkinson (2008)
- Campbell and Bozorgnia (2008)
- Chiou and Youngs (2008)
- Idriss (2008)

Further details of these NGA relationships are provided in Appendix B.

3.1.3 Uncertainties

Two major types of uncertainties are addressed in PSHA. They are as follows:

- Aleatory Uncertainty. Uncertainties in the earthquake recurrence process and in the attenuation of ground motion are the major sources of the aleatory uncertainty in PSHA. This uncertainty is a reflection of the "randomness" inherent to the natural phenomenon of earthquake generation and ground motions. This uncertainty may be based in part on the limited scientific understanding of the natural phenomenon of earthquake generation and seismic wave propagation. This type of uncertainty, in theory, cannot be reduced when additional data or understanding of earthquakes and their effects become available.

- Epistemic Uncertainty. This uncertainty reflects limited available data, limited scientific understanding, and/or limitations in the utility of modeling earthquake and related processes. This type of uncertainty, in theory, can be reduced when additional data or understanding of earthquakes and their effects become available.

The PSHA methodology includes probability models for these two major types of uncertainty. For example, both aleatory uncertainty and epistemic uncertainty are reflected in the logic tree provided for the OBT seismic source fault shown on Figure 2-12 in Section 2.0. Two specific epistemic uncertainties considerations were addressed because of their pertinence to the current PSHA: one is associated with the GMPEs and the other is the NI/RC Fault Zone versus the OBT Fault as the primary seismic source fault.

3.1.3.1 GMPE Uncertainty

In using attenuation relationships, their epistemic uncertainty should be considered. In the past, this epistemic uncertainty was often accommodated by using multiple attenuation relationships. However, given the coordinated process used to develop the NGA relationships, it may not be adequate to address this epistemic uncertainty by just using multiple NGA relationships.

On the basis of the evaluation results presented in Appendix B, an epistemic GMPE uncertainty in addition to the five NGA relationships was used in the current PSHA. This additional uncertainty represents the difference between the GMPE uncertainty that the USGS (2008) is currently using with only three NGA relationships in their seismic hazard mapping program for the building code purposes and the epistemic uncertainty covered by the five NGA relationships and the GMPE uncertainty used in this PSHA.

3.1.3.2 Uncertainty Regarding Strike-slip and Blind Thrust Sources

As discussed in Sections 1 and 2, the seismic sources used in this PSHA consisted of the pertinent time-independent portion of the seismic source fault characterization in UCERF 2 (WGCEP, 2008). For SONGS, the most important seismic source fault in this PSHA's base case set is the NI/RC source, which was also reflected in the 1995 PSHA (SCE, 1995) and a weighted NI/RC and OBT in the 2001 PSHA (SCE, 2001). Since the 2001 PSHA, the OBT has been re-characterized, and new weights have been assigned to the NI/RC (strike-slip) and OBT (blind thrust) models as recommended by the seismic source integration team. Based on the evaluation of the uncertainties associated with both models as discussed in Section 2, the numerically calculated average weights applied to the NI/RC model and the OBT model for use in the PSHA are: 88% and 12% for the strike-slip model and blind thrust end-member models, respectively. The PSHA utilized the above weights applied to the logic trees developed for the NI/RC model as shown

on Figure 2-5 and for the OBT as shown on Figure 2-12. These analysis results are, therefore, provided for a single case and referred to as the "2010 PSHA" results.

3.1.3.3 Recurrence Relationships

The recurrence relationships used for the NI/RC source followed UCERF 2 (WGCEP, 2008) and involved using the characteristic recurrence relationship of Youngs and Coppersmith (1985) with a 2/3 weight and the truncated exponential relationship of Molnar (1979) and Anderson (1979) with a 1/3 weight. For the hypothesized OBT source, a comparison of the recurrence model with the available seismicity data presented in Appendix B indicates that using only the characteristic recurrence relationship is more appropriate.

3.2 PSHA Results

The 2010 PSHA results are presented in terms of hazard curves relating spectral acceleration to annual frequency of exceedance on Figure 3-1 for PGA, 25 Hz, 10 Hz, and 5 Hz; similar results are presented on Figure 3-2 for 3.33 Hz, 2.5 Hz, 2 Hz, and 1 Hz. The 2010 PSHA results are also listed in Table 3-2.

3.2.1 Effects of Seismic Sources

The contributions to the total seismic hazard at the SONGS site from various seismic sources are presented for the 2010 PSHA results on Figures 3-3 and 3-4 corresponding to PGA and 1 Hz, respectively.

As shown on Figures 3-3 and 3-4 for the 2010 PSHA results, the NI/RC-OBT source contributes the most to the total hazard for annual frequency of exceedance less than about 10^{-3} for PGA and 1 Hz. For the higher annual frequency of exceedance, the San Jacinto source, the Southern San Andreas source, and, to a lesser degree, the Elsinore source start to contribute more than the NI/RC source.

3.2.2 Deaggregation Results

Figure 3-5 shows the results of deaggregation for the 2010 PSHA results for a RP of 475 years at PGA and 1 Hz; similarly, Figure 3-6 shows the results of deaggregation for a RP of 2,475 years at PGA and 1 Hz. The RP values of 475 and 2,475 years were selected to correspond to numbers often used in current building codes. For the 2010 PSHA results at 475 year RP, the PGA shaking at SONGS is primarily associated with the NI/RC-OBT source with moment magnitude falling in the 6.5 to 7.5 bin at a distance falling in the 5 to 10 km bin, whereas the 1 Hz shaking is somewhat more controlled by the San Jacinto, South San Andreas, and Elsinore faults with moment magnitude falling in the 7 to 8 bin at a distance falling in the 30 to 100 km bin. At 2,475 year RP, however, the ground motion at the SONGS site is dominated by the NI/RC-OBT source with moment magnitude falling in the 6.5 to 7.5 bin at a distance falling in the 5 to 10 km bin.

3.2.3 Comparison with 1995 PSHA Results

The “weighted hazard curve,” presented previously (SCE, 1995 and 2001), shows the relationship between the weighted spectral acceleration values and annual frequency of exceedance. At each annual frequency of exceedance value evaluated, the weighted spectral values were obtained as follows: spectral accelerations at frequencies 1 Hz and 10 Hz are multiplied by ½ and added to the sum of spectral accelerations at frequencies 5 Hz and 2.5 Hz with the resulting sum divided by 3.

The weighted hazard curves corresponding to the 2010 PSHA and 1995 PSHA results are presented on Figure 3-7. The results shown on Figure 3-7 indicate that the 2010 PSHA results are lower compared to the 1995 PSHA results throughout the range shown. These weighted hazard curves are also tabulated in Table 3-3.

Table 3-1: NGA Relationships and Related Parameters used in PSHA

NGA	Epistemic Weight	Subsurface Parameters†		
		V_{s30}*	$Z_{1.0\text{-km/s}}$**	$Z_{2.5\text{-km/s}}$***
Abrahamson & Silva (2008)	0.20	500-m/s****	0.31-km	3.35-km
Boore & Atkinson (2008)	0.20			
Campbell & Bozorgnia (2008)	0.20			
Chiou & Youngs (2008)	0.20			
Idriss (2008)	0.20			

Notes:

† Used as needed in each NGA relationship.

* V_{s30} is the average shear wave velocity in the upper 30 meters of a soil profile.

** $Z_{1.0\text{-km/s}}$ is the depth at which the shear wave velocity is 1.0 kilometers per second (km/s).

*** $Z_{2.5\text{-km/s}}$ is the depth at which the shear wave velocity is 2.5 km/s.

**** m/s is meters per second.

Table 3-2: Mean Horizontal Ground Motions (g) at Various Frequencies of Exceedance for 2010 PSHA

Annual Frequency of Exceedance	Average Return Period	Spectral Acceleration - g*								
		PGA	25-Hz	10-Hz	5-Hz	3.33-Hz	2.5-Hz	2-Hz	1-Hz	Weighted**
1.00E-04	10,000	0.778	0.936	1.489	1.895	1.832	1.673	1.456	0.852	1.579
2.00E-04	5,000	0.618	0.736	1.178	1.477	1.413	1.284	1.131	0.661	1.227
5.00E-04	2,000	0.430	0.510	0.813	1.019	0.970	0.875	0.776	0.463	0.844
1.00E-03	1,000	0.318	0.372	0.593	0.746	0.716	0.638	0.576	0.353	0.619
2.00E-03	500	0.233	0.269	0.426	0.542	0.525	0.476	0.422	0.266	0.455
5.00E-03	200	0.152	0.176	0.272	0.356	0.348	0.314	0.280	0.176	0.298
1.00E-02	100	0.108	0.124	0.191	0.251	0.248	0.223	0.198	0.123	0.211
2.11E-03	475	0.227	0.263	0.415	0.530	0.515	0.464	0.413	0.261	0.444
4.04E-04	2,475	0.472	0.554	0.895	1.111	1.056	0.949	0.849	0.501	0.920

Notes: * Spectral Accelerations were interpolated at the provided annual frequencies of exceedance

** Weighted Spectral Acceleration (Sa) is determined as follows:

Weighted Sa = $(0.5*Sa_{10\text{-}Hz} + Sa_{5\text{-}Hz} + Sa_{2.5\text{-}Hz} + 0.5*Sa_{1\text{-}Hz})/3$

where $Sa_{x\text{-}Hz}$ is the spectral acceleration at x-Hz

Table 3-3: Comparison of Weighted Hazard Curves 2010 PSHA and 1995 PSHA

Annual Frequency of Exceedance*	Average Return Period	Weighted Spectral Acceleration – g**	
		2010 PSHA	1995 PSHA***
1.00E-04	10,000	1.579	1.656
2.00E-04	5,000	1.227	1.407
5.00E-04	2,000	0.844	1.015
1.00E-03	1,000	0.619	0.884
2.00E-03	500	0.455	0.675
5.00E-03	200	0.298	0.430
1.00E-02	100	0.211	0.310
2.11E-03	475	0.444	0.655
4.04E-04	2,475	0.920	1.077

Notes:

* Spectral Accelerations were interpolated at the provided annual frequencies of exceedance

** Weighted Spectral Acceleration (Sa) is determined as follows:

Weighted Sa = $(0.5*Sa_{10\text{-Hz}} + Sa_{5\text{-Hz}} + Sa_{2.5\text{-Hz}} + 0.5*Sa_{1\text{-Hz}})/3$

where $Sa_{x\text{-Hz}}$ is the spectral acceleration at x-Hz

*** Spectral Acceleration not calculated for annual frequency of exceedance greater than 1.00E-02 in 1995 results.

T:_2009 Projects\09024A SONGS Seismic Hazard Plan\REPORT\Reliability\Section 3 Appendix B

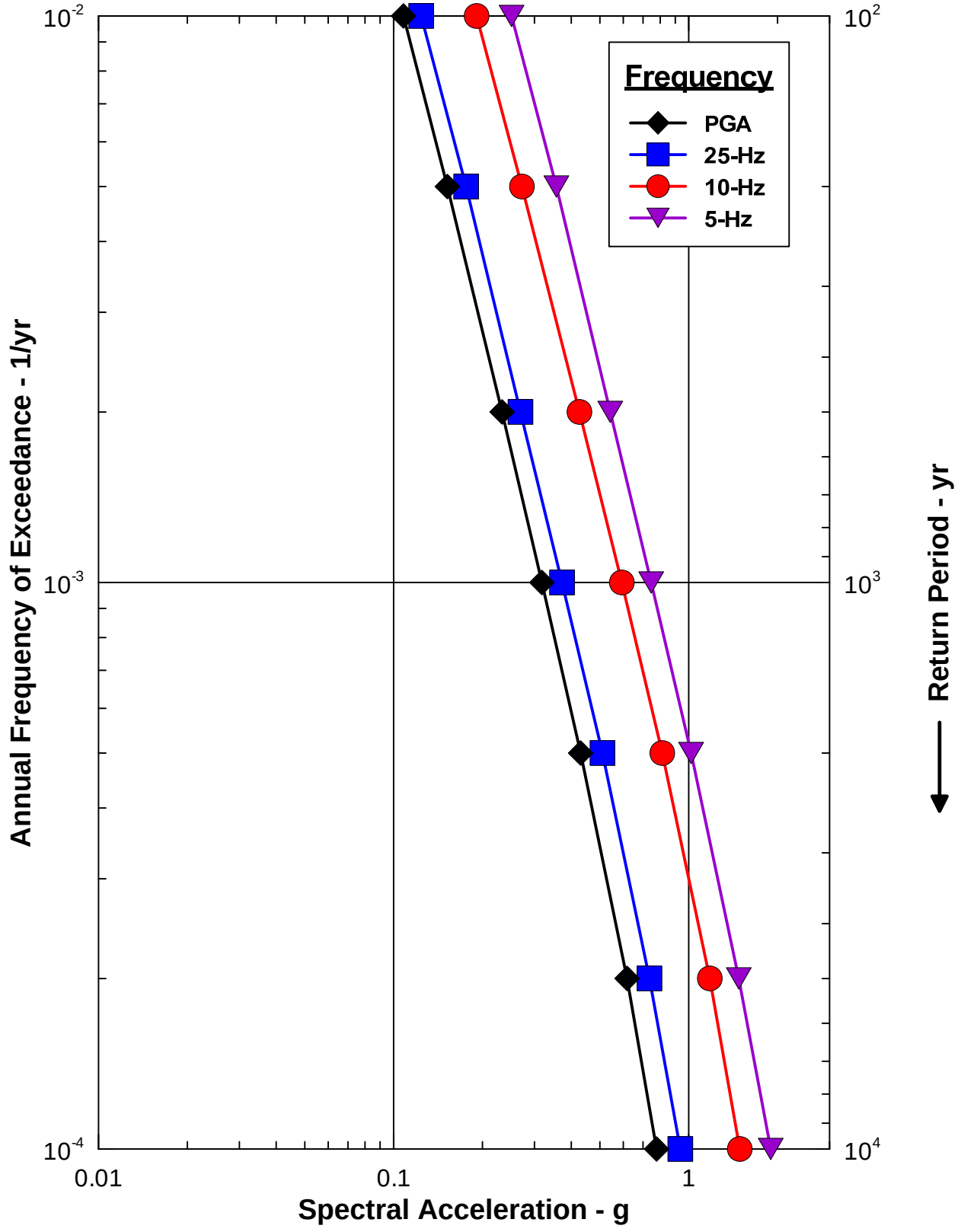

GeoPentech
Geotechnical & Geoscience Consultants

2010 PSHA HAZARD CURVES

FIGURE 3-1

SAN ONOFRE NUCLEAR GENERATING STATION

SEISMIC HAZARD ASSESSMENT PROGRAM

T:_2009 Projects\09024A SONGS Seismic Hazard Plan\REPORT\Reliability\Section 3 Appendix B

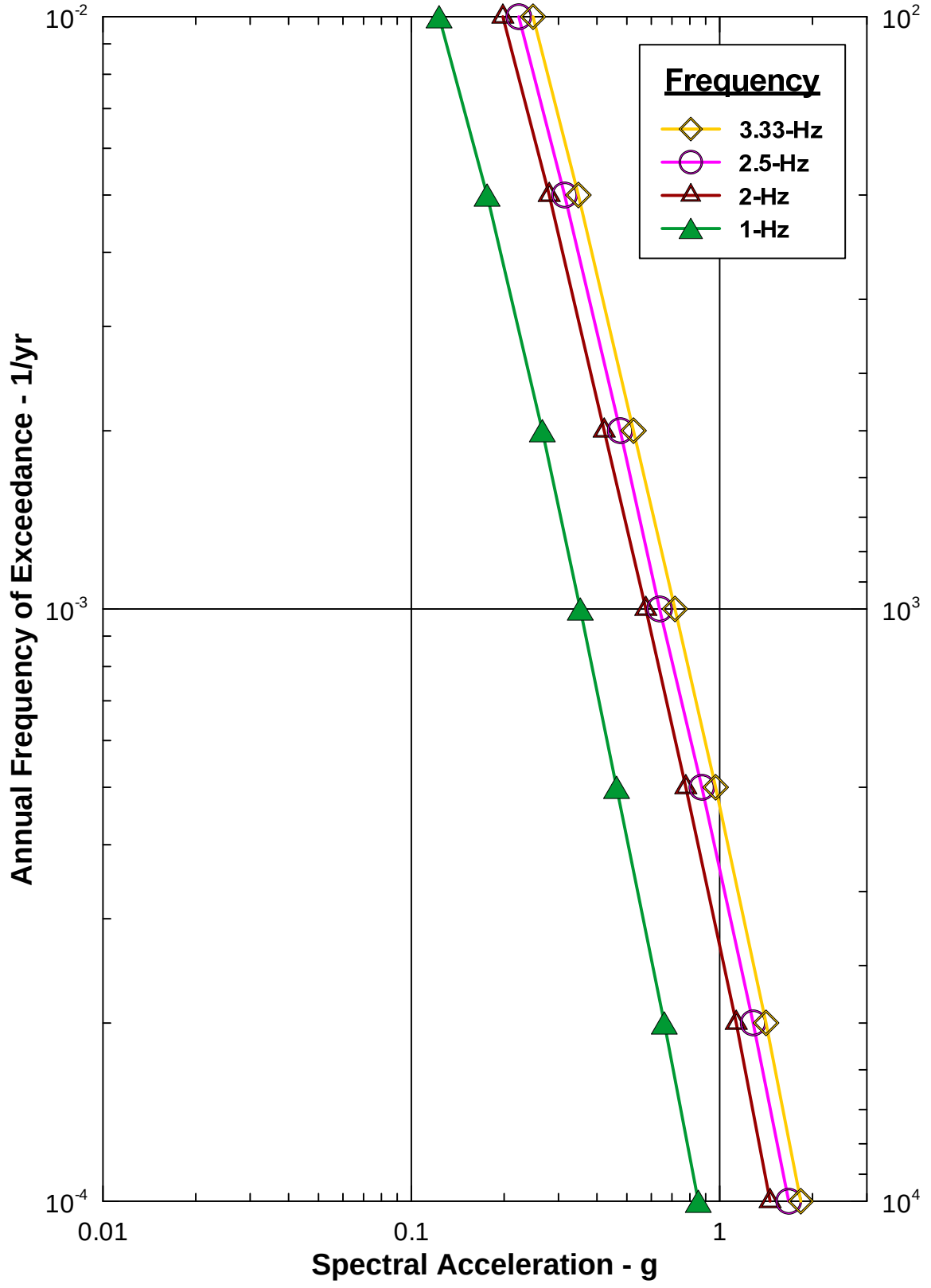

GeoPentech
Geotechnical & Geoscience Consultants

2010 PSHA HAZARD CURVES

FIGURE 3-2

SAN ONOFRE NUCLEAR GENERATING STATION

SEISMIC HAZARD ASSESSMENT PROGRAM

T:_2009 Projects\09024A SONGS Seismic Hazard Plan\REPORT\Reliability\Section 3 Appendix B

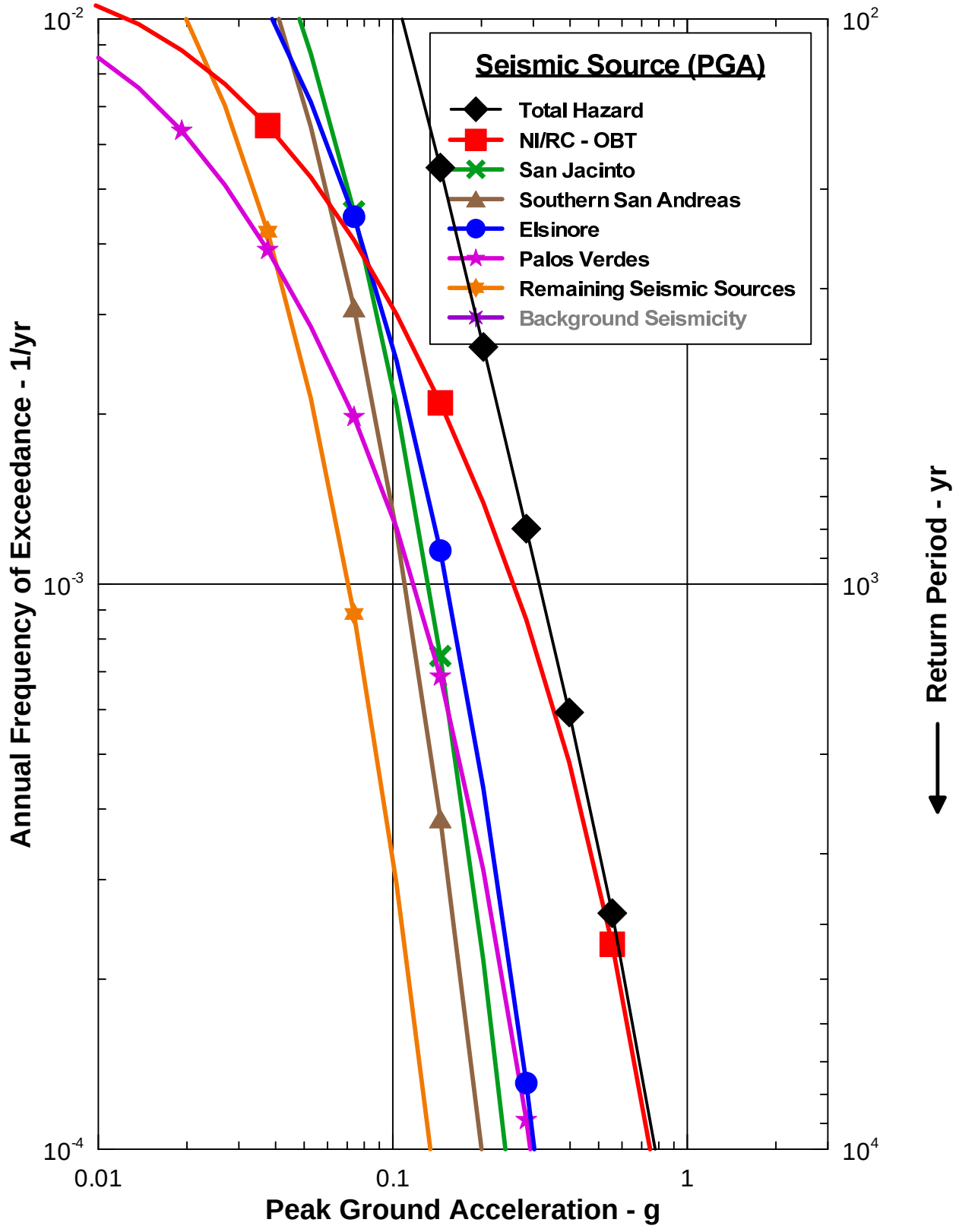

GeoPentech
Geotechnical & Geoscience Consultants

2010 PSHA - PGA SEISMIC SOURCE CONTRIBUTIONS

FIGURE
3-3

SAN ONOFRE NUCLEAR GENERATING STATION

SEISMIC HAZARD ASSESSMENT PROGRAM

T:_2009 Projects\09024A SONGS Seismic Hazard Plan\REPORT\Reliability\Section 3 Appendix B

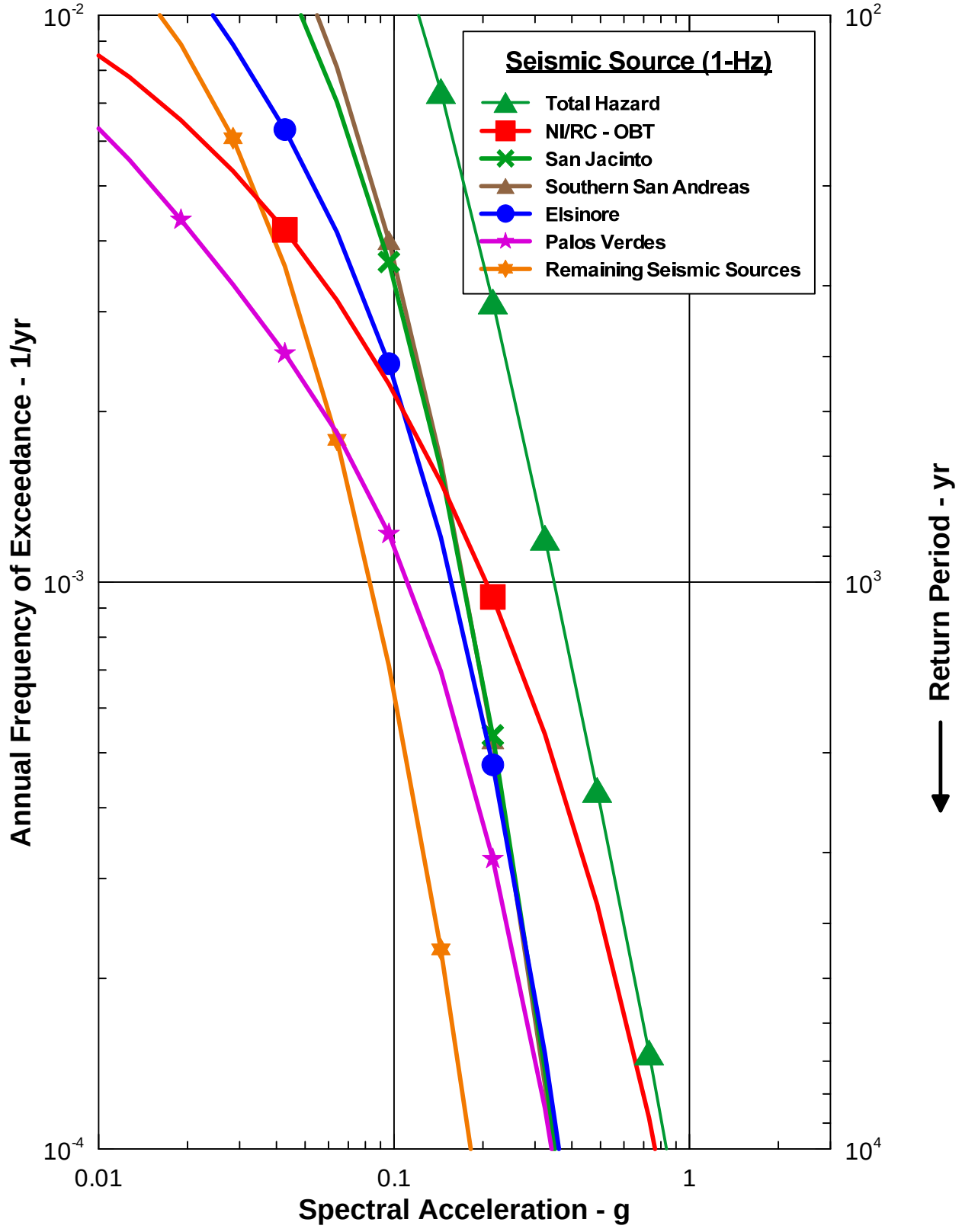

GeoPentech
Geotechnical & Geoscience Consultants

2010 PSHA - 1-Hz SEISMIC SOURCE CONTRIBUTIONS

FIGURE 3-4

SAN ONOFRE NUCLEAR GENERATING STATION

SEISMIC HAZARD ASSESSMENT PROGRAM

PGA

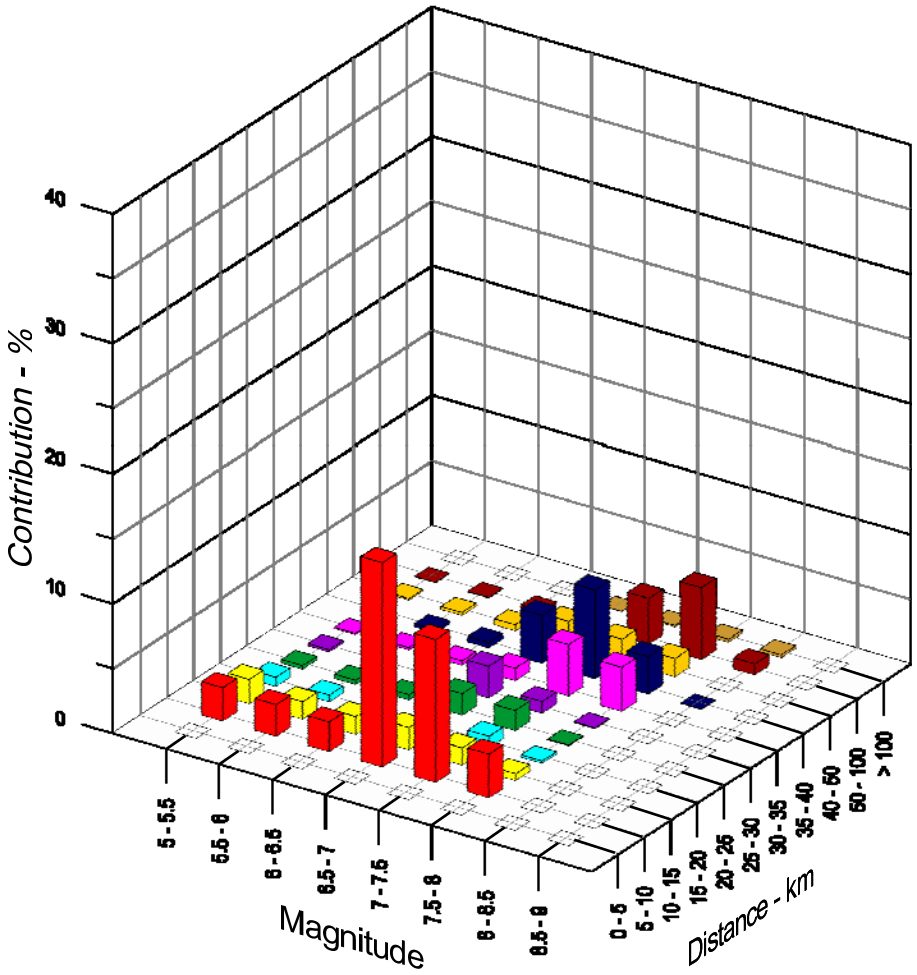

1-Hz

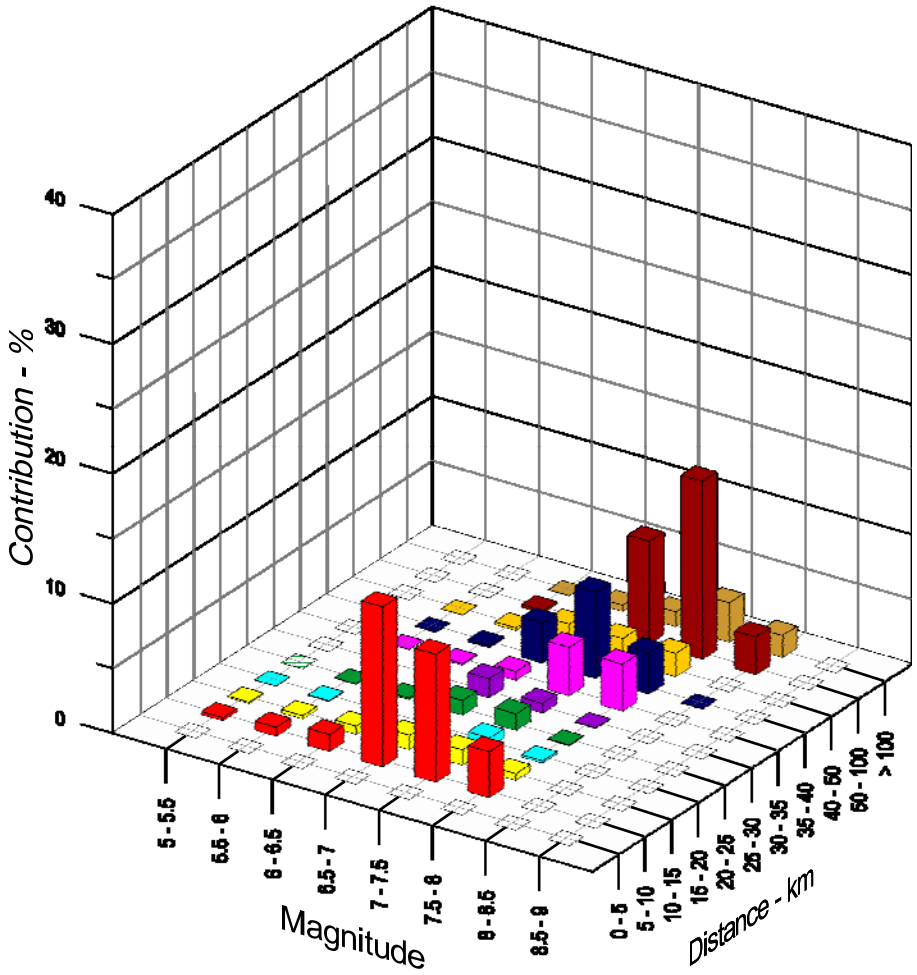

GeoPentech
Geotechnical & Geoscience Consultants

SAN ONOFRE NUCLEAR GENERATING STATION

SEISMIC HAZARD ASSESSMENT PROGRAM

HAZARD DEAGGREGATION
2010 PSHA
FOR 475-yr ARP at PGA and 1-Hz

FIGURE
3-5

PGA

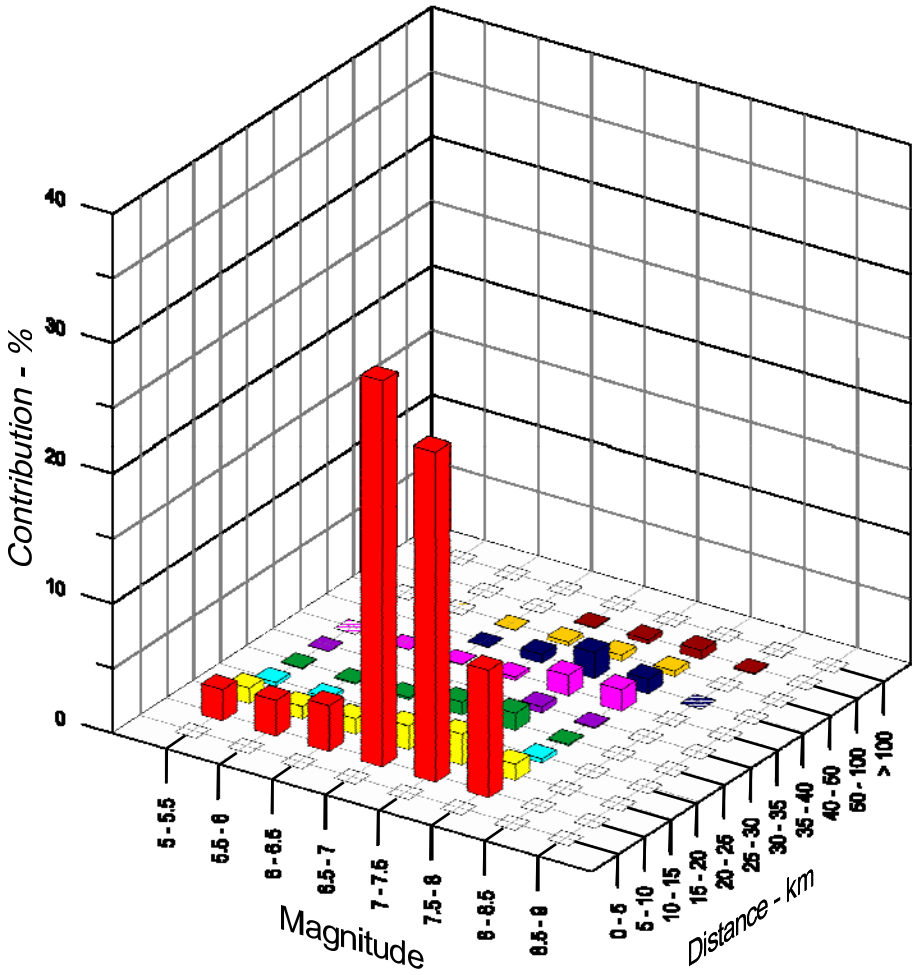

1-Hz

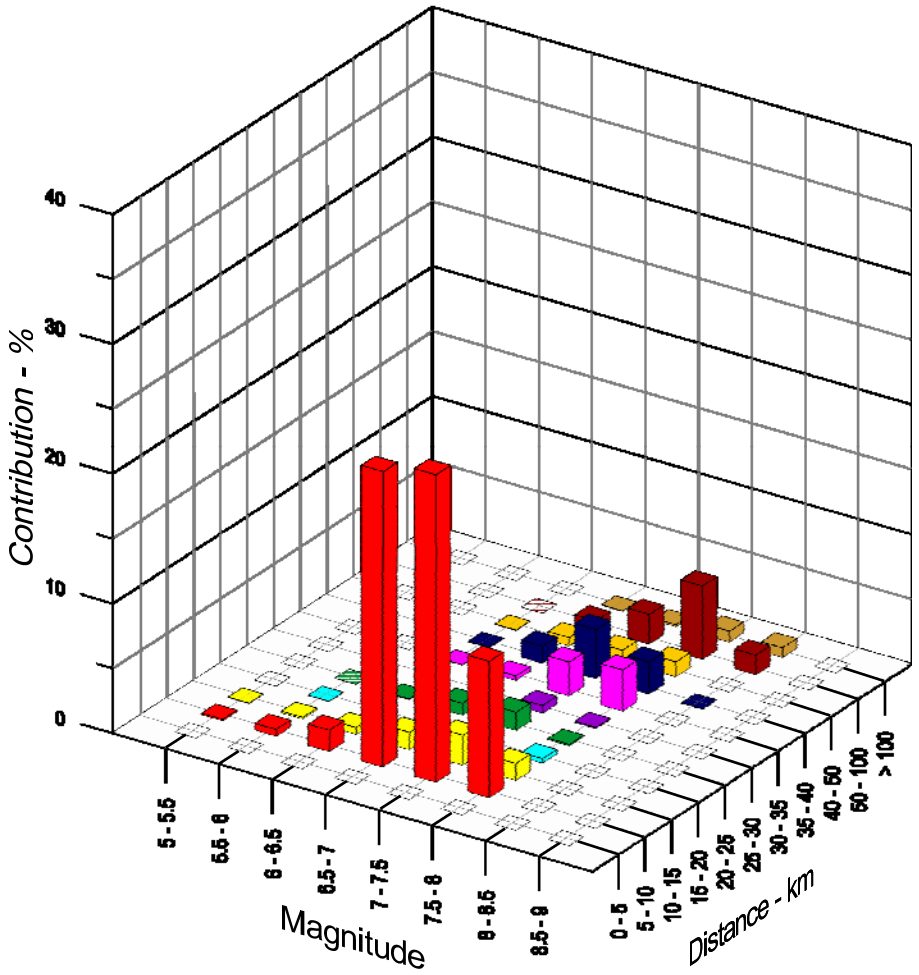

GeoPentech
Geotechnical & Geoscience Consultants

SAN ONOFRE NUCLEAR GENERATING STATION

SEISMIC HAZARD ASSESSMENT PROGRAM

HAZARD DEAGGREGATION OF
2010 PSHA
FOR 2475-yr ARP at PGA and 1-Hz

FIGURE
3-6

T:_2009 Projects\09024A SONGS Seismic Hazard Plan\REPORT\Reliability\Section 3 Appendix B

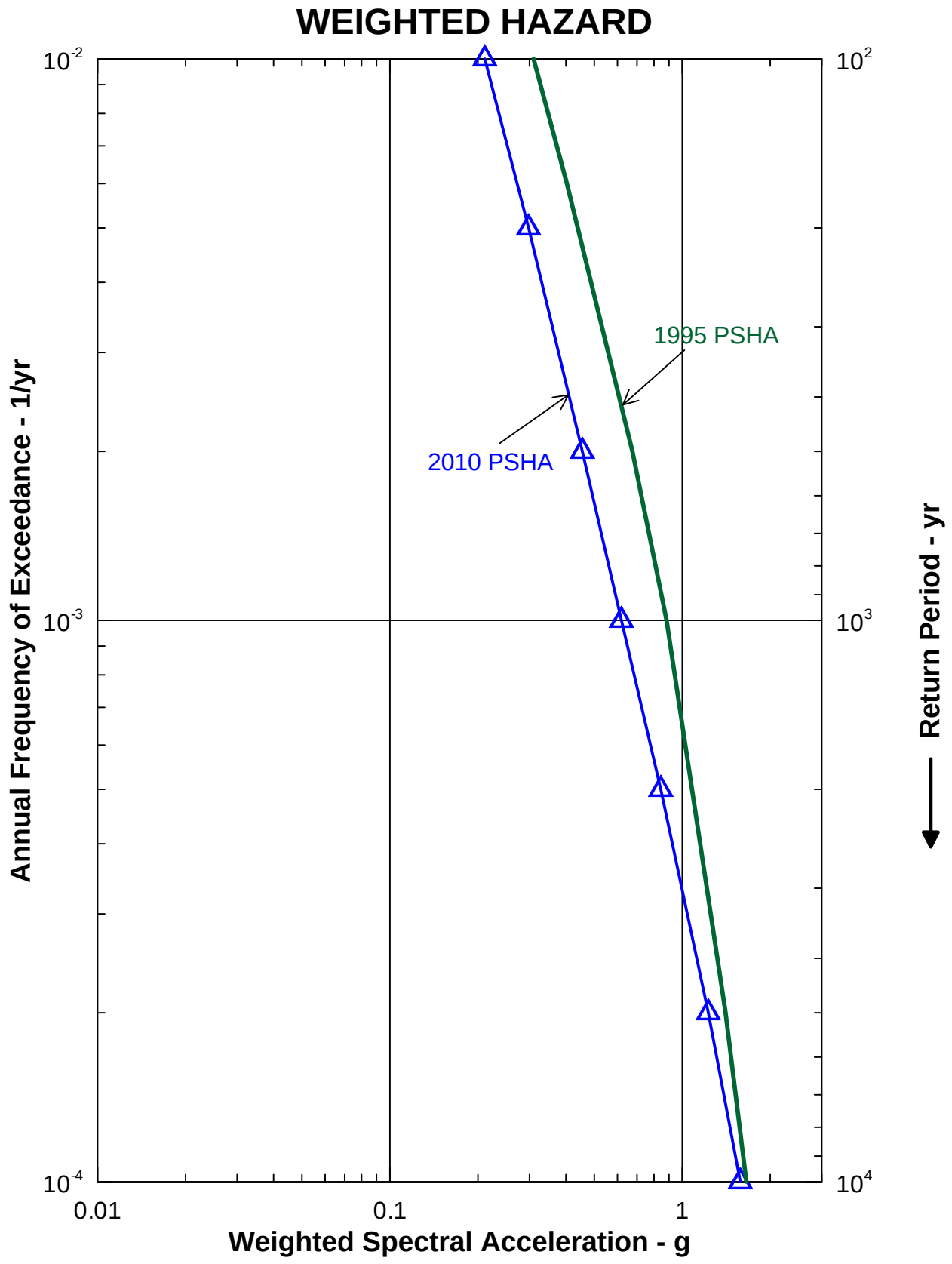

GeoPentech
Geotechnical & Geoscience Consultants

COMPARISON OF WEIGHTED HAZARD CURVES
2010 PSHA AND 1995 PSHA

FIGURE
3-7

SAN ONOFRE NUCLEAR GENERATING STATION

SEISMIC HAZARD ASSESSMENT PROGRAM

4.0 SUMMARY AND CONCLUSIONS

This seismic hazard assessment was completed to evaluate if recent available information has affected the seismic hazard at SONGS. A PSHA was performed utilizing available and regionally relevant seismic geology and seismology information (in particular, the recently released UCERF 2 [WGCEP, 2008], as well as discussions with current academic and USGS researchers) and the recently released five "Next Generation of Ground-Motion Attenuation Models" (NGA, 2008).

On the basis of this analysis, the following conclusions were reached:

- The two fault sources that contribute most to the ground motion hazard at SONGS are the NI/RC Fault Zone, which was the primary source fault governing the licensing of SONGS in the early 1980s, and the recently hypothesized OBT Fault of Rivero et al. (2000) and Rivero (2004). To appropriately represent the generally accepted NI/RC Fault Zone and the recently hypothesized OBT Fault in the 2010 PSHA, the end-member models associated with the NI/RC Fault Zone and OBT were evaluated as described in Section 2 of the report. The relative weights of 88% and 12% were assigned to the NI/RC Fault Zone and the hypothesized OBT, respectively, by the seismic source integration team. The weights are based on the consideration of a number of technical arguments given in the text.

- The mean seismic hazard curves presented on Figures 3-1 and 3-2 are assigned to the combined strike-slip and blind thrust end-member models. The NGA relationships (NGA, 2008) were used in performing this PSHA. This seismic hazard evaluation was limited to annual frequencies of exceedance greater than 10^{-4}. A 10^{-4} annual frequency of exceedance is equivalent to a RP of 10,000 years. At annual frequencies of exceedance lower than 10^{-4}, some issues are to be addressed that potentially could affect the calculated seismic hazard results. These issues consist of those associated with dispersions, i.e., epistemic and aleatory uncertainties in seismic source characterization and ground motion characterization models including the GMPE epistemic uncertainty; and those associated with nonlinear behavior of soils at the site. These issues will be addressed as part of the SONGS on-going seismic hazard program.

- The weighted hazard curves shown on Figure 3-7 indicate that the 2010 PSHA results are lower compared to the 1995 PSHA results throughout the range shown. These weighted hazard curves are also tabulated in Table 3-3.

5.0 REFERENCES

5.1 Publicly Available Publications and Data

Annotated bibliographies of pertinent publications provided in Appendix A, Attachment A-1, are denoted with an asterisk.

Abrahamson, N. and Silva, W., 2008, Summary of the Abrahamson & Silva NGA ground-motion relations: Earthquake Spectra, v. 24, no. 1, p. 67-97.

Allmendinger, R.W., 1998, Inverse and forward numerical modeling of trishear fault-propagation folds: Tectonics, v. 17, no, 4, p. 640-656.

Anderson, J.G., 1979, Estimating the seismicity from geological structure for seismic risk studies: Bulletin of the Seismological Society of America, v. 69, p. 135-158.

Argus, D.F., and Gordon, R.G., 1991, Current Sierra Nevada-North America motion from very long baseline interferometry: implications for the kinematics of the western United States: Geology, v. 19, p. 1085-1088.

*Astiz, L., and Shearer, P.M., 2000, Earthquake locations in the Inner Continental Borderland, offshore Southern California: Bulletin of the Seismological Society of America, v. 90, no. 2, p. 425-449.

Atwater, T., 1998, Plate tectonic history of southern California with emphasis on the western Transverse Ranges and Santa Rosa Island, *in* Weigand, P. W., ed., Contributions to the geology of the Northern Channel Islands, Southern California: American Association of Petroleum Geologists, Pacific Section, MP 45, p. 1-8.

Atwater, T., and Stock, J., 1998, Pacific-North America plate tectonics of the Neogene southwestern United States–an update: International Geological Review, v. 40, p. 375-402.

Axen, G J., and Fletcher, J.M., 1998, Late Miocene-Pleistocene extensional faulting, northern Gulf of California, Mexico and Salton Trough, California: International Geological Review, v. 40, p. 217-244.

Barrows, A.G., 1974, A review of the geology and earthquake history of the Newport–Inglewood Structural Zone, southern California, California Division of Mines and Geology, Special Report 114, 115 pp.

*Bender, E.E., 2000, Late Quaternary uplift and earthquake potential of the San Joaquin Hills, southern Los Angeles basin, California – COMMENT: Geology, v. 28, no. 4, p. 383.

Bennett, R.A., Rodi, W., and Reilinger, R.E., 1996 Global Positioning System constraints on fault slip rates in southern California and northern Baja, Mexico: Journal of Geophysical Research, v. 101, p. 21,943 – 21,960.

*Bohannon, R.G., and Geist, E., 1998, Upper crustal structure and Neogene tectonic development of the California Continental Borderland: Geological Society of America Bulletin, v. 110, n. 6, p. 779-800.

Boore, D.M., and Atkinson, G.M., 2008, Ground-motion prediction equations for the average horizontal component of PGA, PGV, and 5%-damped PSA at spectral periods between 0.01 s and 10.0 s: Earthquake Spectra, v. 24, no. 1, p. 99-138.

Budnitz, R.J., Apostolakis, G., Boore, D.M., Cluff, L.S., Coppersmith, K.J., Cornell, C.A., and Morris, P.A., 1997, Recommendations for Probabilistic Seismic Hazard Analysis: Guidance on Uncertainty and Use of Experts, Report NUREG/CR-6372, Lawrence Livermore National Laboratory, sponsored by the US Nuclear Regulatory Commission, US Department of Energy, and Electric Power Research Institute, 888 pp.

California Geological Survey (CGS), 2002a, California fault parameters-Interactive fault parameter map of California, [http://www.consrv.ca.gov/cgs/rghm/psha/fault_parameters/htm/Pages/index.aspx].

California Geological Survey (CGS), 2002b, California geomorphic provinces, Note 36, December 2002, 4 pp.

California Spatial Information Library (CaSIL), 2006, 1° x 1° Topography DEMs, [http://www.atlas.ca.gov/download.html] extract 1 March 2010.

California State University Monterey Bay (CSUMB), 2010, Seafloor Mapping Lab data library, accessed June 2010 from SFML website, [http://seafloor.csumb.edu/SFMLwebDATA.htm].

Campbell, K.W., and Bozorgnia, Y., 2008, NGA ground motion model for the geometric mean horizontal component of PGA, PGV, PGD and 5% damped linear elastic response spectra for periods ranging from 0.01 to 10 s: Earthquake Spectra, v. 24, no. 1, p. 139-171.

*Campbell, B.A., Sorlien, C.C., Cormier, M., and Alward, W.S., 2009, Quaternary deformation related to 3D geometry of the Carlsbad fault, offshore San Clemente to San Diego [abstract]: Southern California Earthquake Center Proceedings and Abstracts, 12–16 September 2009, v. 19, p. 263.

Cande, S.C., and Kent, D.V., 1995, Revised calibration of the geomagnetic polarity timescale for the late Cretaceous and Cenozoic: Journal of Geophysical Research, v. 100, no. B4, p. 6093-6095.

Cao, T., Bryant, W.A., Rowshandel, B., Branum, D., and Wills, C.J., 2003, The revised 2002 California probabilistic seismic hazard maps June 2003: California Geological Survey, [http://www.consrv.ca.gov/cgs/rghm/psha/fault_parameters/pdf/2002_CA_Hazard_Maps.pdf].

Chiou, B.S.-J., and Youngs, R.R., 2008, An NGA model for the average horizontal component of peak ground motion and response spectra: Earthquake Spectra, v. 24, no. 1, p. 173-215.

Clark, M.M., 1972, Surface rupture along the Coyote Creek Fault: US Geological Survey Professional Paper 787, p. 55-86.

Clark, D.H., Hall, N.T., Hamilton, D.H., and Heck, R.G., 1991. Structural analysis of late Neogene deformation in the central offshore Santa Maria Basin, California: Journal of Geophysical Research, v. 96, no.B4, p. 6435–6457.

*Conrad, J.E., Ryan, H.F., and Sliter, R.W., 2010, Tracing active faulting in the Inner Continental Borderland, Southern California, using new high-resolution seismic reflection and bathymetric data [abstract]: Seismological Society of America 2010 Annual Meeting, Seismological Research Letters, v.81, no. 2, p. 347.

*Crouch, J.K., and Suppe, J., 1993, Late Cenozoic tectonic evolution of the Los Angeles basin and Inner California Borderland: A model for core complex-like crustal extension: Geological Society of America Bulletin, v. 105, p. 1415-1434.

Dames & Moore, 1970, Seismic and foundation studies, proposed units 2 and 3, San Onofre Nuclear Generating Station, for Southern California Edison, 15 April 1970.

DeMets, C., and Dixon, T.H., 1999, New kinematic models for Pacific-North America motion from 3 Ma to present, I: evidence for steady motion and biases in the NUVEL-1A model: Geophysical Research Letters, v. 26, no. 13, p. 1921-1924.

Dorsey, R.J., and Janecke, S.U., 2002, Late Miocene to Pleistocene West Salton detachment fault and basin evolution, southern California: new insights [abstract]: Geological Society of America Abstracts with Programs, v. 34, no. 248.

*Ehlig, P.L., 1977, Geologic report on the area adjacent to the San Onofre Nuclear Generating Station northwestern San Diego County, CA, for Southern California Edison Company, 31 September 1977, 32 pp.

Erslev, E., 1991, Trishear fault-propagation folding: Geology, v. 19, p. 617-620.

Fialko, Y., 2006, Interseismic strain accumulation and the earthquake potential on the southern San Andreas fault system: Nature, v. 441, p. 968- 971, doi: 10.1038/nature04797.

*Fischer, P.J. and Mills, G.I., 1991, The offshore Newport-Inglewood – Rose Canyon fault zone, California: structure, segmentation and tectonics *in* Abbott, P.L., and Elliott, W.J., eds., Environmental Perils San Diego Region: San Diego, San Diego Association of Geologists, p. 17-36.

Fisher, M.A., 2009, Introduction to geologic hazards of offshore southern California *in* Lee, H.J., and Normark, W.R., eds., Earth and Science in the Urban Ocean: The Southern California Continental Borderland: Geological Society of America Special Paper 454, p. 227-228, doi: 10.1130/2009.2454(4.1).

Fisher, M.A., Langenheim, V.E., Nicholson, C., Ryan, H.F., and Sliter, R.W., 2009a, Recent developments in understanding the tectonic evolution of the southern California offshore area: implications for earthquake-hazard analysis *in* Lee, H.J., and Normark, W.R., eds., Earth and Science in the Urban Ocean: The Southern California Continental Borderland: Geological Society of America Special Paper 454, p. 229-250, doi: 10.1130/2009.2454(4.2).

Fisher, M.A., Sorlien, C.C., and Sliter, R.W., 2009b, Potential earthquake faults offshore southern California, from the eastern Santa Barbara Channel south to Dana Point *in* Lee, H.J., and Normark, W.R., eds., Earth and Science in the Urban Ocean: The Southern California Continental Borderland: Geological Society of America Special Paper 454, p. 271-290, doi: 10.1130/2009.2454(4.4).

Franzen, S., Lew, M., and Elliott, P.J., 1998, Multiple investigation methods for fault rupture hazard evaluation, *in* Robertson, and Mayne, eds., Geotechnical Site Characterization, Balkema, Rotterdam, ISBN 90 5410 939 4, p. 139-144.

Freeman, T.S., Heath, E.G., Guptill, P.D., and Waggoner, J.T., 1992, Seismic hazard assessment, Newport-Inglewood fault zone, *in* Engineering Geology Practice in Southern California, Special Publication, no. 4, Association of Engineering Geologists, Southern California Section, p. 211-231.

Glover, E.S., 1876, Bird's Eye View of San Diego, California. Map published by Schneider and Kueppers, San Diego.

*Grant, L.B., and Shearer, P.M., 2004, Activity of the offshore Newport-Inglewood Rose Canyon Fault Zone, coastal southern California, from relocated microseismicity: Bulletin of the Seismological Society of America, v. 94, no. 2, p. 747-752.

*Grant, L.B., and Rockwell, T.K., 2002, A northward propagating earthquake sequence in coastal southern California?: Seismological Research Letters, v. 73, no. 4, p. 461-469.

*Grant, L.B., Ballenger, L.J., and Runnerstrom, E.E., 2002, Coastal uplift of the San Joaquin Hills, southern Los Angeles basin, California, by a large earthquake since A.D. 1635: Bulletin of the Seismological Society of America, v. 92, no. 2, p. 590-599.

*Grant, L.B., Mueller, K.J., Gath, E.M., and Munro, R., 2000, Late Quaternary uplift and earthquake potential of the San Joaquin Hills, southern Los Angeles basin, California – REPLY: Geology, v. 28, no. 4, p. 384.

*Grant, L.B., Mueller, K.J., Gath, E.M., Cheng, H., Edwards, R.L., Munro, R., and Kennedy, G., 1999, Late Quaternary uplift and earthquake potential of the San Joaquin Hills, southern Los Angeles basin, California: Geology, v. 27, p. 1031-1034.

Grant, L.B., Waggoner, J.T., Rockwell, T.K., and von Stein, C., 1997, Paleoseismicity of the north branch of the Newport-Inglewood fault zone in Huntington Beach, California, from Cone Penetrometer Test data: Bulletin of the Seismological Society of America, v. 94, no. 2, p. 277-293.

Greene, H.G., Bailey, K.A., Clarke, S.H., Ziony, J.I., and Kennedy, M.P., 1979, Implications of fault patterns of the Inner California Continental Borderland between San Pedro and San Diego *in* Abbott, P.L., and Elliott, W.J., eds., Earthquakes and Other Perils, San Diego Region, San Diego Association of Geologists, p. 21-29.

Hanks, T.C., and Kanamori, H., 1979, A moment magnitude scale: Journal of Geophysical Research, v. 84, no. B5, p. 2348-2350.

Hanson, K.L., Angell, M., Foxall, W., and Rietman, J., 2002, Evaluation of seismic source characterization of models for the inner borderlands of southern California [abstract]: Eos (Transactions, American Geophysical Union) v. 83, no. 47, Fall Meeting Supplement, abstract S21A-0973, p. F1067.

Harding, T.P., 1973, Newport-Inglewood trend, California – an example of wrenching style of deformation: American Association of Petroleum Geologists Bulletin, v. 57, no. 1, p. 97-116.

*Hauksson, E., 1987, Seismotectonics of the Newport-Inglewood fault zone in the Los Angeles basin, southern California: Bulletin of the Seismological Society of America, v. 77, no. 2, p. 539-561.

*Hauksson, E., and Gross, S., 1991, Source parameters of the 1933 Long Beach earthquake: Bulletin of the Seismological Society of America, v. 81, no. 1, p. 81-98.

Hauksson, E., and Jones, L.M., 1988, The July 1986 Oceanside (M_L = 5.3) earthquake sequence in the Continental Borderland, southern California: Bulletin of the Seismological Society of America, v. 76, no. 6, p. 1885-1906.

Idriss, I.M., 2008, An NGA empirical model for estimating the horizontal spectral values generated by shallow crustal earthquakes: Earthquake Spectra, v. 74, no. 1, p. 217-242.

Jennings, C.W., 1994, Fault activity map of California and adjacent areas with location and ages of recent volcanic eruptions: California Department of Conservation, Division of Mines and Geology, Geologic Data Map Series, Map No. 6 , map with explanatory text, 92 pp., scale 1:750,000.

Kamerling, M.J., and Luyendyk, B.P., 1985, Paleomagnetism and Neogene tectonics of the northern Channel Islands, California: Journal of Geophysical Research, v. 90, p. 12,485-12,502.

Kamerling, M.J., and Luyendyk, B.P., 1979, Tectonic rotations of the Santa Monica Mountains region, western Transverse Ranges, California, suggested by paleomagnetic vectors: Geological Society of America Bulletin, part I, v. 90, p. 331-337.

Kennedy, M.P. and Clarke, S.H., 1996, Analysis of late Quaternary faulting in San Diego Bay and hazard to the Coronado Bridge, prepared for California Department of Transportation (Caltrans).

Kern, J.P., 1977, Origin and history of upper Pleistocene marine terraces, San Diego, California, Geological Society of America Bulletin, v. 88, p. 1553-1566.

*Kern, J.P., and Rockwell, T.K., 1992, Chronology and deformation of Quaternary marine shorelines, San Diego County, California *in* Kern, J.P., and Rockwell, T.K., eds., Quaternary Coasts of the United States: Marine and Lacustrine Systems, Special Publication no. 48, Society for Sedimentary Geology, 377-382.

*Kier, G., and Mueller, K., 1999, Flexural modeling of the northern Gulf of California Rift: relating marine terrace uplift to the forebulge on a subsiding plate: Southern California Earthquake Center 1999 internship final report, 11 pp., [http://www.scec.org/education/college/internships/1999/99grant.pdf].

Kies, R.P. and Abbott, P.L., 1983, Rhyolite clast populations and tectonics in the California continental borderland: Journal of Sedimentary Research, v. 53, no. 2, p. 461-475.

Klinger, R.E. and Rockwell, T.K., 1989, Flexural-slip folding along the eastern Elmore Ranch fault in the Superstition Hills earthquake sequence of November 1987: Bulletin of the Seismological Society of America, v. 79, no. 2, p. 297-303.

Lajoie, K.R., Ponti, D.J., Powell, C.L., Mathieson, S.A., and Sarna-Wojcicki, A.M., 1992, Emergent marine strandlines and associated sediments, coastal California: A record of Quaternary sea- level fluctuations, vertical tectonic movements, climatic changes and coastal processes, *in* Heath, E., and Lewis, L., eds., The regressive Pleistocene shoreline in southern California: Santa Ana, California, South Coast Geological Society annual Field Trip guidebook 20, p. 81-104.

Law/Crandall, Inc., 1993, Report of potential fault displacements Wastewater Treatment Plant Number 2 Huntington Beach, California for County Sanitation Districts of Orange County, 2661.30140.0001, 16 September 1993, 10 pp, 7 plates.

Lee, H.J., Greene, G.H., Edwards, B.D., Fisher, M.A., and Normark, W.R., 2009, Submarine landslides of the southern California Borderland Point *in* Lee, H.J. and Normark, W.R., eds., Earth and Science in the Urban Ocean: The Southern California Continental Borderland: Geological Society of America Special Paper 454, p. 251-269, doi: 10.1130/2009.2454(4.3).

*Legg, M.R., 1991, Developments in understanding the tectonic evolution of the California Continental Borderland: Special Publication no. 46, Society for Sedimentary Geology, p. 291-312.

*Legg, M.R., Goldfinger, C., Kamerling, M.J., Chaytor, J.D., and Einstein, D.E., 2007, Morphology, structure and evolution of California Continental Borderland restraining bends *in* Cunningham, W.D., and Mann, P., eds., Tectonics of Strike-Slip Restraining and Releasing Bends: Geological Society, London, Special Publications, 290, p. 143-168, doi: 10.1144/SP290.3.

Legg, M.R., Kamerling, M.J., and Francis, R.D., 2004, Termination of strike-slip faults at convergence zones within continental transform boundaries: examples from the California Continental Borderland in Grocott, J., McCaffrey, K.J.W., Taylor, G., and Tikoff, B., eds., Vertical Coupling and Decoupling in the Lithosphere, Geological Society of London, p. 65-82.

Leon, L.A., Dolan, J.F., Shaw, J.H., and Pratt, T.L., 2009, Evidence for large Holocene earthquakes on the Compton thrust fault, Los Angeles, California: Journal of Geophysical Research, v. 114, no. B12305, 14 pp., doi: 10.1029/2008JB006129.

Lindvall, S.C., and Rockwell, T.K., 1995, Holocene activity of the Rose Canyon fault zone in San Diego, California: Journal of Geophysical Research, v. 100, no. B12, p. 24,121-24,132.

Lutz, A.T.; Dorsey, R.J.; Housen, B.A.; and Janecke, S.U., 2006, Stratigraphic record of Pleistocene faulting and basin evolution in the Borrego Badlands, San Jacinto fault zone, southern California: Geological Society of America Bulletin, v. 118, p. 1377-1397.

Medwedeff, D., 1992, Geometry and kinematics of an active, laterally propagating wedge thrust, Wheeler Ridge, California, *in* Mitra, S., and Fischer, G. W., eds., Structural geology of fold and thrust belts: Baltimore, Maryland, Johns Hopkins University Press, p 3-28.

Minerals Management Services (MMS), 2001, Oil and gas resources in the Pacific outer continental shelf as of January 1, 1999: an expanded update to the 1995 National Assessment of United States Oil and Gas Resources: US Department of the Interior Minerals Management Services OCS Report MMS 2001-014, February 2001, 21 pp.

Molnar, P., 1979, Earthquake recurrence intervals and plate tectonics: Bulletin of the Seismological Society of America, v. 69, p. 115-133.

Morton, D.M., and Matti, J.C., 1993, Extension and contraction within an evolving divergent strike-slip fault complex: the San Andreas and San Jacinto fault zones at their convergence in southern California. *in* Powell, R.E. Weldon, R.J., and Matti, J.C., eds., The San Andreas Fault system: displacement, palinspastic reconstruction, and geologic evolution, Geological Society of America Memoirs, v. 178, p. 217-230.

Moody, J.D., and Hill, M.J., 1956, Wrench-fault tectonics: Geological Society of America Bulletin, v. 67, p. 1207-1246.

*Moore, G.W., 1972, Offshore extension of the Rose Canyon fault, San Diego, California: US Geological Survey Professional Paper 800-C, C113-C116.

Moriwaki, Y., Tan, P., and Barneich, J.A., 2002, Evaluation of alternative seismic source models using SCIGN data [abstract]: Eos (Transactions, American Geophysical Union) v. 83, no. 47, Fall Meeting Supplement, 19 November 2002.

Mount, V., Suppe, J., and Hook, S., 1990, A forward modeling strategy for balancing cross sections: American Association of Petroleum Geologist Bulletin, v. 74, p. 521-531.

*Mueller, K., Kier, G., Rockwell, T., and Jones, C.H., 2009, Quaternary rift flank uplift of the Peninsular Ranges in Baja and southern California by removal of mantle lithosphere: Tectonics, v. 28, TC5003, doi:10.1029/2007TC002227.

Mueller, K.J., Grant, L.B., and Gath, E., 1998, Late Quaternary growth of the San Joaquin Hills anticline—a new source of blind thrust earthquakes in the Los Angeles basin [abstract]: Seismological Society of America 1998 Annual Meeting, Seismological Research Letters, v. 69, no. 2, p. 161-162.

NOAA, 2008, Geophysical Data System (GEODAS) bathymetry points, Volume 1, Version 5.0.11.

NOAA, 2001, Geophysical Data System (GEODAS) bathymetry points, Volume 1, Version 4.1.

NGA, 2008, Earthquake Spectra, v. 24, no. 1, p. 1-341.

Nicholson, C., Sorlien, C.C., Atwater, T., Crowell, J.C., and Luyendyk, B.P., 1994, Microplate capture, rotation of the western Transverse Ranges, and initiation of the San Andreas transform as a low-

angle fault system: Geology, v. 22, p. 491-495.

Petersen, M.D., Bryant, W.A., Cramer, C.H., Cao, T., and Reichle, M., 1996, Probabilistic seismic hazard assessment for the State of California: U.S. Geological Survey Open File Report 96-706, 19 pp.

Plesch, A., Shaw, J.H., Benson, C., Bryant, W.A., Carena, S., Cooke, M., Dolan, J., Fuis, G., Gath, E., Grant, L., Hauksson, E., Jordan, T., Kamerling, M., Legg, M., Lindvall, S., Magistrale, H., Nicholson, C., Niemi, N., Oskin, M., Perry, S., Planansky, G., Rockwell, T., Shearer, P., Sorlien, C., Suss, M. P., Suppe, J., Treiman, J., and Yeats, R., 2007, Community Fault Model (CFM) for southern California: Bulletin of the Seismological Society of America, v. 97, no. 6, p. 1793-1802.

Ponti, D.J., 2010, USGS investigations of stratigraphy and neotectonics of the Los Angeles basin [abstract]: US Geological Survey, 5 pp.

*Ponti, D.J., 2001, Changing deformation rates through time: insights from new Quaternary stratigraphic studies in the Los Angeles basin, California [abstract]: American Geophysical Union 2001 Fall Meeting, 10–14 December 2001, abstract #S12E-11.

*Ponti, D.J., and Ehman, K.D., 2009, A 3-D sequence-based structural model for the Quaternary Los Angeles basin, California [abstract]: Southern California Earthquake Center Proceedings and Abstracts, 12–16 September 2009, vol. 19, p. 262-263.

Rentz, P, 2010, The influence of tectonics, sea level, and sediment supply on coastal morphology in the Oceanside littoral cell, CA, unpublished M.S. Thesis: University of California, San Diego.

*Rivero, C.A., 2004, Origin of active blind-thrust faults in the southern Inner California Borderlands, unpublished Ph.D. Dissertation: Harvard University, 146 pp.

*Rivero, C., and Shaw, J.H., 2010, in press, Active folding and blind-thrust faulting induced by basin inversion processes, Inner California Borderlands: Tectonics, submitted for consideration of publication 2010, 45 pp.

*Rivero, C., and Shaw, J.H., 2005, Fault-related folding in reactivated offshore basins, California *in* Interpretations of Contractual Fault-Related Folds, An American Association of Petroleum Geologists Seismic Atlas, Studies in Geology, No. 53, Department of Earth and Planetary Sciences: Harvard University, Cambridge, MA, 3 pp.

*Rivero, C., and Shaw, J.H., 2001, 3D geometry and seismogenic potential of the Inner California Borderland blind thrusts system [abstract]: Southern California Earthquake Center Proceedings and Abstracts, 23–26 September 2001, p. 105-106.

*Rivero, C., Shaw, J.H., and Mueller, K., 2000, Oceanside and Thirtymile Bank blind thrusts: implications for earthquake hazards in coastal southern California: Geology, v. 28, no. 10, p. 891-894.

Rockwell, T., 2010a, The Rose Canyon Fault Zone in San Diego; Proceeding of Fifth International Conference on Recent Advances in Geotechnical Earthquake Engineering and Soil Dynamics and Symposium in Honor of Professor I.M. Idriss; Paper No. 7.06c, 9pgs.

Rockwell, T., 2010b, The non-regularity of earthquake recurrence in California: Lessons from long paleoseismic records from the San Andreas and San Jacinto faults in southern California, and the north Anatolian fault in turkey, Proceeding of Fifth International Conference on Recent Advances *in* Geotechnical Earthquake Engineering and Soil Dynamics and Symposium in Honor of Professor I.M. Idriss, Paper No. EQ 5, 9 pp.

Rockwell, T., 2010c, Fault hazard characterization for a transportation tunnel project in Coronado, California *in* Geotechnical Earthquake Engineering and Soil Dynamics and Symposium in Honor of Professor I.M. Idriss, Paper No. 7.02c, 13 pp.

Rockwell, T.K. and Murbach, M., 1999, Holocene earthquake history of the Rose Canyon fault zone. USGS Award No. 1434-95-G-2613 Final Technical Report 36 pp (plus appendix).

*Rockwell, T.K., Lindvall, S.C., Haraden, C.C., Hirabayashi, C.K., and Baker, E., 1992, Minimum Holocene slip rate for the Rose Canyon fault in San Diego, California, *in* Heath, E.G., and Lewis, W.L., eds., The Regressive Pleistocene Shoreline Coastal Southern California: South Coast Geological Society, Inc., 1992 Annual field Trip Guide Book No. 20, p. 55-64.

Rockwell, T.K., Lindvall, S.C., Haraden, C.C., Hirabayashi, C.K., and Baker, E., 1991, Minimum Holocene slip rate for the Rose Canyon fault in San Diego, California *in* Abbott, P.L., and Elliott, W.J., eds., Environmental Perils San Diego Region: San Diego, San Diego Association of Geologists, p. 37-46.

*Ryan, H.F., Legg, M.R., Conrad, J.E., and Sliter, R.W., 2009, Recent faulting in the Gulf of Santa Catalina: San Diego to Dana Point *in* Lee, H.J., and Normark, W.R., eds., Earth and Science in the Urban Ocean: The Southern California Continental Borderland: Geological Society of America Special Paper 454, p. 291-315, doi: 10.1130/2009.2454(4.5).

SCE, UFSAR, San Onofre Nuclear Generating Station, Units 2 & 3, Updated Final Safety Analysis Report, submitted to the U.S. Nuclear Regulatory Commission (NRC).

SCE, 2001, San Onofre Nuclear Generating Station Units 2 and 3 Seismic Hazard Study of Postulated Blind Thrust Faults, prepared by Geomatrix Consultants, GeoPentech, and Southern California Edison for the Nuclear Regulatory Commission, 26 December 2001, 165 pp.

SCE, 1995, Seismic Hazard at San Onofre Nuclear Generating Station, prepared by Risk Engineering, Inc. for Southern California Edison Co., 2244 Walnut Grove Avenue, Rosemead, California 91770, 25 August 1995, 340 pp.

SCE, 1979, Report of the Evaluation of Maximum Earthquake and Site Ground Motion Parameters Associated with the Offshore Zone of Deformation San Onofre Nuclear Generating Station, prepared by Woodward-Clyde Consultants for Southern California Edison, P.O. Box 800, Rosemead, California 91770, June 1979, 243 pp.

SSHAC, 1997, Recommendations for probabilistic seismic hazard analysis: Guidance on uncertainty and use of experts, prepared by Senior Seismic Hazard Analysis Committee, Lawrence Livermore National Laboratory, Volume 1, Main Report, NUREG/CR-6372, UCRL-ID-122160, 280 pp.

Schneider, C.L., Hummon, C., Yeats, R.S., and Huftile, G.L., 1996, Structural evolution of the northern Los Angeles basin, California, based on growth strata: Tectonics, v. 15, no. 2, p. 341-355.

Scripps Orbit and Permanent Array Center (SOPAC), 2010, SOPAC refined velocities, accessed June 2010, from SOPAC website, [http://sopac.ucsd.edu/cgi-bin/refinedModelVelocities.cgi].

Seeber, L, and Sorlien, C.C., 2000, Listric thrusts in the western Transverse Ranges, California: Geological Society of America Bulletin, v. 112, p. 1067-1079.

Shaw, J., and Suppe, J., 1996, Earthquake hazards of active blind-thrust faults under the central Los Angeles basin, California: Journal of Geophysical Research, v. 101, no. B4, p. 8623-8642.

Shlemon, R.J., 1987, The Cristianitos fault and Quaternary geology, San Onofre State Beach, California *in* Geological Society of America Continental Field Guide—Cordilleran Section, p. I126-I129.

Shlemon, R.J., 1978, Late Quaternary rates of deformation Laguna Beach–San Onofre State Beach Orange and San Diego Counties, California, prepared by Roy J. Shlemon & Assoc. for Southern California Edison Company and San Diego Gas & Electric Company, October 1978, 31 pp.

Shlemon, R.J., Elliott, P., and Franzen, S., 1995, Holocene displacement history of the Newport-Inglewood, north branch fault splays, Santa Ana River floodplain, Huntington Beach, California [abstract]: Geological Society of America Abstracts with Programs 1995 Annual Meeting, 6–9 November 1995, v. 27, no. 6, p. A-375.

*Sliter, R.W., Ryan, H.F., and Normark, W.R., 2001, Does recent deformation at the base of slope provide evidence of a connection between the Newport-Inglewood and the Rose Canyon fault zones offshore southern California? [abstract]: American Geophysical Union 2001 Fall Meeting, 10–14 December 2001, abstract #S11A-0531.

*Sorlien, C.C., Campbell, B.A., Alward, W.S., Seeber, L., Legg, M.R., and Cormier, M., 2009a, Transpression along strike-slip restraining segments vs. regional thrusting in the Inner California Continental Borderland [abstract]: Southern California Earthquake Center Proceedings and Abstracts, 12–16 September 2009, v. 19, p. 264.

*Sorlien, C.C., Campbell, B.A., and Seeber, L., 2009b, Geometry, kinematics, and activity of a young mainland-dipping fold and thrust belt: Newport Beach to San Clemente, California, USDI/USGS Award No. 08HQGR0103 Final Technical Report, 25 pp.

Sorlien, C.C., Kamerling, M.J., and Mayerson, D., 1999, Block rotation and termination of the Hosgri strike-slip fault system, California, from 3-D map restoration: Geology, v. 27, p. 1039-1042.

Suppe, J., 1983. Geometry and kinematics of fault bend folding: American Journal of Science, v. 283, p. 684–721.

Suppe, J., and Medwedeff, D.A., 1990, Geometry and kinematics of fault-propagation folding: *Eclogae* Geologicae Helvetiae., v. 83, p. 409-454.

Thomas, P., Wong, I., and Abrahamson, N., 2010, Verification of probabilistic seismic hazard analysis computer programs: PEER Report 2010/106, Pacific Earthquake Engineering Research Center, College of Engineering, University of California, Berkeley, May 2010, 176 pp.

Treiman, J., 1993, The Rose Canyon fault zone, southern California: California Division of Mines and Geology, Open File Report 93-02, 45 pp.

USGS, 2009, Quaternary fault and fold database for the United States, accessed 25 October 2010, from USGS website, [http//earthquakes.usgs.gov/regional/qfaults/].

USGS, 2008, Documentation for the 2008 update of the United States National Seismic Hazard Maps, prepared by Petersen, M. D., Frankel, A. D., Harmsen, S. C., Mueller, C. S., Hallar, K. M., Wheeler, R. L.,

Wesson, R. L., Zeng, Y., Boyd, O. S., Perkins, D. M., Luco, N., Field, E. H., Wills, C. J., and Rukstales, K. S., U.S. Geological Survey Open File Report 2008-1128, 128 pp.

WGCEP, 2008, The Uniform California Earthquake Rupture Forecast, Version 2 (UCERF 2), prepared by 2007 Working Group on California Earthquake Probabilities: US Geological Survey Open File Report 2007-1437 and California Geological Survey Special Report 203, [http://pubs.usgs.gov/of/2007/1497/].

WGCEP, 1995, Seismic hazards in southern California: probable earthquakes, 1994-2024: Bulletin of the Seismological Society of America, v. 85, p. 379-439.

Weichert, D.H., 1980, Estimation of the earthquake recurrence parameters for unequal observation periods for different magnitudes: Bulletin of the Seismological Society of America, v. 70, no. 4, p. 1337-1346.

Wells, D.L., and Coppersmith, K. J., 1994, New empirical relationships among the magnitude, rupture length, rupture width, rupture area, and surface displacement: Bulletin of the Seismological Society of America, v. 84, p. 974-1002.

Wentworth, C.M., 1990, Structure of the Coalinga region and thrust origin of the earthquake, in The Coalinga, California earthquake of May 2, 1983: US Geological Survey Professional Paper 1487, p. 41-68.

Wesnousky, S.G., 2008, Displacement and geometrical characteristics of earthquake surface ruptures: Issues and implications for seismic-hazard analysis and the process of earthquake rupture: Bulletin of the Seismological Society of America, v. 98, p. 1609-1632.

Western Geophysical Company, 1972, Final Report: San Onofre Offshore Investigations, *in* SCE, 2001, SONGS Units 2 and 3 Seismic Hazard Study of Postulated Blind Thrust Faults, offshore marine reflection seismic data, Plate 2-3, 26 December 2001.

Weston Geophysical, 1971, Seismic Velocity Measurements, San Onofre Nuclear Generating Station, *in* Woodward-McNeill and Associates, 1972, Material Property Studies, San Onofre Nuclear Generating Station, Appendix C, 15 March 1972.

*Wetmore, P.H., Malservisi, R., Fletcher, J., Alsleben, H., Callihan, S., Springer, A., and González-Yajimovich, O., 2010, in review, Transtension within a restraining bend domain of a transform plate boundary: the role of block rotations and the reactivation of preexisting crustal structures: Geological Society of America Lithosphere, submitted for consideration of publication 2010, 17 pp.

Wilcox, R.E., Harding, T.P., Seely, D.R., 1973, Basic Wrench Tectonics: American Association of Petroleum Geologists Bulletin, v. 57, no.1, p. 74-96.

Woodward-Clyde Consultants, 1980, Response to NRC Questions San Onofre 2 & 3, Question 361.61, 4 pp., 3 figures, April 1980.

Woodward-McNeill and Associates, 1972, Material Property Studies, San Onofre Nuclear Generating Station, Appendix E, 15 March 1972, 8 pp.

*Wright, T.L., 1991, Structural geology and tectonic evolution of the Los Angeles basin, California *in* Biddle, K.T., ed., Active margin basins: American Association of Petroleum Geologists Memoir 52, p. 35–134.

Yeats, R.S., 1987, Late Cenozoic structure of the Santa Susana fault zone, California: U.S. Geological Survey Professional Paper 1339, p. 137-160.

Yeats, R.S., 1973, Newport-Inglewood fault zone, Los Angeles basin, California: American Association of Petroleum Geologists Bulletin, v. 57, no. 1, p. 117-135.

Yerkes, R.F., 1990, Tectonic setting, in The Coalinga, California earthquake of May 2, 1983: US Geological Survey Professional Paper 1487, p. 13-22.

Youngs, R.R., and Coppersmith, K.J., 1985, Implications of fault slip rates and earthquake recurrence models to probabilistic seismic hazard analysis: Bulletin of the Seismological Society of America, v. 75, no. 4, p. 939-964.

5.2 Personal Communication

Details of personal communication summarized in Appendix A, Attachment A-1, are denoted with an asterisk.

Abrahamson, N., 2010, personal communication.

*Ponti, D., 2010, personal communication.

*Rockwell, T., 2010, personal communication.

Rockwell, T., 2001, personal communication.

*Ryan, H., 2010, personal communication.

USGS, 2009, Harmsen, S., personal communication on 20 October 2009.

USGS, 2007, Kendrick, C., personal communication.

6.0 GLOSSARY

ALEATORY UNCERTAINTY: Uncertainty arising from or associated with the inherent, irreducible, natural randomness of a system or process

ANNUAL FREQUENCY OF EXCEEDANCE: Mean number of seismic events per year exceeding a specified value

BASE: United States Marine Corps Base at Camp Pendleton

CFM: Community Fault Model of southern California developed by Plesch et al. (2007)[1]

CGS: California Geological Survey

CPT: Cone Penetration Test

dgnd: The median or spectral acceleration uncertainty for any given attenuation relationship

EPISTEMIC UNCERTAINTY: Uncertainty associated with a model of a system or process and its parameters that arises from limitations of the data available or on causal understanding

GMPEs: Ground motion prediction equations

GPS: Global Positioning System

HAZ4.2: PSHA computer program developed by Dr. Norman Abrahamson (2010, PC)[1]

HAZARD CURVE: Plot of the relationship between a ground motion parameter and the mean number of seismic events per year in which the ground motion parameter at the site exceeds a specified value; herein, the ground motion parameters of interest are the peak ground acceleration and spectral acceleration

HECTARE: Unit of surface area equal to 10,000 square meters (i.e., 100 meters by 100 meters); also equal to 2.47 acres

Hz: Hertz

ICB: Inner Continental Borderland

InSAR: Interferometric Synthetic Aperture Radar

ka: Thousand years ago

km: Kilometers

km/s: Kilometers per second

Ma: Million years ago

MIS 5e/5a: Marine Isotope Stages 5e/5a; part of a series of stages 1 through 6

MMS: Minerals Management Services

mm/yr: Millimeters per year

m_j: A variable used in PSHA calculations representing an earthquake of a particular magnitude

m/s: Meters per second

M: A quantity characteristic of the total energy released by an earthquake

M_L: Local magnitude scale developed by Richter in the 1930s

Mw: Moment magnitude scale as presented by Hanks and Kanamori (1979)[1]

NGA: Next Generation Attenuation relationships presented as part of the NGA Relations Project, a five year research program designed to improve earthquake ground motion attenuation relationships for shallow crustal earthquakes in the western United States[1]

NI: Newport-Inglewood (Fault)

NI/RC: Newport-Inglewood/Rose Canyon Fault Zone

NSHM: National Seismic Hazard Maps as presented by USGS (2008; 2009, PC)[1]

$\dot{N}_s(m_j)$: A variable used in PSHA calculations representing the mean number of earthquakes per year having an earthquake magnitude m_j

OBT: Oceanside Blind Thrust Fault as characterized by Rivero et al. (2000)[1], Rivero and Shaw (2001)[1], Rivero (2004)[1], Rivero and Shaw (2005)[1], and Rivero and Shaw (2010, in press)[1]

OZD: Offshore Zone of Deformation

PC: Personal communication

PEER: Pacific Earthquake Engineering Research

PGA: Peak ground acceleration

PSHA: Probabilistic Seismic Hazard Analysis

POISSON PROCESS: A random function which describes the number of random events in a specified interval of time or space; the random events have the following properties: (i) the probability of more

than one event during the specified time interval is negligible; (ii) the probability of an event during the specified time interval does not depend on what happened prior to the specified time

QA/QC: Quality Assurance/Quality Control

RC: Rose Canyon (Fault)

RP: Return Period in years; inverse of annual frequency of exceedance value

RECURRENCE RELATIONSHIP: Relationship showing the annual recurrence of earthquakes of various magnitudes up to a maximum magnitude; used to determine the mean number of earthquakes per year

r_k: A variable used in PSHA calculations representing the distance between the site and a fault rupture plane

SA: Spectral Acceleration

SCE: Southern California Edison

SCOZD: South Coast Offshore Zone of Deformation

SDT: San Diego Trough

SONGS: San Onofre Nuclear Generating Station

SOPAC: Scripps Orbit and Permanent Array Center

SSHAC: Senior Seismic Hazard Analysis Committee

STAB: Seismic Technical Advisory Board for SONGS Seismic Hazard Analysis

TMBT: Thirtymile Bank Blind Thrust Fault as characterized by Rivero (2004)[1] and Plesch et al. (2007)[1]

TECHNICAL COMMUNITY: As used in this report, this term refers to geoscientists and engineers that have demonstrated expertise in relevant ground motion and seismotectonic fields of study in the area around SONGS

TYPE-A FAULT: Seismic sources with detailed earthquake recurrence models where the timing of past events and event displacements are available; earthquakes on Type-A Faults are modeled as characteristic earthquakes; faults as presented by WGCEP (2008)[1] and USGS (2008)[1]

TYPE-B FAULT: Seismic sources with measurable slip rates but lacking information of the timing of past events, fault segmentation, and/or event displacements; earthquakes on Type-B Faults are modeled as characteristic earthquakes that rupture the full fault length; faults as presented by WGCEP (2008)[1] and USGS (2008)[1]

TYPE-C ZONE: Regions of distributed shear in which overall rate and style of deformation are unknown; zones as presented by WGCEP (2008)[1] and USGS (2008)[1]

UCERF 2: Uniform California Earthquake Rupture Forecast, Version 2 as developed by the 2007 WGCEP (WGCEP, 2008)[1]

UFSAR: Updated Final Safety Analysis Report

V_{s30}: A variable used in the NGA relationships for the average shear wave velocity from the ground surface to a depth of 30 m

$v(Z \geq z)$: A function used in PSHA calculations representing the annual frequency of exceedance

USGS: United States Geological Survey

WGCEP: Working Group(s) on California Earthquake Probabilities

WEIGHTS: A weight as used in this report is a number between zero and one assigned to a branch of logic trees in such a way that the sum of the weights assigned to the branches associated with any single branching point (a point from which all the branches under considerations are shown) is one. A weight assigned to a branch usually represents the assigner's or assigners' combined judgment regarding how that branch should be counted with respect to the other branches associated with that branching point in the analysis of the probabilistic model represented by the entire logic tree.

Z: A variable used in PSHA calculations representing the ground motion parameters peak ground acceleration (PGA) and spectral acceleration (SA)

z: A variable used in PSHA calculations representing a specified ground motion parameter threshold

$Z_{1.0}$: A variable used in the NGA relationships for the approximate depth to 1.0 km/s shear wave velocity material

$Z_{2.5}$: A variable used in the NGA relationships for the approximate depth to 2.5 km/s shear wave velocity material

[1] Citation contained in Section 5.0 References

APPENDIX A
SEISMIC SOURCE CHARACTERIZATION

APPENDIX A OUTLINE

APPENDIX A

SEISMIC SOURCE CHARACTERIZATION

A1.0 INTRODUCTION

This Appendix provides additional background information to support the judgments regarding the weights assigned to the alternative strike-slip and blind thrust end-member seismic source characterization models discussed in Section 2.0 of the main report. Brief summaries of key seismic hazard assessments that have been conducted specifically for the SONGS Units 2 and 3 and of the current community seismic source characterization model are given in Section A-2. Section A-3 outlines the geologic and tectonic setting and history of the study region. Sections A-4 and A-5 provide additional discussion of the data and studies supporting the strike-slip fault source model (NI/RC as the primary fault source) and the blind thrust fault source model (OBT as the primary fault source), respectively. The following three Attachments are included in this Appendix and provide additional background information:

A-1 Annotated Bibliographies, which contain abstract summaries of selected references.

A-2 Seismic Source Characterization of Onshore RC Fault by Dr. Thomas Rockwell of San Diego State University.

A-3 Seismic Source Characteristics of Inner California Borderland's Blind Thrust Fault Systems by Dr. John Shaw and Dr. Andreas Plesch of Harvard University.

A2.0 CHRONOLOGY OF PREVIOUS RELEVANT SEISMIC HAZARD ASSESSMENTS

During the 1970s and early 1980s, SCE, with the assistance of firms such as Dames & Moore, Fugro, Western Geophysical, Woodward-Clyde Consultants, and several independent consultants completed rigorous onshore and offshore investigations to identify and characterize nearby fault sources and to evaluate their impact on potential earthquake ground motion and tsunami hazards for licensing SONGS Units 2 and 3 (SCE, UFSAR). During these SCE licensing investigations, what was referred to then as the Offshore Zone of Deformation (OZD), was part of a system of faults that included the onshore NI to the north, the offshore South Coast Offshore Zone of Deformation (SCOZD) in the middle, and the RC Fault to the south as illustrated on Figure A-1a. The SCOZD, the closest of these OZD source faults, is located offshore about 8 km southwest of SONGS. This system of faults was identified as the controlling earthquake source in the deterministic assessment of earthquake ground motions completed at that time.

The Cristianitos Fault, which is the closest mapped fault (refer to Figures A-1a, b, and c), is exposed in the sea cliff 915 m southeast of SONGS. Based on this exposure, the Cristianitos Fault was found by SCE (UFSAR) and Shlemon (1987) to have not displaced a 125 ka old marine terrace platform. Therefore, the Cristianitos Fault was not considered to be a fault source in the licensing earthquake ground motion assessment (SCE, UFSAR).

Other fault sources considered during the licensing of Units 1 and 2 to be capable of producing significant earthquake ground motions at SONGS included the onshore San Andreas, San Jacinto, and

the Elsinore fault zones, and the offshore Palos Verdes, Coronado Banks, Santa Catalina, San Diego Trough, and San Clement faults, as illustrated in Figures A-1a and b.

An updated seismic hazard assessment was conducted by SCE in 1995, with the assistance of Geomatrix Consultants, Risk Engineering, and Woodward-Clyde Consultants. During the 1995 PSHA (SCE, 1995), offshore and onshore data relevant to the OZD, in particular the SCOZD, that had become available since the preparation of the SCE UFSAR, were evaluated. The results of a PSHA, which was completed in this study, also showed that the NI, the SCOZD, and the RC fault sources were the controlling sources for seismic hazard at SONGS.

In 2001, with the assistance of Fugro West, Geomatrix Consultants, and GeoPentech, SCE completed a re-assessment of the seismic source characteristics of the NI/SCOZD/RC and conducted a PSHA that specifically addressed the newly postulated blind fault sources in the vicinity of SONGS. Alternative source characterizations for this 2001 seismic hazard analysis were developed to capture the range of plausible fault geometries and interactions between postulated thrusts, including the OBT (Rivero et al., 2000) and the San Joaquin Hills Blind Fault (SJBF) (Grant et al., 1999 and 2000), and strike-slip faults, including the NI/SCOZD/RC faults. Analysis of geodetic GPS data conducted as part of this assessment showed relative motion more consistent with north-northwest shear with little or no convergence across the ICB Province, or evidence of a regional “driving” force that would reactivate a large seismogenic thrust fault (SCE, 2001; Hanson et al., 2002; Moriwaki et al., 2002). Quaternary slip rates assigned to offshore blind thrust fault sources were modified from postulated higher long-term post-Pliocene slip rates (Rivero et al., 2000) to reflect constraints provided by the geodetic data and coastal marine terrace uplift rates.

UCERF 2, which was published by the 2007 WGCEP in 2008, represents the USGS current seismic source model for the southern California region. UCERF 2 primarily updated the state of knowledge on the southern California portion of the San Andreas Fault and the San Jacinto and Elsinore faults over what had previously been reported by a WGCEP in 1995. Postulated onshore blind thrust faults, such as the SJBF (Grant et al., 1999) were included in UCERF 2. However, postulated blind thrust faults in the ICB Province are not included in the source model used in UCERF 2, but were flagged by the authors of UCERF 2 as potential sources for future consideration.

There is ongoing debate within the technical community (e.g., Rivero and Shaw, 2001; Grant et al., 2002; Grant and Rockwell, 2002; Rivero, 2004; Grant and Shearer, 2004; Rivero and Shaw, 2005; Ryan et al., 2009; Sorlien et al., 2009b; Rentz, 2010; Rivero and Shaw, 2010, in press; and many others) as to whether high-angle strike-slip faults or low angle reverse or thrust faults are the primary tectonic structures or faults accommodating the crustal motions in the vicinity of SONGS. The present study utilizes two end-member tectonic structural models (referred to as the strike-slip and blind thrust system models) to facilitate the characterization of the closest offshore faults that have been demonstrated to dominate the earthquake shaking hazard for SONGS. UCERF 2 was selected as the basis or reference for one end-member model because it represents the most recent technical community’s consensus seismic source characterization model for California faults. In this strike-slip end-member model, the NI/RC Fault Zone is characterized as the closest, active, primary strike-slip fault to SONGS. The source parameters from UCERF 2 used to characterize the NI/RC Fault Zone in the USGS (2008) and USGS (2009, PC) seismic hazard mapping studies are used in this study. For the blind thrust end-member model, the OBT is characterized as the primary contributing seismic source for SONGS. The OBT is

included in the CFM (Plesch et al., 2007) and is identified in UCERF 2 as a potential fault source that should be given future consideration.

A3.0 TECTONIC AND GEOLOGIC SETTING

Southern California is divided into several physiographic regions, or provinces based on the makeup of their geologic and tectonic characteristics. Refer to Figure 2-1 in the main portion of this report and Figures A-2a, b, c, and d for the location of these provinces relative to SONGS and illustrations of their long and complex tectonic evolution. SONGS is located in the Peninsular Ranges Province, just east of its boundary with the ICB Province and to the south of the Transverse Ranges Province.

A summary of the geologic and tectonic characteristics of these physiographic provinces (Section A3.1) and a tectonic history that outlines the development of their key geologic and tectonic structures (Section A3.2 and Figures A-2a, b, c, and d) provide additional perspectives on the relationships between strike-slip and thrust faults in the region.

A3.1 Physiographic Provinces in the Study Region

As seen on Figure A-2a, the Peninsular Ranges Province extends from Colorado Desert Province in Coachella/Imperial Valley on the east, well into Baja California on the south, and to the Transverse Ranges Province on the north. To the west, the ICB Province is almost entirely offshore, including Santa Catalina and San Clemente Islands. This province also includes the Palos Verdes Peninsula and the western portion of the Los Angeles (LA) Basin. Similar to the Peninsular Ranges Province, the ICB Province is also bounded on the north by the Transverse Ranges Province and also extends to the south offshore of Baja California. The Outer Continental Borderland Province (MMS, 2001 and Crouch and Suppe, 1993) bounds the ICB Province on the west.

The Peninsular Ranges and ICB provinces are dominated by northwest-southeast trending mountain ranges and intervening basins that extend from within Baja California to the southern border of the Transverse Ranges Province (CGS, 2002b). The Transverse Ranges province is dominated by east-west trending mountain ranges and intervening basins that extend from the Twenty-Nine Palms/Palm Springs area on the east to offshore of Point Conception and the Channel Islands on the west. The basins and ranges in the Peninsular Ranges, ICB, and Transverse Ranges Provinces are commonly separated by fault zones that trend parallel to the ranges and valleys. The LA Basin, located at the juncture of these three physiographic provinces, includes faults and folds with differing orientations resulting from the complex interaction between the northwest-trending Peninsular Ranges and ICB Provinces and the east-west-trending Transverse Ranges Provinces.

As mentioned above, the physiography of both the ICB and the Peninsular Ranges provinces are composed of generally similar northwest-oriented faulted ridges and basins, with relatively steep slopes on the flanks of the uplifted ridges. However, there are distinct differences between the ICB and Peninsular Ranges provinces in their underlying basement rock composition and their structural relief their overlying sedimentary rocks, which suggest that it is appropriate to keep these two provinces separated. The ICB Province is underlain by the Catalina Schist basement rock complex and the Peninsular Ranges Province is underlain by a batholithic and older basement rock complex, as illustrated on Figures A-2c and A-2d. The ICB Province is bounded on the east by the NI/RC Fault Zone near the coast. The East Santa Cruz Basin Fault bounds the ICB Province on the west. The Peninsular Ranges

Province is bound on the west by the NI/RC Fault Zone and on the east by the Coachella and Imperial valleys with their San Andreas Fault System (refer to Figures A-2a and A-3).

A3.2 Tectonic History of the Inner Continental Borderland and Transverse Ranges

Southern California's current complex tectonic and geologic setting resulted from a long and complicated history in crustal plate interaction that has culminated in today's San Andreas Fault being the dominate player in the predominate right-lateral strike-slip boundary between the Pacific and North American crustal plates (Figures A-2b and 2c) (Atwater, 1998; Nicholson et al., 1994; Bohannon and Geist, 1998; Fisher 2009; and Fisher et al., 2009a). This complex deformational history and resulting tectonic setting form the basis for interpreting the stratigraphy, faults and folds, and present seismotectonic setting of the Peninsular Ranges and ICB provinces in the area around SONGS. Essentially, there have been three different phases of the crustal deformation, each with a distinct style and pattern of deformation and resulting geology.

A3.2.1 Phase 1 - Collision and Subduction

In the Cretaceous and early Tertiary, the western side of the Continental Borderland was a convergent (subduction) plate boundary (Figure A-2b). During Cretaceous and Paleogene time (>24 Ma), the oceanic Farallon plate was subducting beneath the continental crust of western North America, resulting in a continental margin arc-trench system. The subduction-related geology of California, when reconstructed, includes the Sierra Nevada granitic batholith that formed the roots of a magmatic arc, the metamorphic rocks along the arc front that form the foothills belt of the Sierra Nevada, the Great Valley Sequence of marine sedimentary rocks formed in the submarine fore-arc basin, the Coast Range ophiolite that was the oceanic floor of the fore-arc basin, and the Franciscan complex of accreted terrain metamorphic rocks formed in the accretionary wedge at the subduction front. These major geologic units are still recognizable in southern California, but, as illustrated on Figures A-2c and 2d, they have been broken up and re-organized by subsequent tectonic events (Atwater, 1998; Nicholson et al., 1994; Bohannon and Geist, 1998; Fischer, 2009; and Fisher et al., 2009a).

A3.2.2 Phase 2 - Oblique Extension

Beginning in the late Oligocene and early Miocene (17 to 24 Ma), subduction gradually ceased along the western margin of North America when the East Pacific Rise (source of the Farallon and Pacific Plates) encountered the continental margin and, along with the Farallon Plate, was, in turn, subducted beneath North America (Figure A-2b). A new plate boundary configuration resulted with the Pacific Plate in direct contact with the North American Plate along the strike-slip San Andreas Fault. The relative motion between the Pacific and North American Plates was no longer convergent, but rather largely right-lateral translational in nature.

During the Miocene (5 to 24 Ma), various crustal blocks along the North American margin became attached to the northward-moving Pacific Plate (Atwater, 1998). This microplate capture led to extensional deformation of the upper plate of the subduction zone, rotation and translation of large crustal blocks, normal faulting, widespread Middle Miocene Volcanism, and a zone of oblique extension (transtension) in the Borderland (Kamerling and Luyendyk, 1979 and 1985; Wright, 1991; Nicholson et al., 1994; Fisher, 2009; and Fisher et al., 2009a). This oblique extension continued into the middle Pliocene (~4 Ma) and caused extensive ridge and basin (horst and graben) morphology (similar to block

faulting in the Basin and Range Province) to occur in the ICB. This formed many of the generally northwest-trending basins and ridges of the ICB that are apparent today.

As schematically illustrated by Nicholson et al. (1994) in the sequence of maps shown on Figure A-2b, the western Transverse Ranges Province was one of these several captured rotating crustal blocks. These blocks, while simultaneously being translated northward, were also rotated as much as 90 to 110 degrees in a clockwise direction (also refer to Figure A-2c) forming the east-west trending, western portion of the Transverse Ranges Province (Kamerling and Luyendyk, 1985; Crouch and Suppe 1993; and Bohannon and Geist, 1998). As the Transverse Ranges Province moved northward and rotated into its present position and the transform plate boundary continued to develop along the eastern edge of the rotating block, significant extension occurred in the Los Angeles Basin and ICB Province resulting in rapid basin subsidence and sedimentation accumulation during the Miocene and early Pliocene. Approximately 4 to 5 Ma (during the early Pliocene), another reorientation of the plate boundary in southern California and northern Mexico occurred. The plate boundary south of the Borderland and west of Baja California migrated eastward, splitting Baja California and coastal southern California off from the rest of North America, attaching these crustal blocks to the Pacific Plate (Figure A-2b). Since that time (about 5 Ma), the relative plate motion vector between the North American and Pacific Plates has been oriented approximately N37°W (Cande et al., 1995; Atwater and Stock, 1998). The southern San Andreas Fault was the manifestation of this new shift eastward of the plate boundary in southern California. The southern San Andreas and the northern San Andreas are now connected through the well-known, large left restraining bend in the fault trace, (now referred to as the Mojave segment) thereby producing convergence across a wide area of the southern California, expressed most proximately in the Transverse Ranges Province (Clark et al., 1991; Wright, 1991; Schneider et al., 1996; Sorlien et al., 1999; and Seeber and Sorlien, 2000).

Thus, overall, the tectonic setting in this portion of southern California changed in the Pliocene from predominately transtensional to predominately transpressional. The increased convergence commonly resulted in diversely-striking Miocene normal faults being reactivated as reverse faults, and inversion of half-graben basins into anticlines (Yeats, 1987; Clark et al., 1991; Seeber and Sorlien, 2000). Significant transpression occurred across the newly-developing Transverse Ranges and portions of the LA Basin on numerous oblique reverse and blind faults, many of which are inverted normal faults (Pasadenan orogeny). Large scale, rapid uplift of crustal blocks north of the LA Basin occurred concurrently with gradual uplift of the Palos Verdes Peninsula and the San Joaquin Hills, and subsidence and rapid sedimentation in the LA Basin (Wright, 1991).

A3.2.3 Phase 3 - Transform Plate Boundary (Present)

The present-day Pacific-North American Plate boundary south of the Transverse Ranges Province in southern California is dominated by a broad zone of distributed right-lateral strike-slip motion. This motion affects an area extending from the San Andreas Fault in the east to the offshore San Clemente Fault in the west (Figure A-1a).

Various studies have estimated that approximately 48 to 52 millimeters per year (mm/yr) of right-lateral shear occurs across southern California (Bennett et al., 1996; DeMets and Dixon, 1999). The San Andreas Fault and several other strike-slip fault zones accommodate most of the slip across the plate boundary (Jennings, 1994; Petersen et al., 1996). The Eastern California Shear Zone (east of San Andreas Fault) is believed to accommodate about 10 mm/yr of right-lateral slip (Bennett et al., 1996). The slip

rate on the San Andreas Fault is variable, but ranges from about 10 to 35 mm/yr in southern California. The most recent information from paleoseismic studies suggests that the San Jacinto Fault has a slip rate of about 15 to 20 mm/yr (C. Kendrick, USGS, 2007, PC), which exceeds the 12 mm/yr reported by the CGS and the SCEC. Geologic data suggest that the Whittier-Elsinore, NI onshore, and Palos Verdes faults have slip rates of about 5, 1, and 3 mm/yr, respectively (Cao et al., 2003).

Quaternary to Holocene offsets on the major fault zones within the Continental Borderland are interpreted to be primarily right-lateral strike-slip faults with a lesser vertical slip component, commonly referred to as oblique-slip faults. The San Pedro Basin Fault and the San Clemente Fault are two of the most active faults in the Borderland, but their slip-rates are largely unknown. Based on regional slip budgets and offsets of Miocene volcanic rocks, estimates of the slip-rates of the key faults in the ICB are as follows: the San Pedro Basin Fault has a slip-rate of 1 to 2 mm/yr and individual splays of the San Clemente Fault Zone (including the Santa Cruz-Catalina Ridge and Pilgrim Banks-Santa Barbara Island faults) have slip-rates of 1 to 4 mm/yr. GPS observations between 1986 and 1995 indicate that the total relative slip between the North American and Pacific plates is 49 ± 3mm/yr. The estimated total relative slip-rate between the North American and Pacific Plates is reported by DeMets and Dixon (1999) to be about 52 mm/yr. While there are no permanent GPS stations on the eastern edge of the Pacific Plate, stations on Santa Catalina, San Clemente and San Nicolas Islands have shown 45.5, 47.5 and 48.5 mm/yr of slip with respect to stable North America, respectively (SOPAC, 2010). As shown in Figure A-3, the station on San Clemente Island, ***scip,*** is moving at a rate of 6 mm/yr with an azimuth of 41 degrees west of north relative to station, ***scms,*** in San Clemente (11 miles northeast of SONGS). These GPS velocities would suggest that the upper limit of postulated slip-rates for the offshore right-lateral strike-slip faults is slightly overestimated.

Using this more regional perspective and stepping closer to the area surrounding SONGS, two end models were utilized to facilitate the characterization of the closest offshore faults that have been demonstrated to dominate the seismic shaking hazard for SONGS. In this regard, UCERF 2 was selected as the basis for reference because it represents the most recent regionally documented seismic source characterization for California faults. Therefore, for the first end-member model, the NI/RC Fault Zone was selected because it was the only UCERF 2 model utilized by the USGS (2008) and USGS (2009, PC) in developing the seismic hazard maps for the building code that applies to the area near SONGS. Similarly, the other end-member model selected was the OBT because of its postulated ability to generate large magnitude earthquakes on a fault plane that was proposed to extend eastward, under the coastline and beneath SONGS.

A4.0 DATA AND OBSERVATIONS SUPPORTING THE NI/RC AS THE PRIMARY FAULT SOURCE

This section provides more detailed discussion of the available and relevant structural, geomorphology, paleoseismicity, seismology and GPS information that have been used to identify and characterize the NI/RC Fault Zone as a predominantly high-angle, right-lateral, strike-slip fault. The NI/RC Fault Zone is the closest primary seismic source fault to SONGS in the strike-slip end-member seismic source model included in this 2010 PSHA. Attachment A-2 presents Dr. Tom Rockwell's summary of current information concerning the NI/RC Fault Zone.

A4.1 Geometry and Structural Analyses

The geometry of a fault, as well as its flanking lithology, provide the geologic and tectonic structural information for estimating how that fault will rupture in the future; this information in turn is needed to

model the resulting earthquake ground motions that will impact facilities, such as SONGS. In addition to geometry and structural geologic information about the San Andreas Fault and other active strike-slip faults in the world, subsurface data from the oil fields under the LA Basin along the onshore NI portion of the NI/RC Fault Zone lead to the development of the classic theory of wrench fault tectonics (Moody and Hill, 1956; Wilcox et al., 1973; Harding, 1973; Yeats, 1973; Barrows, 1974; Harding 1985). In simplistic terms, as illustrated on Figure A-4a, the primary principal behind wrench fault theory is that, as high-angle, crustal-through-going, strike-slip faults progressively propagate through overlying more recently deposited sediments, they initially form a broad, near-surface zone of subsidiary faults in a flower-like pattern (refer to Figure A-4b). The orientation of these subsidiary faults is at oblique angles to the primary strike-slip fault and the direction of crustal deformation. These conjugate subsidiary faults vary in their geometry and style of faulting (i.e., normal, reverse, thrust, strike-slip, or oblique-slip) depending on their orientations relative to the strike and dip of the primary strike-slip fault. As the displacement of these more recently deposited sediments increases, the broad, flower-like pattern progressively narrows into the primary trace of the fault. The subsidiary fault patterns are most prominent in en echelon step-overs or bends in the trace of the primary, high-angle, strike-slip fault. As illustrated on Figures A-4a and A-4b, for right-lateral strike-slip faults right step-overs produce localized zones of tension expressed in subsiding blocks bracketed by normal or transtensional oblique slip faults. Examples of the en echelon right step-overs along the NI/RC Fault Zone are the subsiding San Diego Bay and Bolsa Chica and Anaheim Bay wetlands. Left step-overs produce localized zones of compression expressed in rising blocks bracketed by thrust, reverse, or transpressional oblique slip faults. Examples of these left step-overs along the NI/RC Fault Zone are Mount Soledad, Signal Hill, Domingues Hills, and Baldwin Hills.

SCE (UFSAR), with the assistance of Woodward-Clyde Consultants (1980), completed a thorough re-analysis of the oil well records and available geologic data from the oil fields between Newport Beach and Westwood (an example is provided on Figure A-5). This independent assessment concluded that the oil field data supported the wrench fault model and that a high-angle, right-lateral strike-slip fault dominated by the NI Fault Zone, and estimated that the long term slip rate on the fault was about 0.5 mm/yr. More recent work in examining oil well and groundwater well data from western Los Angeles County by Dr. Dan Ponti of the USGS (2010, PC) further supports the dominance of the high-angle strike-slip fault in the NI Fault Zone as illustrated in Figure A-6.

Data supporting the characteristics of the offshore part of the NI/RC Fault Zone are more limited. The continuity of the NI/RC Fault Zone, between its southern onshore trace near La Jolla and its onshore traces north of Newport Beach was first suggested by Moore (1972). SCE (UFSAR), through Western Geophysical Company, completed rigorous offshore marine seismic reflection surveys to assess potential faulting offshore of SONGS (Western Geophysical Company, 1972). Track lines of these surveys and their interpreted faults are shown on Figure A-7a. This offshore work supported the conclusion that the closest primary seismic source fault to SONGS is the offshore continuation of the high-angle, right-lateral, strike-slip NI/RC Fault Zone, whose characteristics are reflected in the wrench fault style of tectonics present in the northern and southern onshore portions of the fault zone.

Little has changed in the geoscience community's overall assessment of the NI/RC Fault Zone characterization as a strike-slip fault zone since the SCE's original investigations were completed. Some refinements were made in the mapped offshore traces of the faults by Fischer and Mills (1991) (Figure A-7b); Ryan et al. (2009) (Figure A-7c); Sorlien et al. (2009b) (Figure A-7d); and Conrad et al. (2010) (Figure A-7e). Figure A-7f illustrates a map containing the USGS (2009) Quaternary Fault and Fold

Database in the ICB. The changes in the NI/RC Fault Zone's seismic characteristics by Fischer and Mills (1991) were incorporated in the source models used in SCE (1995 and 2001) and those by Ryan et al. (2009), Sorlien et al. (2009b), and Conrad et al. (2010) were considered in this PSHA. Other research, including Grant and Shearer (2004), Fisher (2009), Fisher et al. (2009a), Fisher et al. (2009b), Lee et al. (2009), Rockwell (2010a and 2010c), proprietary work completed by Fugro, Inc., and work currently underway by Dr. Dan Ponti of the USGS along the onshore NI Fault and its subsidiary traces north of Long Beach, further supports the weights assigned herein to a high-angle, strike-slip characterization of the NI/RC Fault Zone as the closest primary source fault to SONGS in the strike-slip end-member model incorporated into this PSHA.

Most notable of this more recent research is the work completed by Ryan et.al. (2009), which essentially is an independent assessment of the available data reviewed during SCE's earlier work (Western Geophysical Company, 1972) on the characteristics of the faults located offshore of SONGS. Some of the proprietary marine geophysical survey data recently obtained by the USGS from WesternGeco and used by Ryan et al. (2009) was purchased by SCE years ago. Ryan (2010, PC) indicated that the results of the USGS's independent assessment of the data are in general agreement with the results of SCE's previous investigations and analysis of the faulting off-shore of SONGS, as seen by comparing Figure A-7a and A-7c.

USGS (2009) considers the NI/RC Fault Zone to be a primary, high-angle, right-lateral, strike-slip seismic source fault, with relatively minor alternatives to its most northern on-shore geometry.

A4.2 Evidence for Activity

A4.2.1 Paleoseismicity

The results of the SCE (UFSAR) (Woodward-Clyde) analysis of the oil field data (see example on Figure A-5 from Freeman et al., 1992) showed that, although the quality of the data varied between the different oil fields, the best fit of that data indicated about 0.5 mm/yr of strike-slip displacement across the main trace of the NI Fault. Slip rate estimates for the northern on-shore part of the NI/RC Fault Zone have been made by Fischer and Mills (1991), Freeman et al. (1992), Law/Crandall, Inc. (1993), Shlemon et al. (1995), Grant et al. (1997), and Franzen and Elliott (1998). In combination, these estimates suggest a wide range in slip-rate between 0.4 to 3.0 mm/yr for the onshore RC segment. More thorough and extensive paleoseismic investigations conducted by Lindvall and Rockwell (1995) and Rockwell (2010a and 2010c) support seismic source characteristics assigned to the southern onshore portion of the NI/RC Fault Zone in the San Diego area (summarized in Attachment A-2). Detailed 3D fault trenching in that work further supports the dominate high-angle, right-lateral, strike-slip style of faulting along the NI/RC Fault Zone with slip-rates estimated to be between 1.5 and 2.5 mm/yr. Offshore the paleoseismic data along the NI/RC Fault Zone has been more limited. Fischer and Mills (1991), based on their re-assessment of seismic reflection data available at that time, estimated a slip-rate of about 0.8 mm/yr, but were careful to qualify their estimate based on the limitations of their available data. Recent, high resolution marine geophysical surveys, like the USGS (Conrad et al., 2010) survey over the San Diego Trough Fault and the Rentz (2010) survey off the coast over the inner shelf between Dana Point and Carlsbad (refer to Figure A-8a), are providing more useable data to assess the paleoseismic record beneath the ICB.

High-resolution seismic data on the inner shelf has been used to constrain the recency of displacement on the Cristianitos Fault. Using this data, which is illustrated on Figure 8b, Rentz (2010) notes that what

subtle surface relief is observed locally on the inner shelf is of eroded, partially buried, bedrock remnants of "…adjacent geologic formations with different erosive properties." As Rentz (2010) suggests, "this differential erosion may be responsible for the trend of the San Mateo promontory, the highstand relief in the seismic profiles, and the ~9.6 km wide shelf," off of the coast between Dana Point and Carlsbad. Further, they conclude that in the area of their survey, "There is no observed offset of the overlying Holocene sediment packages, which would be expected if deformation was ongoing"; further supporting the SCE (UFSAR) conclusion that the Cristianitos Fault is inactive.

A4.2.2 Geomorphology

The geomorphology along the onshore parts of the NI/RC Fault Zone clearly supports the dominance of a high-angle strike-slip fault. As Dr. Rockwell presents in more detail in Attachment A-2, displaced stream channels in RC Fault are predominately offset right-laterally. Although the location and geomorphology defined by the NI/RC Fault Zone is less obvious in other parts of San Diego due to urban development, Dr. Rockwell presents in Attachment A-2, a late 19th century cartographer's sketch that shows a linear topographic lineament, which correlates with the present known location of the NI/RC Fault Zone. The pattern of this lineament across San Diego's hilly terrain supports the presence of an active near-vertical, right-lateral fault plane along this trace of the NI/RC Fault Zone.

The linear surface trace of the NI/RC Fault Zone through the western part of the LA Basin, particularly between Newport Beach and Long Beach, and the presence of localized uplifted hills and plateaus and intervening subsiding lowlands and wetlands is consistent with the presence of an underlying strike-slip dominated wrench fault system.

Between Newport Beach and La Jolla, the onshore geomorphology is characterized by a flight of emergent marine terraces (Figure A-9). The relatively uniform altitude of these surfaces suggests uniform uplift that does not appear to be consistent with the varying dips and long-term rates of slip postulated for the OBT. The sequence of emergent marine terraces have been mapped and described by Shlemon (1978), Kern and Rockwell (1992), Lajoie et al. (1992), and Grant et al. (1999) (refer to Figure A-9). Dating of the emergent MIS 5e/5a marine terraces at 125/80 ka by these authors, suggests regionally uniform coast uplift at a rate of about 0.13 to 0.14 mm/yr. Along the coastal San Joaquin Hills, the uplift rate may be as high as 0.21 to 0.27 mm/yr (Grant et al., 1999).

The presence and regionally persistent elevations of these onshore marine terraces, which are subparallel with the trend of the NI/RC Fault Zone, are more in concert with a nearby strike-slip faulting rather than a regionally persistent underlying thrust fault with changing dip angles, as proposed by Rivero et al. (2000) and Rivero (2004). As suggested by Mueller et al. (2009), the uniform uplift of these late Pleistocene uplifted marine terraces is more likely tied to regional tilting or "flexure of the crust driven largely by heating and thinning of the upper mantle beneath the Gulf of California and eastern Peninsular Ranges." Locally, this regional uplift is amplified by transpressional bends and en echelon step overs in the NI/RC Fault Zone leading to the higher uplift rates such as those tied of the San Joaquin Hills (Grant et al., 1999, 2000, and 2002) and Mount Soledad (Rockwell, 2010).

A relatively low-relief offshore continental shelf and the consistent 400-foot depth of its shelf break, is evident in the bathymetry extending along the coast between Palos Verde Peninsula to the Mexican Border, as illustrated in Figure A-10. This geomorphology also is inconsistent with a regionally persistent underlying thrust fault with changing dip angles, as proposed by Rivero et al. (2000) and Rivero (2004).

This uniform low-relief surface, which correlates to the last glacial maximum sea level low-stand at approximately 19 to 21 ka, is more consistent with a through-going strike-slip fault, such as the NI/RC.

Recent marine geophysical surveys along this shelf by Rentz (2010) are consistent with this conclusion by associating the wider shelf offshore between Dana Point and Carlsbad Canyon, in contrast to the width of the rest of the self between Newport Beach and Dana Point and between Carlsbad Canyon and La Jolla, to more erosion resistant bedrock formations. However, agreeing that the width of the shelf is at least in part is controlled by erosion patterns, based on new multibeam data acquired by the USGS in November 2010, Dr. Ryan (2010, PC) notes that there are major changes in erosion patterns across the San Mateo Point area and suggest that the San Mateo fold and thrust belt, located to the west of the NI/RC Fault Zone, does contributes to the shelf width. She also noted that the shelf morphology would be primarily controlled by sea level cycles, especially considering the low slip rate estimates for the offshore reverse and thrust faults.

A4.2.3 Seismology

Seismology data from the ICB, as a tool to help resolve the location and geometry of faults in this province, has limitations due to the paucity of nearby stations, limited azimuthal coverage, and uncertainties in the underlying velocity structure. Recognizing these limitations, Astiz and Shearer (2000) used improved methods to refine the locations of earthquakes that occurred in the Borderland between 1981 and 1997. Rivero et al. (2000) and Rivero (2004) utilized Astiz and Shearer (2000), in particular the 1986 M_L 5.3 Oceanside Earthquake, to support the offshore thrust fault models as discussed below in Section A-5.

Grant and Shearer (2004) also re-analyzed the 1981 M <3.0 cluster of earthquakes located about 10 km northwest of Oceanside and a 2,000 cluster of seismic events offshore of Newport Beach (refer to Figure A-11). Their work, especially the analysis of earthquakes northwest of Oceanside, supports a high-angle fault plane at depths of 12.5 to 13 km, This orientation of hypocenters and the their depth suggest the presence of a deep-rooted, high-angle, strike-slip fault (i.e., the NI/RC Fault Zone), rather than a low-angle reverse or thrust fault (i.e., the OBT). This supports the high-angle, strike-slip, end-member model containing the NI/RC Fault Zone as the closest primary seismic source fault to SONGS.

The 2,000 cluster of earthquakes offshore of Newport Beach also indicate a high-angle fault, such as the NI/RC Fault Zone, but this cluster is located west of the surface trace of the NI/RC Fault Zone and occurs at a depth of 6.5 to 7 km. The shallow depth of these earthquakes, however, does not preclude the possible presence of a seismogenic thrust fault plane passing beneath the high-angle structure.

Marrying the epicenter data from the M 5.3, 1986 Oceanside Earthquake with the new trace of the San Diego Trough Fault, recently re-located by new USGS offshore marine geophysical surveys (Conrad et al., 2010 and Ryan, 2010, PC) is in contrast with the thrust mechanism of that event being correlated with the Thirtymile Bank Blind Thrust (TMBT) as suggested by Rivero et al. (2000) and Rivero (2004). As seen on Figure A-12, the Oceanside event occurred near the San Diego Trough Fault at a left bend in that fault's trace. This relationship supports the occurrence of a thrust event within a high-angle, right-lateral, strike-slip fault system and not the occurrence of a thrust event on a regionally persistent underlying blind thrust fault.

A4.2.4 GPS

Clockwise rotation of crustal blocks in the ICB Province, suggested in SCE (2001), has been emphasized by Ryan et al. (2009). The rotating block proposed by Ryan et al. (2009) has been plotted along with geodetic data on Figure A-13 to qualitatively analyze whether geodetic data collected in southern California supports possible block rotation. Figure A-13 shows the best estimate of long-term velocities for permanent continuous GPS stations with respect to station ID ***scms*** in San Clemente. As shown on Figure A-13, stations in the southern portion of the Peninsula Range crustal block (shown in purple) appear to show slight clockwise rotation about the ***scms*** reference station. It is noted that the velocity vectors are presented in an exaggerated scale (1 inch equals 15 mm/yr) for effect. The tension and compression caused by this block rotation would likely lead to the reactivation of some portions of the Oceanside detachment as thrust faults and some portions as normal faults. Some portions would likely remain inactive, making it kinematically incompatible with the postulated through-going, regional thrust model. Conversely, Late Quaternary inactivity of the OBT fault offshore of Carlsbad and La Jolla, as suggested by Sorlien et al. (2009b), is consistent with this block rotation model.

Similarly, a qualitative analysis of geodetic data was prepared with respect to San Clemente Island as previously shown in Figure A-3. The visual trend of the relative velocities presented on Figure A-3 is in strong agreement with the strike-slip end-member seismic source characterization model for the ICB Province. It is noted that the velocities are presented in a smaller scale than in the previous figure (1 inch equals 5 mm/yr). In a qualitative sense, no tension or compression is observed in the relative velocities between Santa Catalina or San Clemente Islands and the Peninsula Range as would be expected in the blind thrust end-member model. The geodetic data (velocities and uncertainties) presented on Figures A-3 and A-13 are based on the public archive preserved by the Scripps Orbit and Permanent Array Center (SOPAC) and includes all permanent continuous GPS stations installed in southern California between 1995 and 2008 with at least 1.5 years of data collected.

A5.0 DATA AND OBSERVATIONS SUPPORTING THE OBT AS THE PRIMARY FAULT SOURCE

This section provides more detailed discussion of the available and relevant structural, geomorphology, paleoseismicity, seismology and GPS information that have been used to identify and characterize the OBT as the closest primary seismic source fault to SONGS. This summary is based primarily on Rivero (2004), Rivero and Shaw (2005), and Rivero and Shaw (2010, in press). Attachment A-3 presents Dr. John Shaw's and Dr. Andreas Plesch's assessment of the seismic source characteristics and current information concerning the OBT Fault based primarily on the work summarized in these publications. Figures A-14 through A-27 present illustrations supporting the data and observations described in this section of Appendix A. This information forms the basis for the blind thrust seismic source characterization end-member model used in the 2010 PHSA.

The OBT model is based on recognition of an extensive offshore low-angle fault by previous workers (Fischer and Mills, 1991; Crouch and Suppe, 1993; Rivero et al., 2000; Rivero and Shaw, 2010, in press). Rivero et al. (2000) first postulated that regional offshore thrust faults are primary, regional-scale active faults. These workers suggest that Mesozoic subduction zones (Phase 1) were reactivated as detachment surfaces during rotation of the Transverse Ranges in the Miocene (Phase 2), and that subsequent transpression in the Pliocene and Quaternary has resulted in structural inversion (Phase 3). According to Rivero et al. (2000) the OBT forms a regionally continuous fault extending from Laguna Beach to at least the US-Mexican Border. Fault rupture scenarios by Rivero et al. (2000) suggest the

potential to generate large (M_W 7.1-7.6) earthquakes that would control seismic hazards in the adjacent coastal area.

These regionally extensive blind thrusts are inferred to interact at depth coevally with displaced high angle, strike-slip or oblique-slip faults, such as the NI/RC Fault Zone and the other high-angle, strike-slip faults in the ICB, which are illustrated in Figure A-14. This blind thrust system model was further developed and described by Rivero (2004), Rivero and Shaw (2005), and Rivero and Shaw (2010, in press). Figure 2-2 in the main text provides a copy of the CFM developed by Plesch et al. (2007), which illustrates the OBT and TMBT fault sources included in this alternative seismic source model. These postulated blind thrust fault sources were addressed in UCERF 2 (WGCEP, 2008) as being considered for future deformation model development, but they are not in the current USGS source characterization model (USGS, 2009, PC).

Utilizing available seismic data Rivero and Shaw (2010, in press) and Shaw and Plesch (Attachment A-3) characterized the blind thrust fault sources (i.e., the OBT and TMBT) and associated hanging wall and footwall subsidiary faults. Possible structural scenarios that represent potential interactions between the steeply-dipping strike-slip faults and the low-angle blind thrust fault sources are outlined in Figure A3-2. Steeply-dipping, right-lateral strike-slip faults, such as the NI and RC, are incorporated into Rivero's (2004) blind thrust seismic source characterization model as highly segmented and offset faults under the argument that continuous, through-going, strike-slip faults, as primary fault sources are not kinematically compatible with the several km of shortening documented on the OBT Fault.

The key data and analyses that Rivero (2004), Rivero and Shaw (2005), and Rivero and Shaw (2010, in press) present in support of the OBT as a primary regional-scale active blind thrust are discussed in the following sections.

A5.1 Geometry and Structural Analysis

A5.1.1 Geometry

The geometry and style of faulting associated with the OBT are less well understood than for many other faults in southern California. Until recently, studies of blind faults and large oblique reverse faults in southern California focused primarily on the Transverse Ranges Province and the LA Basin where higher rates of contractional strain were expected. The work of Shaw and Suppe (1996) identified the Compton blind thrust as part of an active regional fault bend fold system in the western LA Basin. The OBT may be inferred to be an analog and possible extension of this system further to the southeast into the ICB Province. Although the offshore setting of the ICB Province poses challenges to the identification and characterization of blind thrust faults, the Oceanside detachment surface that is interpreted to be the OBT is clearly imaged in many offshore seismic reflection profiles.

The prominent reflector in the seismic data, now interpreted to be the OBT, originally was mapped by Western Geophysical Company (1972). Western Geophysical mapped a regional unconformity or disconformity at the top of acoustical basement, and mapped faults in 'cover sediments' offsetting upper Miocene strata above this surface (Figure A-7a). Subsequent studies described the regional disconformity as an extensional breakaway detachment fault surface (Figure A-2a-d), and identified it throughout much of the ICB Province (e.g., Crouch and Suppe, 1993 and Bohannon and Geist, 1998). The exposed detachment surface became an erosional unconformity that was subsequently covered by Miocene and younger sediments.

Rivero (2004) presents a detailed map (Figure 2-6) showing the locations of seismic profile data used to constrain the location and geometry of the OBT as developed by Rivero et al. (2000) and described by Rivero and Shaw (2005), and Rivero and Shaw (2010, in press). More than 10,000 km of industry seismic reflection profiles, well data, seismicity, and seafloor geologic maps were analyzed. The structural analysis employed kinematic and forward modeling techniques based on quantitative structural relationships between fold shape and fault geometry (Suppe, 1983; Suppe and Medwedeff, 1990; Mount et al., 1990; Erslev, 1991; and Almendinger, 1998). Advanced three–dimensional modeling techniques were used to generate full representations of fault surfaces and key stratigraphic markers. The lateral extent and geometric segmentation of the active blind–thrust ramps were determined by mapping of direct fault plane reflections and associated fold trends throughout the basin areas covered by the seismic grid. The three–dimensional modeling also was used to quantify the distribution of dip slip on the active fault system, and to further constrain the geometrical analysis (Rivero, 2004).

The geometry of the two segments of the OBT as represented in the CFM (Plesch et al., 2007), which is used to characterize the OBT for this study, therefore, is based on a systematic and comprehensive analysis of offshore deep seismic reflection data.

The geometry of the OBT as mapped by Rivero and Shaw consists of two segments of differing sizes and dips. The OBT has been mapped over an area of more than 1800 km^2, and extends to the south beyond the mapped limits of the fault at the US-Mexican Border. The northern segment averages 14 degree dip, and the southern segment averages 25 degree dip (Rivero et al., 2000). The geometry of the OBT is described in greater detail in Attachment A-3 and Rivero (2004).

A5.1.2 Structural Analysis

Rivero (2004) presents a comprehensive structural analysis of faults in the ICB, focusing on the tectonic reactivation of the Oceanside and Thirtymile detachments as blind–thrust faults. As an outgrowth of the studies presented in Rivero et al. (2000), this analysis generated more precise three–dimensional representations of the faults and estimates of long–term slip rates. More advanced three–dimensional modeling techniques and fault–related fold theories were employed to identify and to describe active blind–thrust faulting and folding induced by the reactivation of the OBT and the TMBT in the Dana Point, Carlsbad and TMBT regions. Over 10,000 km of industry seismic reflection profiles, well data, seismicity, and geologic maps were used. Rivero (2004) performed kinematic and forward modeling structural analysis techniques based on quantitative structural relationships between fold shape and fault geometry. He also used advanced 3D modeling techniques to generate full representations of fault surfaces and key stratigraphic horizons, and provided evidence for present day strain partitioning produced by the interaction of the low-angle thrusts and vertical strike-slip faults (Figures A-16, A-18 through A-20, A-22, and A-26).

The structural analysis led Rivero and Shaw to postulate Pliocene and Quaternary oblique compression and structural reactivation processes as the originating mechanism of the regional blind–thrust fault system (Rivero and Shaw, 2010, in press). This reactivation generated regional structural wedges cored by faulted basement blocks that inverted sedimentary basins (Figures A-15 and A-16) in the hanging wall of the Miocene detachments (Rivero, 2004). The Miocene detachment break-away zone and Pliocene through Quaternary reactivated blind thrust, as well as emergent thrust faults such as the San Onofre Thrust, located in the hanging wall of the OBT, were mapped (Figures A-17 through A-20). From these results, earthquake scenarios based on the structural interaction of active blind–thrust faults and major

strike–slip faults were developed for the ICB Province (see discussion in Attachment A-3). By defining new long–term slip rates, Rivero (2004) concluded that simple and complex earthquake sources could produce large earthquakes (M 7.0 to M 7.6) with recurrence intervals from 970 to 1,810 years (Attachment A-3).

Rivero (2004) notes that it is not possible to directly measure the long–term amount of contractional slip on the OBT because it is generally blind. However, since the location of the OBT is constrained in the region, he used area balancing methods to constrain fault slip. He also evaluated alternative slip values derived from balanced structural interpretations located across several of the major contractional trends observed in the study area as an additional constraint. Excess–area balancing methods were modified and used to invert for the amount of contractional slip consumed by the OBT (Figures A-24 and A-25), since the spatial location and geometry (dip value) of this fault were assumed by Rivero 2004 to be well–known in the study region.

Balanced and restored cross sections based on available seismic data and well data suggest approximately 2.2 to 2.7 km of shortening across the OBT during the last 1.8 to 2.4 Ma (Rivero and Shaw, 2010, in press; Attachment A-3). This suggests an average slip rate of about 1 mm/yr on the OBT, although shortening rate estimates vary significantly along strike (Figures A-24 and A-25).

A5.2 Evidence for Activity

Blind thrusts by definition do not extend to the surface and thus cannot be observed directly. Secondary deformation related to folding and faulting in the hanging wall of the blind thrust is used to identify and characterize recent movement on such fault sources. The following two subsections (4.2.1 Paleoseismicity and 4.2.2 Geomorphology) describe evidence and methods used to evaluate evidence for activity and provide constraints slip rates for the OBT and related structures.

A5.2.1 Paleoseismicity

Fault trenching or other paleoseismic data are not available for the OBT. The offshore location of the near-surface projected traces of the main thrust and back thrusts mapped by Rivero (2004) precludes direct observation of the surface deformation that may be associated with these tectonic structures. The Compton blind thrust, which is postulated to be an onshore equivalent of the OBT, may provide an analog to the OBT.

Leon et al. (2008) employed a multidisciplinary methodology that uses a combination of high-resolution seismic reflection profiles and borehole excavations to suggest a link between blind faulting on the Compton thrust at seismogenic depths directly to near-surface folding. They concluded from these studies that the Compton blind thrust fault is active and has generated at least six large-magnitude earthquakes (M_W 7.0 to 7.4) during the past 14,000 years that deformed the Holocene strata record. Growth strata (discrete sequences that thicken sequentially across a series of buried fold scarps) are interpreted to be associated with uplift events on the underlying Compton thrust ramp.

Rivero et al. (2000) interpret the San Joaquin Hills Blind Thrust (SJHBT) as a backthrust to the OBT. Rivero (2004) estimates that M 7.1 and M 7.3 events would occur on average every 1,070 to 1,430 and 1,480 to 1,960 years, respectively, on the OBT where the SJHBT is linked with the OBT. Grant et al. (1999) also suggest that a backthrust that soles into the OBT is a viable structural model, although less preferred than one in which movement of the SJHB is the product of partitioned strike-slip and

compressive shortening across the NI/RC Fault Zone. They calculated average recurrence times of 1,650 to 3,100 years for moderate-magnitude earthquakes (based on an average uplift event of 1.3 m; Grant et al., 2002).

A5.2.2 Geomorphology

Rivero et al. (2000) provides a viable structural model that explains the localized uplift of the San Joaquin Hills as a backthrust in the hanging wall of the OBT (Figure A-21). They interpret an offshore extension of this structure that is imaged in seismic data as forming above a shallow blind thrust ("Shelf Monocline Trend" on Figure A-21) with an average southwest dip value of 23 degrees. This shallow fault is restricted to the hanging wall of the OBT at depth, and they interpret that this shallow fault soles into the OBT forming a structural wedge (Medwedeff, 1992; Mueller et al., 1998 and Rivero, 2004) (Figure A-21 and A-26). Quaternary uplift of the San Joaquin Hills as manifested by emergent marine terraces, therefore, is interpreted as evidence of Quaternary reactivation of the OBT (Figure A-23).

On a more regional scale, Rivero and Shaw suggest that emergent marine terraces along the entire coast between southern Orange County and northern Baja California show evidence for regional uplift of approximately 0.13 to 0.14 mm/yr (Kern and Rockwell, 1992), and may be the surface manifestation of Quaternary uplift in the hanging wall to the OBT (Rivero et al., 2000 and Rivero, 2004; Attachment A-3).

Seafloor fold and fault scarps associated with the OBT (Figures A-4b, A-16, A-18, A-19, and A-20) also suggest recent contractional activity (Rivero et al., 2000 and Rivero, 2004). Structural inversion and associated reactivation of normal faults commonly produce broad regions of positive structural relief characterized by the development of broad anticlines located directly on top of extensional rollovers and syn-extensional stratigraphic wedges (Figure A-15). Rivero (2004) concludes that thrust motion on the OBT generated four prominent contractional fold trends. Three of these trends are foreland–directed structures, namely the San Mateo, the San Onofre and the Carlsbad trends (Figures A-17 through A-20). These active structures are characterized by thrust sheets that extend laterally for 10 to 20 km, and produce prominent fold and fault scarps on the sea floor. The fourth trend is characterized by hinterland thrusting, which is manifested in a laterally continuous monocline that controls the relief and bathymetric expression of the continental shelf. This monocline is interpreted to result from the interaction between a shallow west–dipping back thrust system and the deep–seated, east–dipping OBT.

Geomorphically, youthful seafloor scarps and folds above fault tiplines have been documented on multibeam bathymetry data and seismic reflection data. Growth folding and offset of Late Quaternary strata are locally apparent on the seismic records, documenting active seafloor uplift on the continental slope in the vicinity of the San Mateo, San Onofre, and Carlsbad faults (Sorlien et al., 2009b; Ryan et al., 2009 and Rivero and Shaw, 2010, in press).

A5.2.3 Seismology

Seismicity in the offshore region is generally diffuse and scattered as compared to more spatially correlated patterns associated with many strike-slip active faults in the Peninsular Ranges on the mainland (Astiz and Shearer, 2000). The focal mechanism of the 1986 M_L 5.6 Oceanside event suggests that the main shock during that event had reverse motion (Hauksson and Jones, 1988). Most importantly, Astiz and Shearer (2000) document a shallow, east-dipping plane of seismicity at a depth of between 10 and 15 km beneath the continental slope and shelf west of San Diego based on relocation of

1981–1997 earthquakes (Figure A-27). The standard errors associated with these earthquake locations are less than 1.5 km. Astiz and Shearer (2000) suggest that these focal mechanisms document the existence of an active, low-angle east-dipping fault in the Coronado Banks Region that may be part of a larger system of offshore thrust faults like the OBT. Rivero (2004) cites this low angle plane of seismicity as evidence for contractional activity on the OBT.

A5.2.4 GPS

As previously noted, the geodetic data (velocities and uncertainties) presented on Figures A-3 and A-13 are based on the public archive preserved by the Scripps Orbit and Permanent Array Center (SOPAC) and includes all permanent continuous GPS stations installed in southern California between 1995 and 2008 with at least 1.5 years of data collected. The GPS data collected to date generally does not support regional compression or extension normal to the postulated OBT. However, it is noted that the current status of geodetic data can be considered inconclusive due to the following:

- Data reduction has quantitative limitations due to the uncertainty caused by locking effects that are dependent upon the characterization of major strike-slip faults in the Continental Borderlands.

- Currently, GPS stations in the vicinity of SONGS are either located on what would be the locked part of the OBT where resolution of low postulated slip rates are within the uncertainty of the GPS measurements or they are located too close to the Elsinore Fault to show any gradient of shortening across the area in question.

- There are very few GPS stations in the vicinity of SONGS and even fewer in the offshore region of the Continental Borderlands; one continuous station exists on San Clemente Island and two on Catalina Island.

- There are many sources with unknown slip-rates in the ICB Province making it difficult to resolve the low magnitude of slip postulated on either the OBT or the NI/RC Fault Zone system.

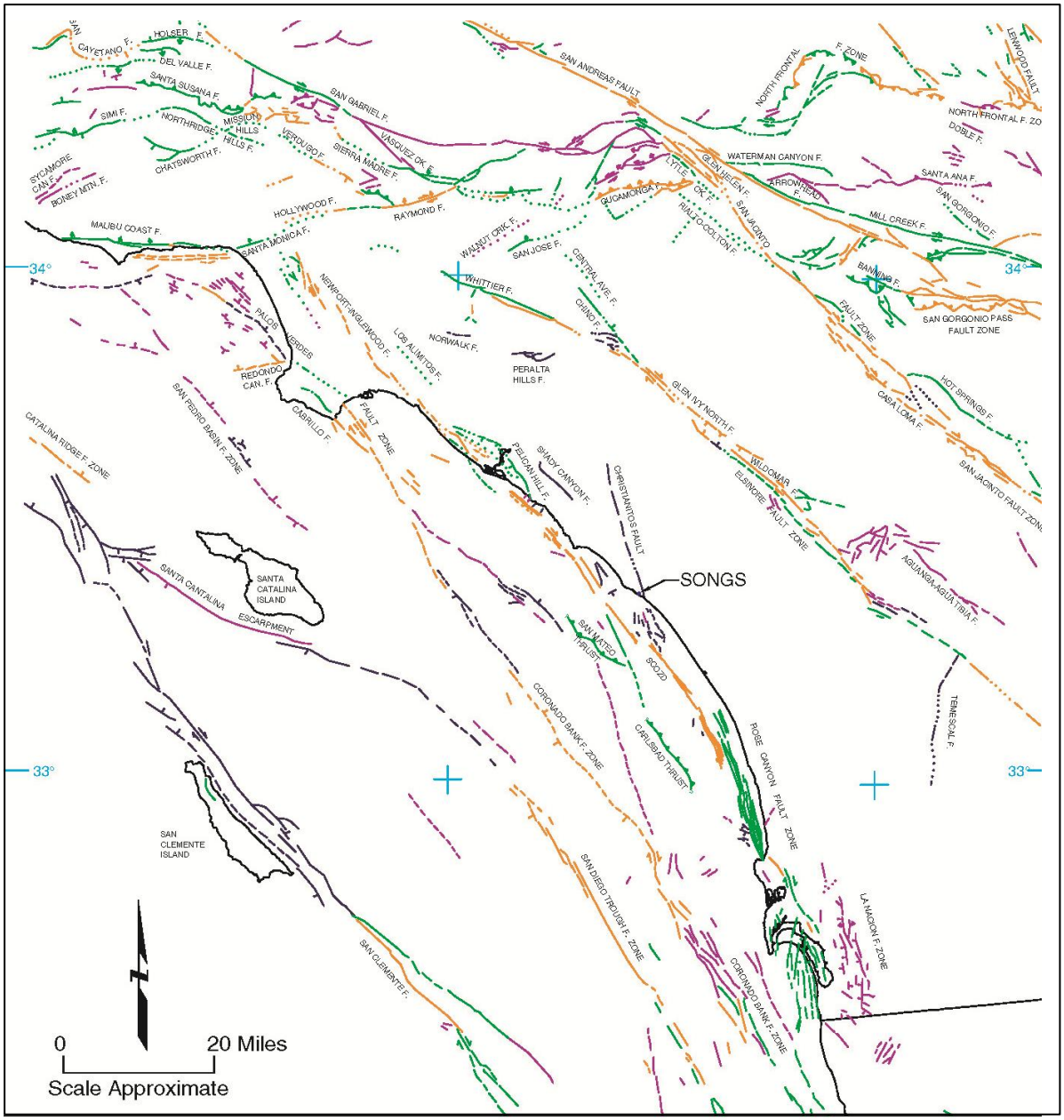

FAULT RECENCY CLASSIFICATION

- Faults that displace Holocene (~ 10 ka) or latest Pleistocene (~ 20 ka) deposits or geomorphic surfaces
- Faults that displace late Quaternary (~ 780 ka) deposits or geomorphic surfaces
- Quaternary faults (1.8 Ma)
- Faults that displace pre-Quaternary deposits. Receny of last displacement for offshore faults generally not known. Only selected faults from Jennings (1992) are shown.

GeoPentech
Geotechnical & Geoscience Consultants

SCE (2001) QUATERNARY FAULT MAP

FIGURE A-1a

SAN ONOFRE NUCLEAR GENERATING STATION

SEISMIC HAZARD ASSESSMENT PROGRAM

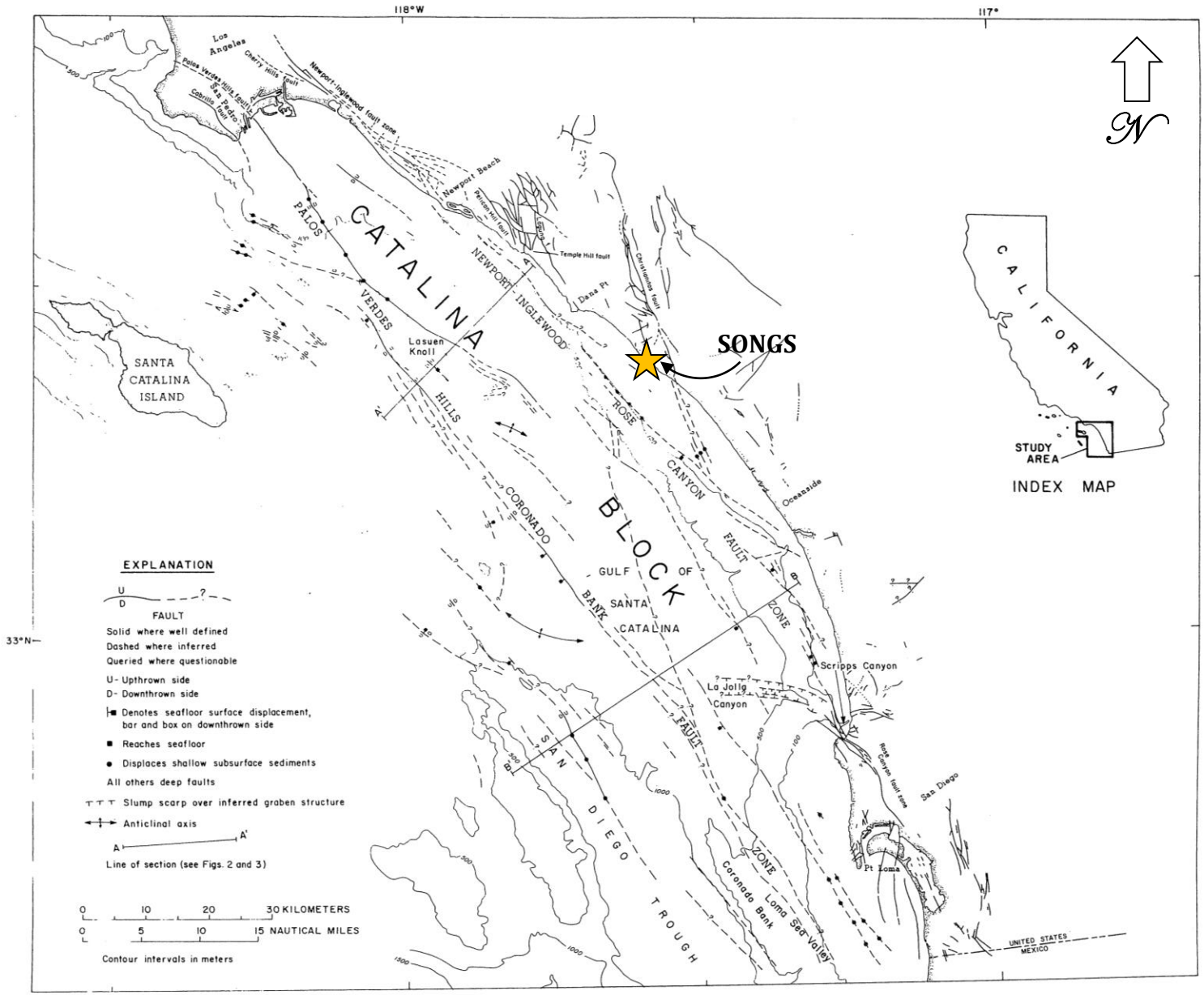

Modified from Greene et al. (1979)

GeoPentech Geotechnical & Geoscience Consultants	**SAN ONOFRE NUCLEAR GENERATING STATION** SEISMIC HAZARD ASSESSMENT PROGRAM	**CONTINENTAL BORDERLAND STRUCTURAL GEOLOGY MAP**	FIGURE A-1b

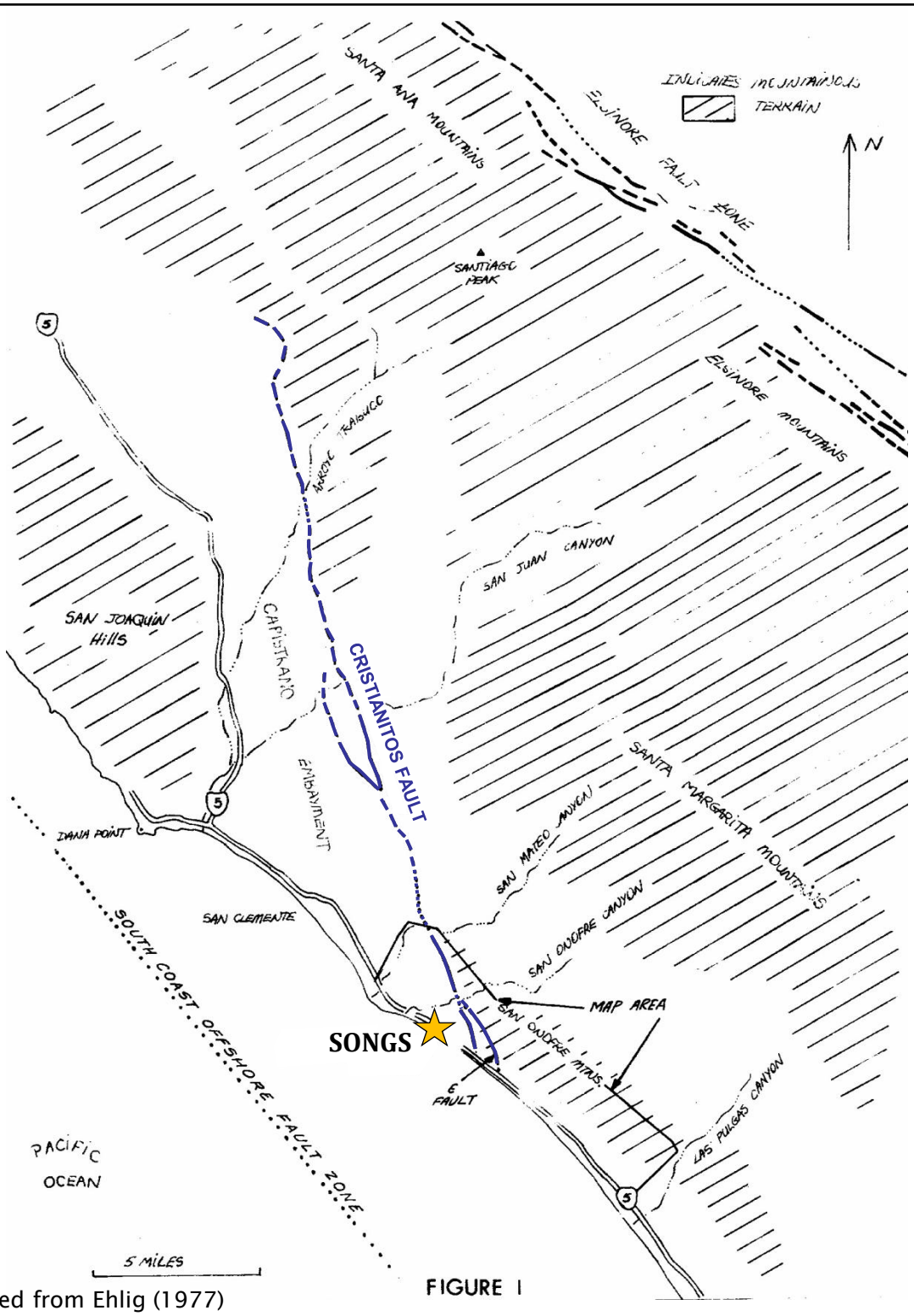

FIGURE 1

Modified from Ehlig (1977)

GeoPentech Geotechnical & Geoscience Consultants	MAP OF CRISTIANITOS FAULT ZONE	FIGURE A-1c
	SAN ONOFRE NUCLEAR GENERATING STATION SEISMIC HAZARD ASSESSMENT PROGRAM	

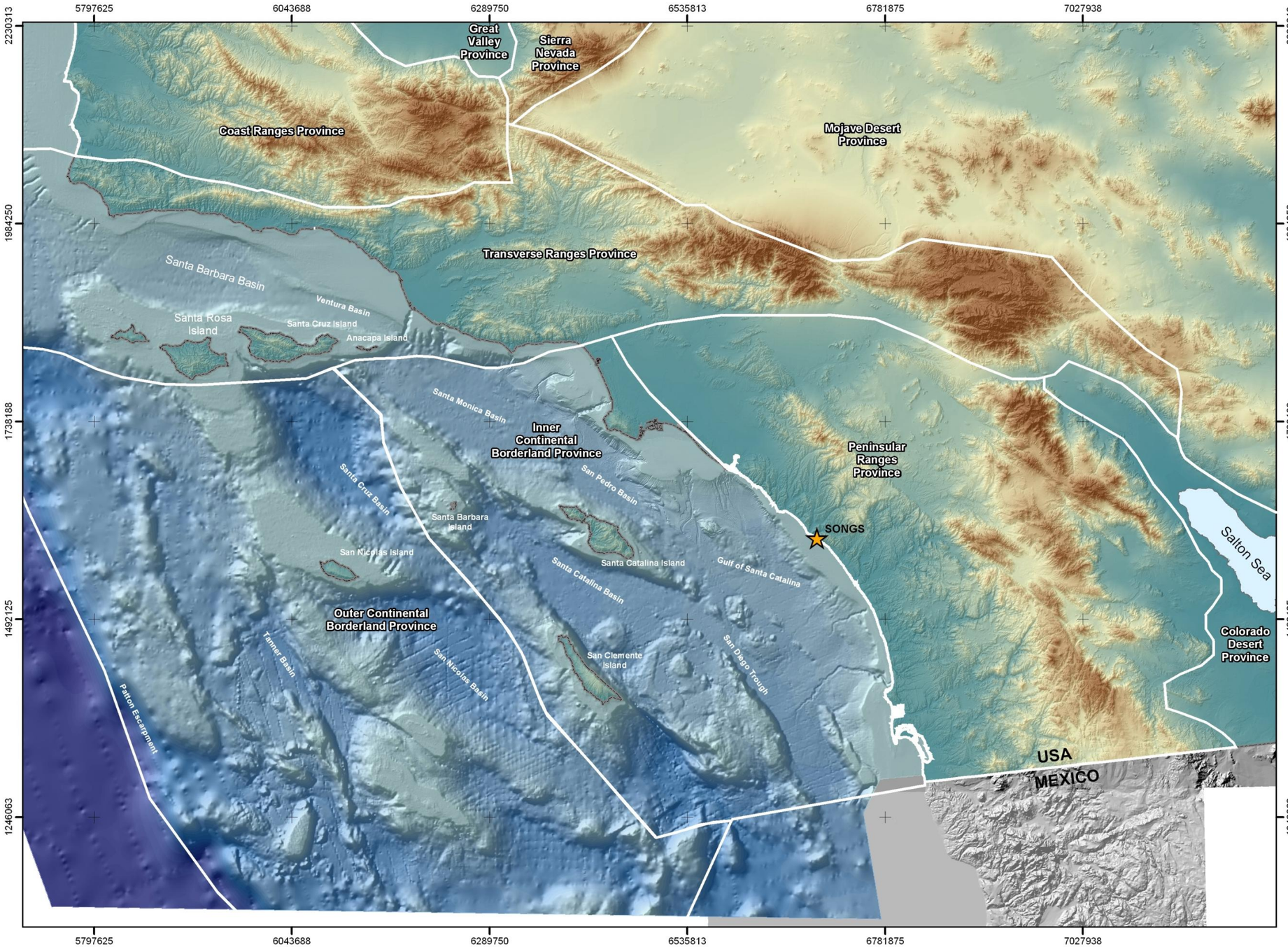

LEGEND

Approximate Geomorphic Province Boundary

Coordinate Grid: CA State Plane Zone 5, NAD83, Feet

Source: CGS (2002b) and Fisher et al. (2009a)

N

1:1,500,000

20 10 0 20 Miles

GeoPentech
Geotechnical & Geoscience Consultants
By Fugro West, Inc. (2010)

SAN ONOFRE NUCLEAR GENERATING STATION

SEISMIC HAZARD ASSESSMENT PROGRAM

GEOMORPHIC PROVINCES OF SOUTHERN CALIFORNIA

FIGURE
A-2a

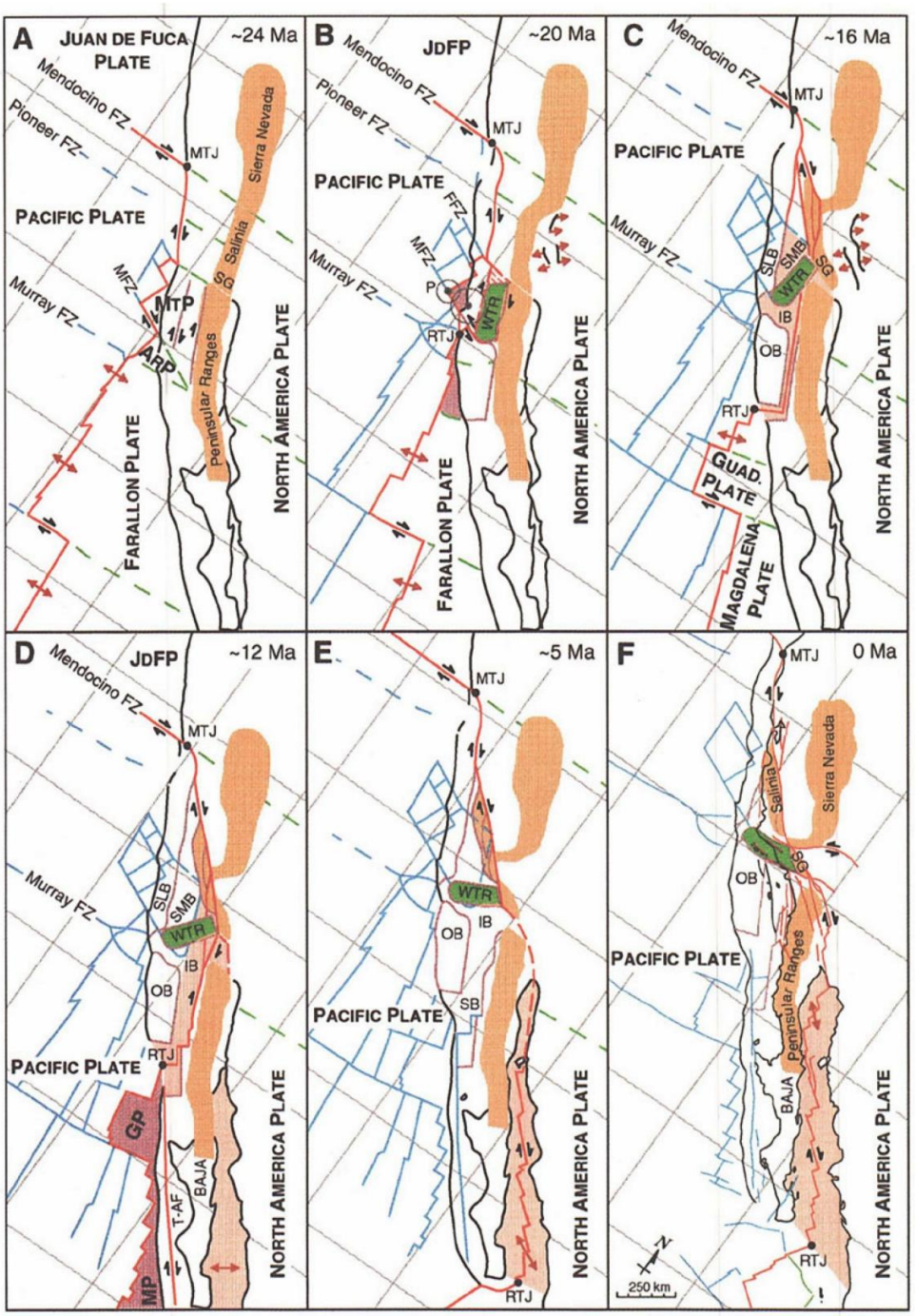

Simple tectonic model of Pacific–North America plate interactions since 24 Ma. Model assumes constant rate and direction of Pacific plate motion and constant rate of western Transverse Ranges (WTR) rotation. When partially subducted Monterey (20 Ma), Arguello (17.5 Ma), and Guadalupe and Magdalena (12 Ma) microplates are captured, part of North America upper plate is transferred to Pacific plate. Fine gray lines provide reference grid tied to fixed North America; error circles in B are estimated uncertainties in position P from this model and Stock and Molnar (1988). ARP—Arguello plate; GP—Guadalupe plate; MTP—Monterey plate; SG—San Gabriel block; JDFP—Juan de Fuca plate; SLB—Santa Lucia Bank; SMB—Santa Maria basin; IB, OB, SB—inner, outer, and southern borderland, respectively; T-AF—Tosco-Arbreojos fault; MP—Magdalena plate; red areas—regions of transtension; purple areas—captured or soon-to-be captured microplates. See Figure 2 for other abbreviations.

Source: Nicholson et al. (1994)

GeoPentech
Geotechnical & Geoscience Consultants

CENOZOIC EVOLUTION OF THE PACIFIC – NORTH AMERICA PLATE BOUNDARY

FIGURE A-2b

SAN ONOFRE NUCLEAR GENERATING STATION

SEISMIC HAZARD ASSESSMENT PROGRAM

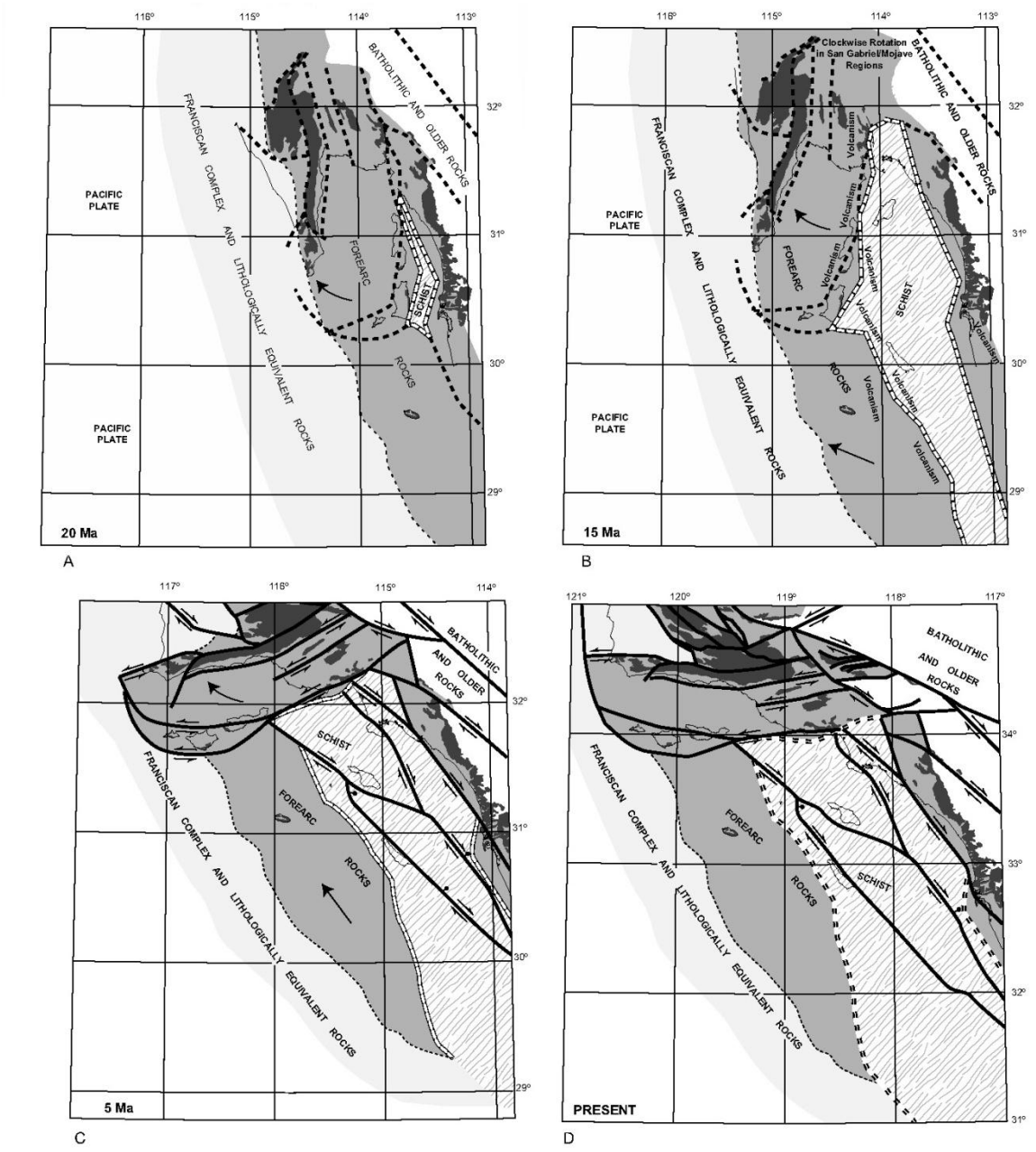

Palinspastic maps of California continental borderland and adjacent regions for past 20 m.y. Light gray areas are accretionary rocks of Franciscan Complex or belts that are lithologically similar to that complex. Medium gray areas are underlain by forearc strata. Dark gray areas are known outcrops of forearc strata. Area in wavy lined pattern is Catalina Schist belt. White areas are floored by batholithic basement rocks. Fine line is modern shoreline and island configuration, shown deformed and displaced for reference in earlier models. Heavy lines are major faults that are thought to be active during time represented. Dashed double line is fault-bounded margin of Catalina Schist belt. Dashed boxed line is active margin of extending region within Catalina Schist belt. Arrows show approximate trajectories of areas with respect to North America. (A) 20 Ma; time period prior to most of the deformation. (B) 15 Ma; time period in migrating-hinge phase of extension. (C) 5 Ma; time period in dispersed right-normal-slip phase of extension. (D) Present-day configuration.

Source: Bohannon and Geist (1998)

GeoPentech Geotechnical & Geoscience Consultants	**LATE CENOZIC PALINSPASTIC RECONSTRUCTION MAPS OF THE CONTINENTAL BORDERLAND**	FIGURE A-2c
	SAN ONOFRE NUCLEAR GENERATING STATION SEISMIC HAZARD ASSESSMENT PROGRAM	

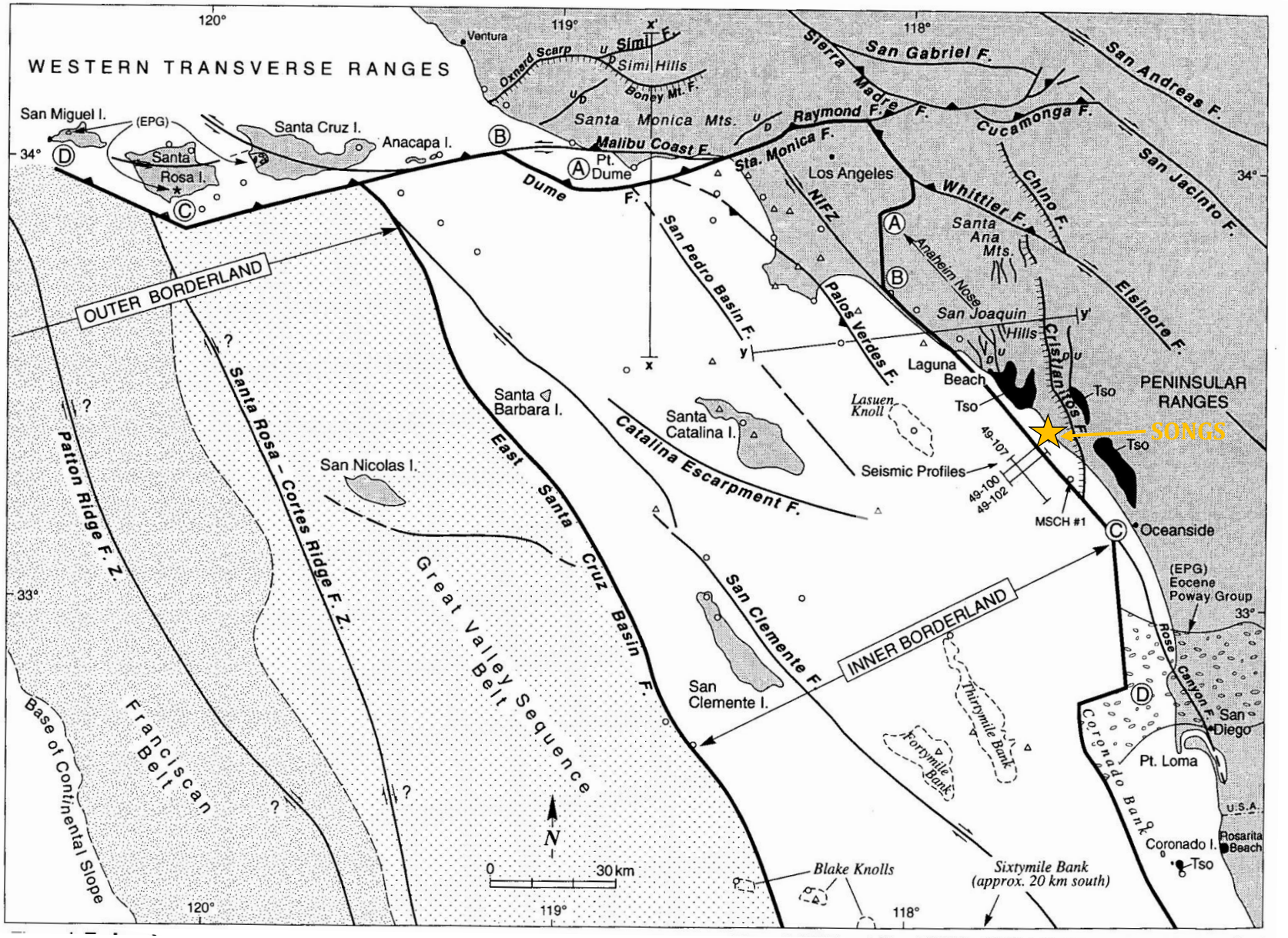

NOTES: (1) Modified from Crouch and Suppe (1993)
(2) Presented in SCE (2001)

GeoPentech
Geotechnical & Geoscience Consultants

SAN ONOFRE NUCLEAR GENERATING STATION
SEISMIC HAZARD ASSESSMENT PROGRAM

SIMPLIFIED MAP OF CALIFORNIA BORDERLAND PROVINCES WITH ONSHORE AND OFFSHORE FAULT TRACES

FIGURE
A-2d

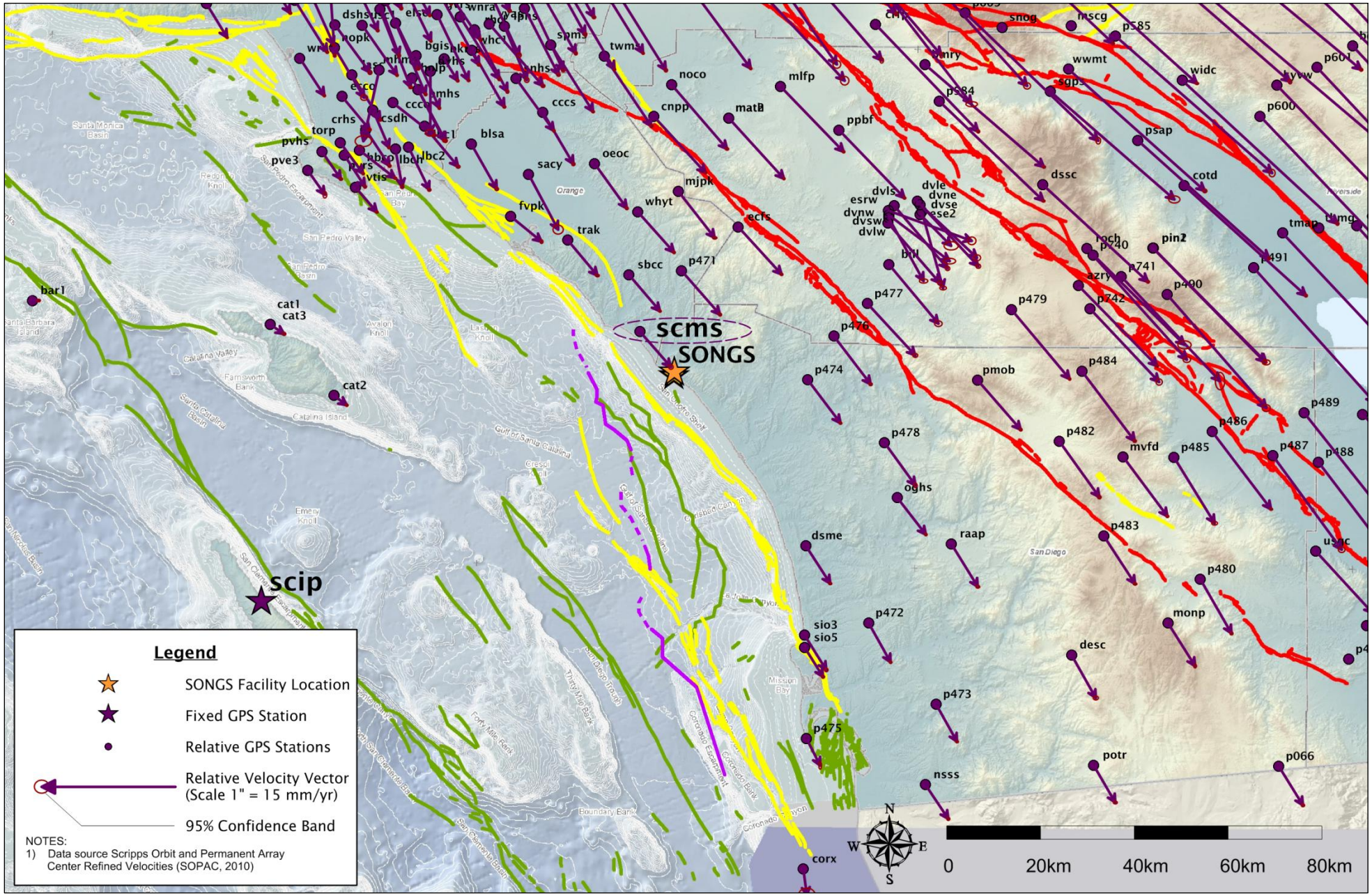

GeoPentech
Geotechnical & Geoscience Consultants

SAN ONOFRE NUCLEAR GENERATING STATION
SEISMIC HAZARD ASSESSMENT PROGRAM

GEODETIC DATA
VELOCITY RELATIVE TO SCIP

FIGURE
A-3

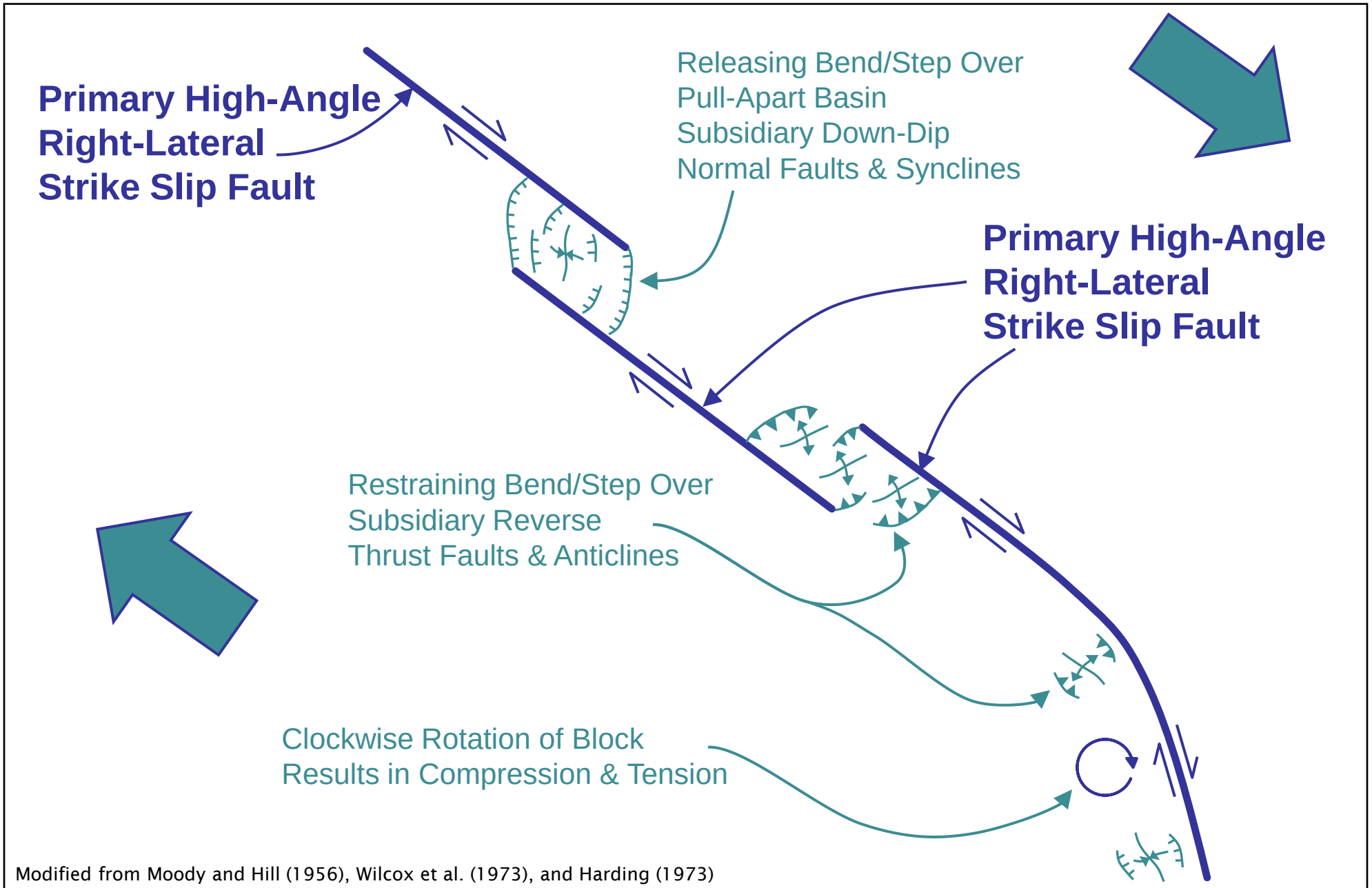

Modified from Moody and Hill (1956), Wilcox et al. (1973), and Harding (1973)

GeoPentech Geotechnical & Geoscience Consultants	**SAN ONOFRE NUCLEAR GENERATING STATION** SEISMIC HAZARD ASSESSMENT PROGRAM	**BASIC WRENCH FAULT TECTONICS**	FIGURE A-4a

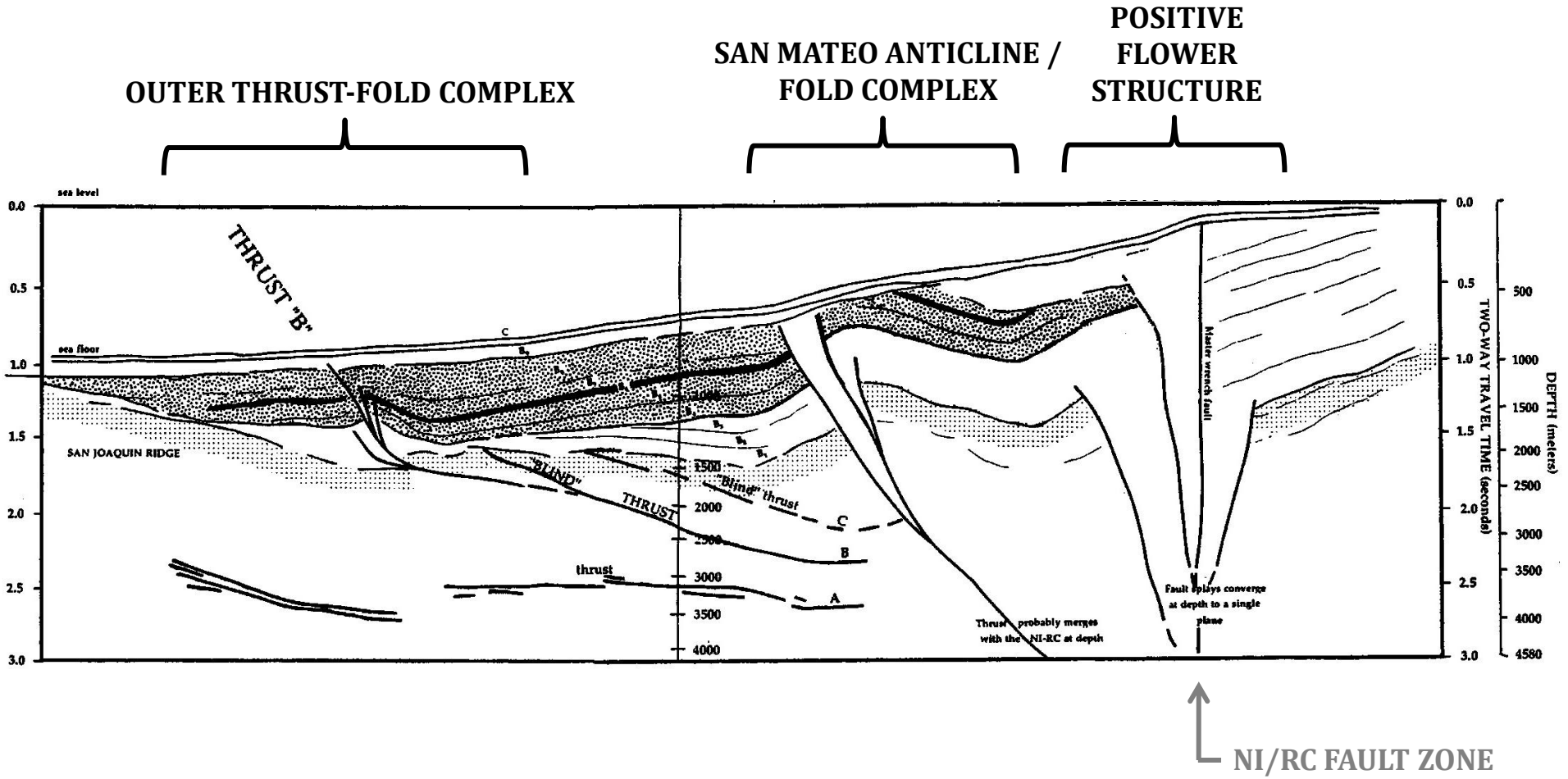

NOTES: (1) Modified from Fischer and Mills (1991)
(2) Presented in SCE (2001)

GeoPentech Geotechnical & Geoscience Consultants	**SAN ONOFRE NUCLEAR GENERATING STATION** SEISMIC HAZARD ASSESSMENT PROGRAM	**EXAMPLE OF A POSITIVE FLOWER STRUCTURE**	FIGURE A-4b

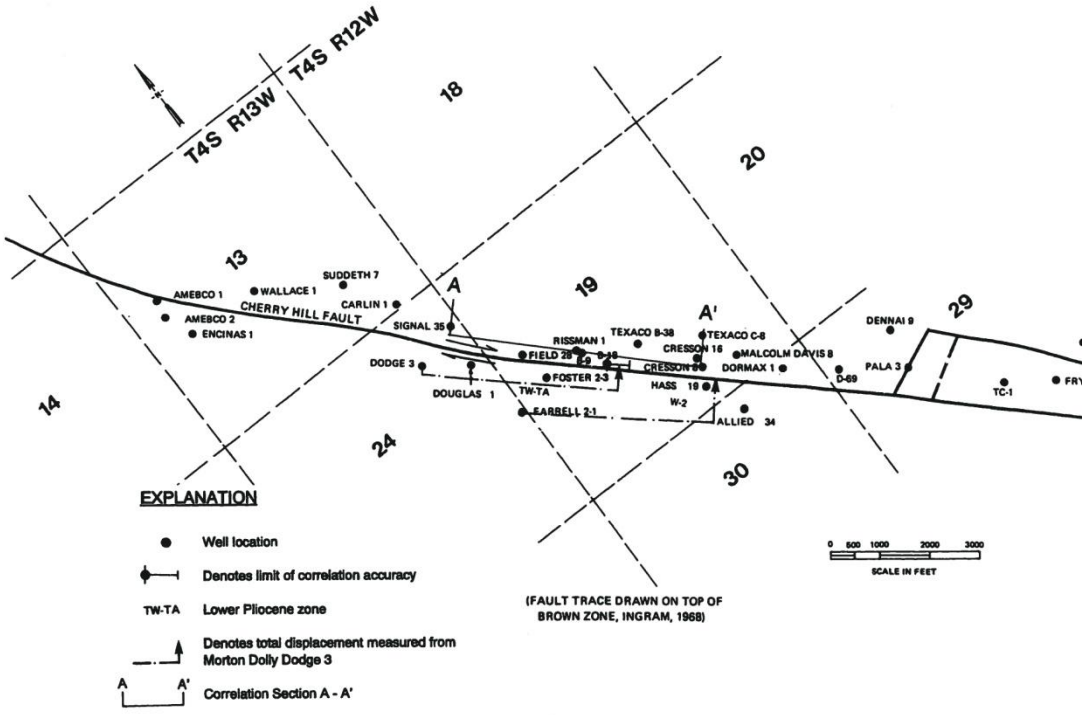

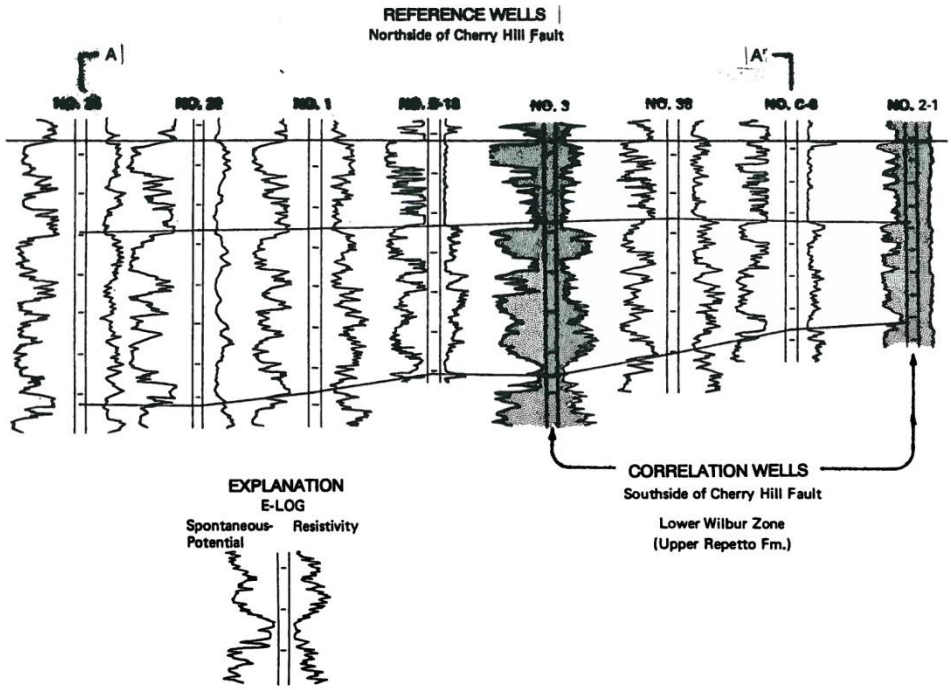

Source: Freeman et al. (1992)

GeoPentech Geotechnical & Geoscience Consultants	**LONG BEACH OIL FIELD WELL MAPS AND LOGS**	FIGURE A-5
	SAN ONOFRE NUCLEAR GENERATING STATION SEISMIC HAZARD ASSESSMENT PROGRAM	

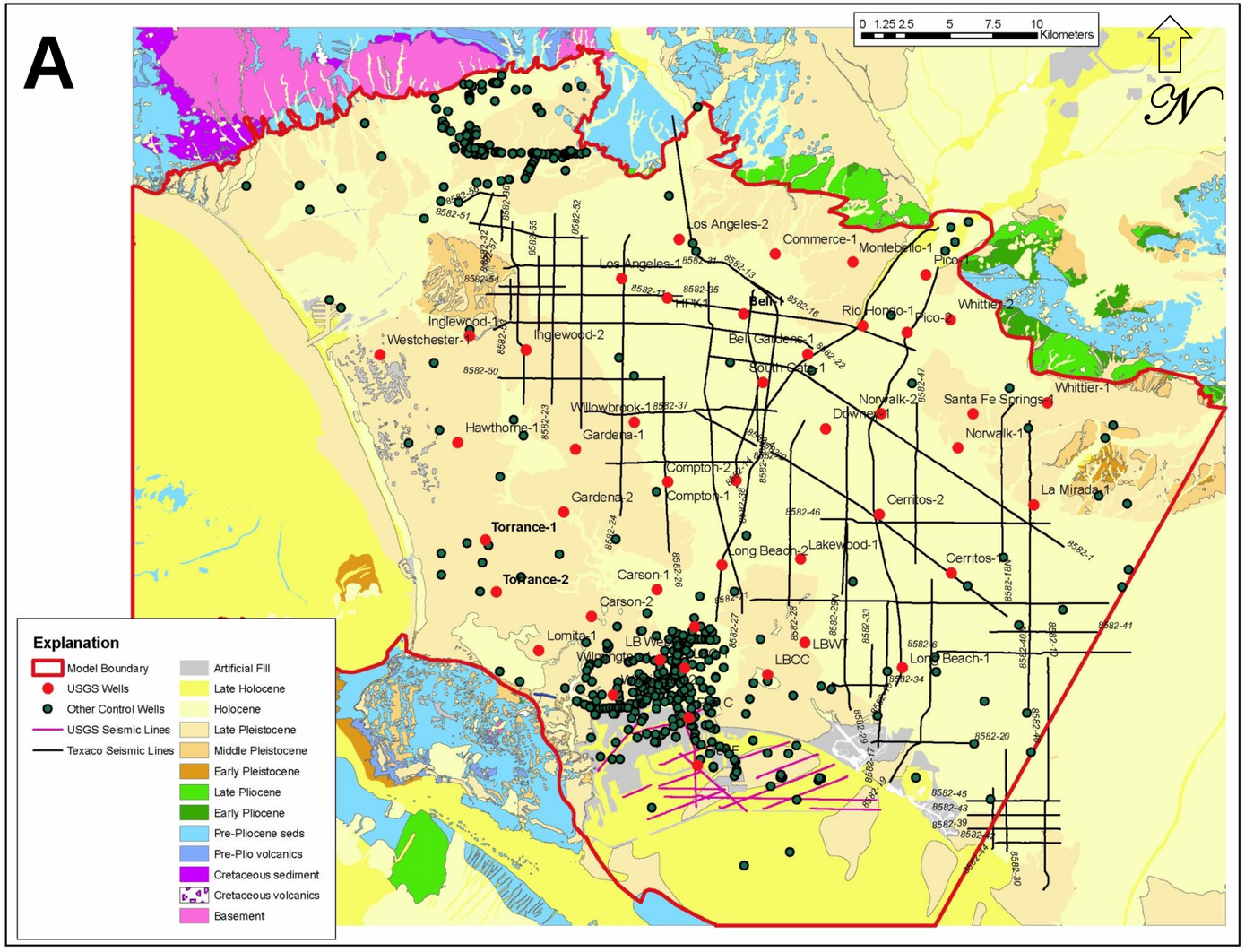

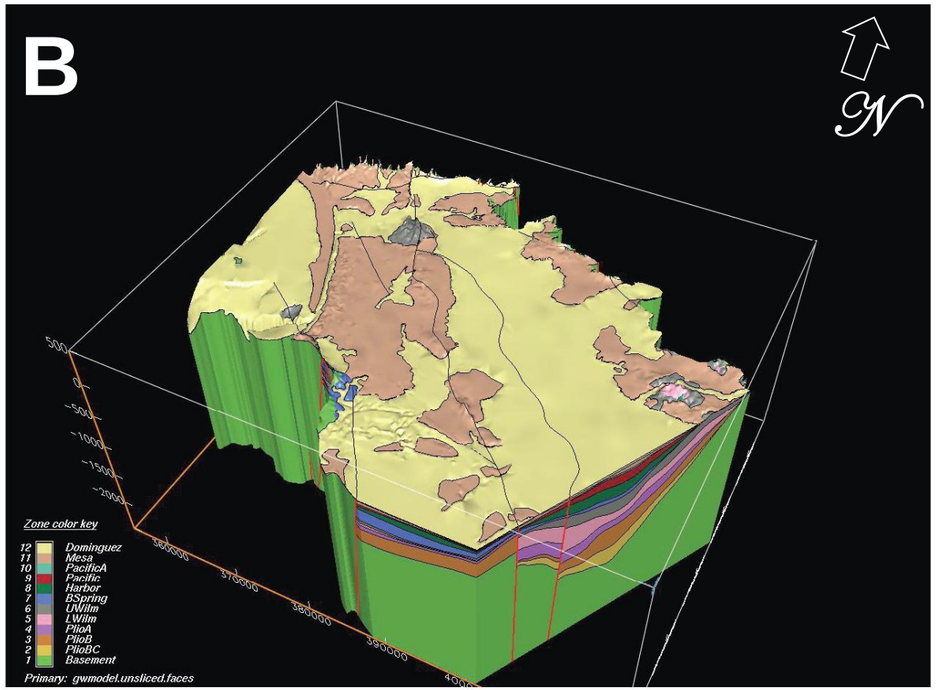

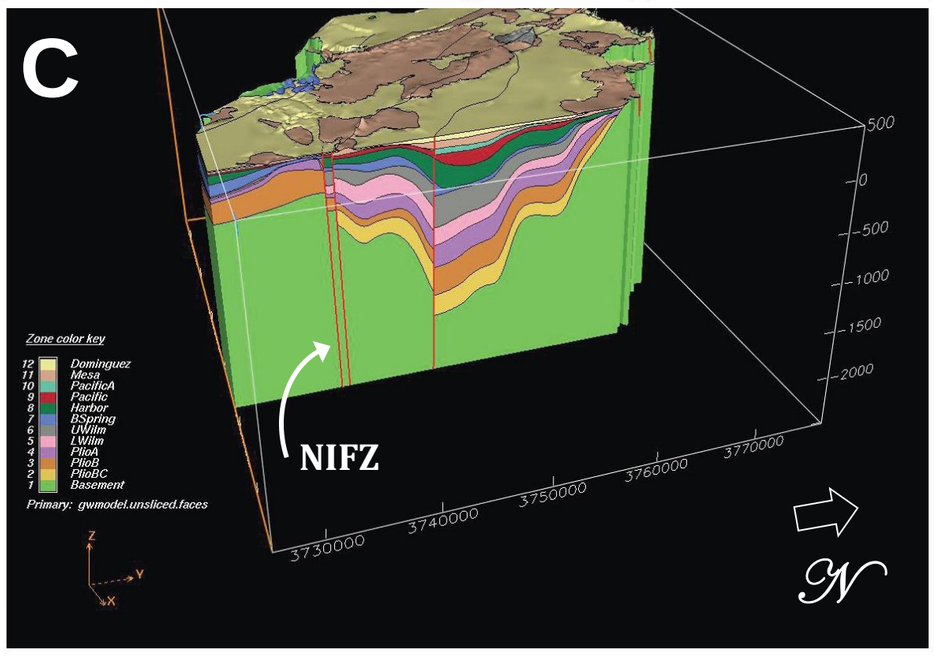

Modified from Ponti (2010)

GeoPentech
Geotechnical & Geoscience Consultants

SAN ONOFRE NUCLEAR GENERATING STATION

SEISMIC HAZARD ASSESSMENT PROGRAM

MAP AND 3D STRUCTURAL MODEL OF THE LA BASIN

FIGURE
A-6

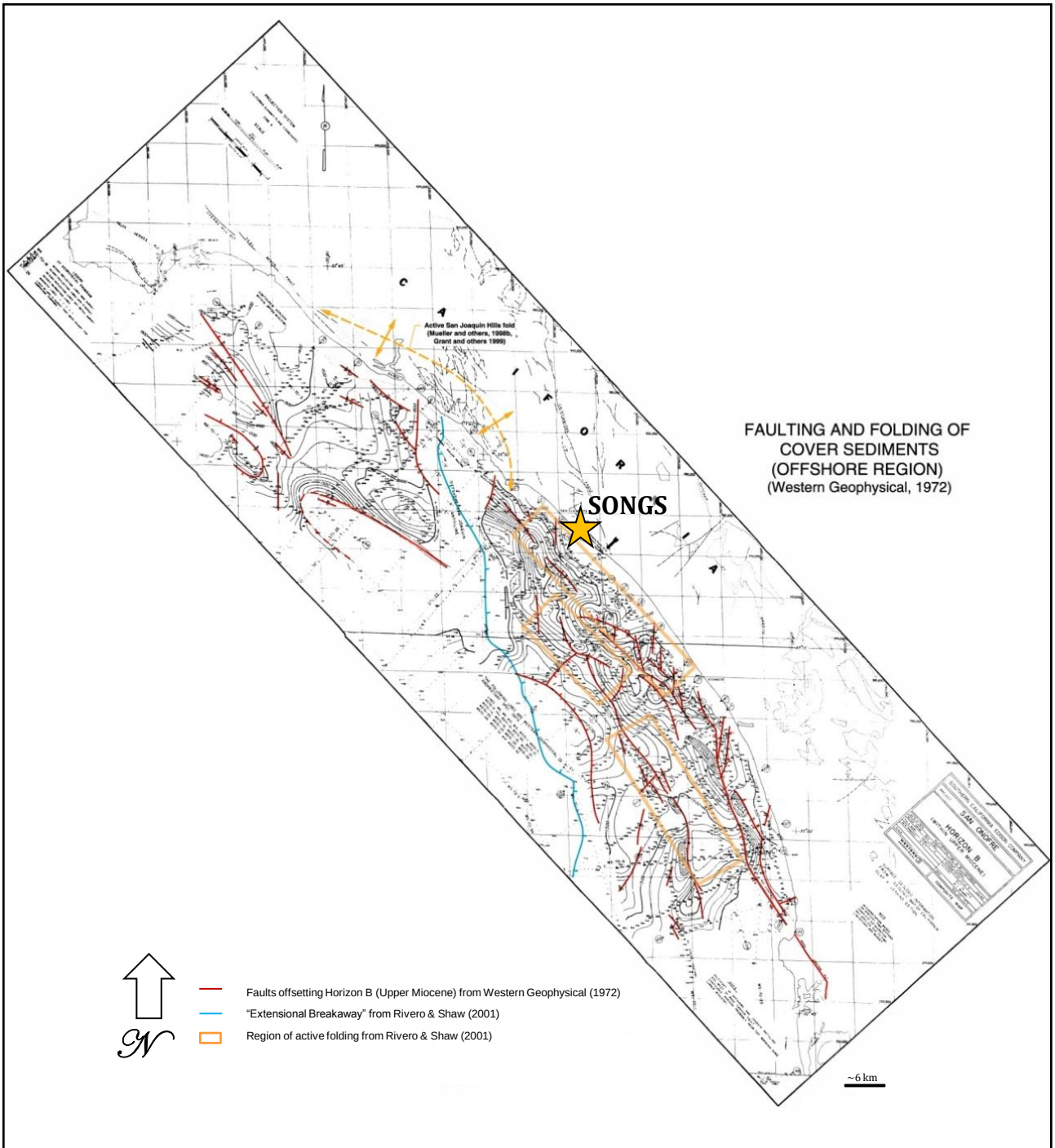

NOTES: (1) Modified from Western Geophysical (1972) and Rivero and Shaw (2001)
(2) Presented in SCE (2001)

GeoPentech
Geotechnical & Geoscience Consultants

OFFSHORE FAULT AND FOLD MAP BY WESTERN GEOPHYSICAL (1972)

FIGURE A-7a

SAN ONOFRE NUCLEAR GENERATING STATION

SEISMIC HAZARD ASSESSMENT PROGRAM

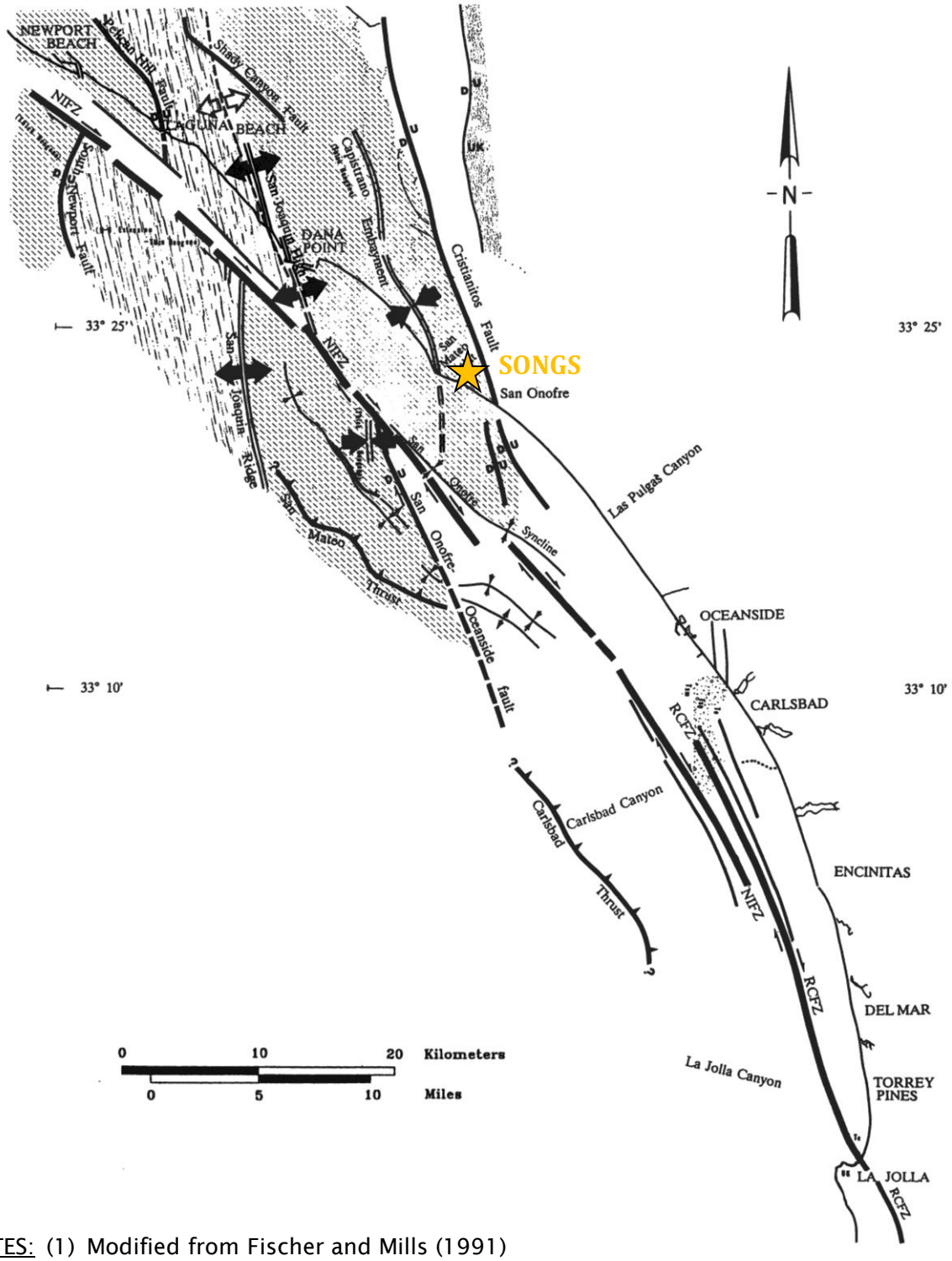

NOTES: (1) Modified from Fischer and Mills (1991)
(2) Presented in SCE (2001)

GeoPentech
Geotechnical & Geoscience Consultants

FAULT AND FOLD MAP OF THE INNER CONINENTAL BORDERLAND AND COASTAL REGION

FIGURE A-7b

SAN ONOFRE NUCLEAR GENERATING STATION

SEISMIC HAZARD ASSESSMENT PROGRAM

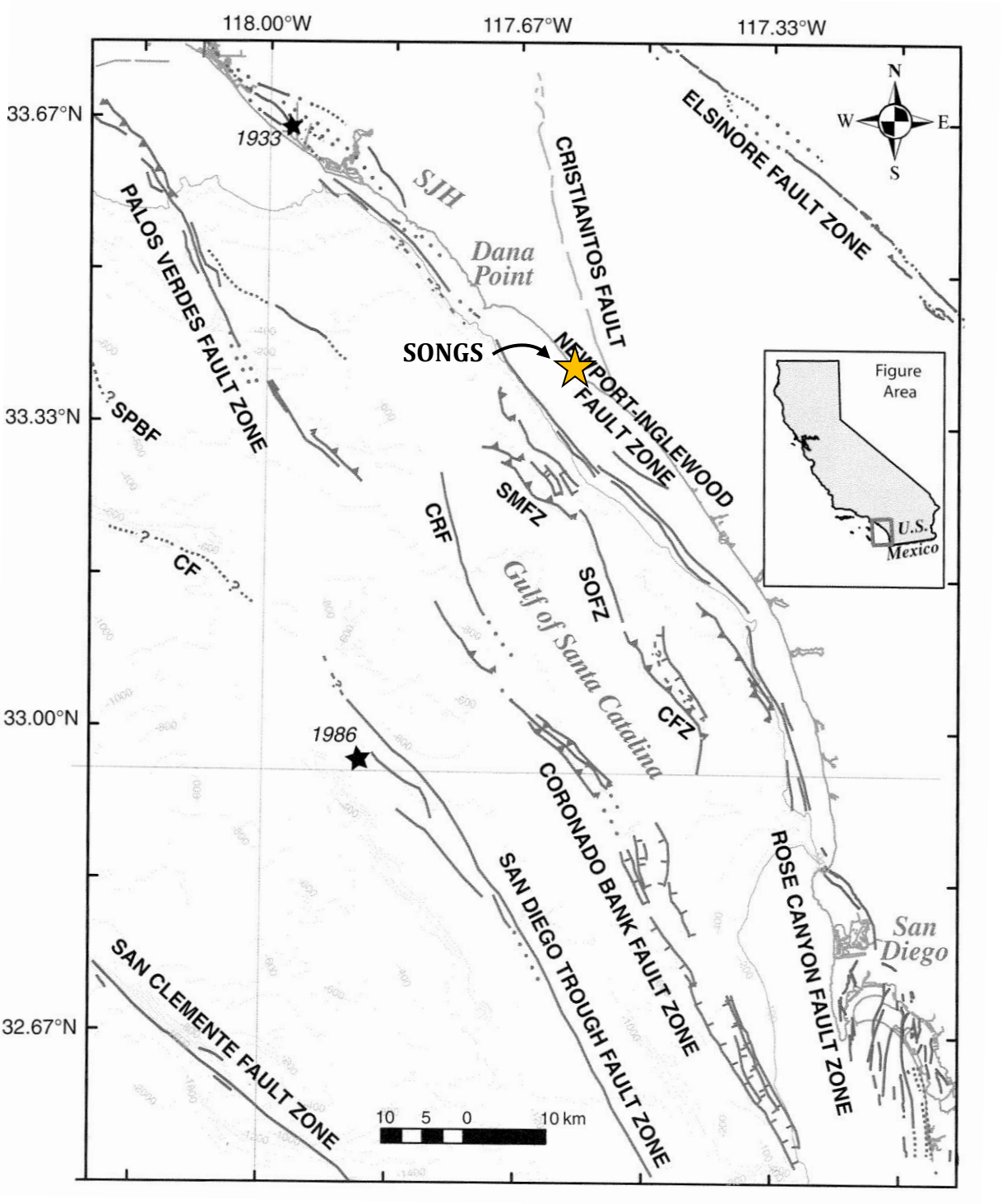

GeoPentech Geotechnical & Geoscience Consultants	OFFSHORE FAULT MAP BY RYAN ET AL. (2009)	FIGURE A-7c
	SAN ONOFRE NUCLEAR GENERATING STATION SEISMIC HAZARD ASSESSMENT PROGRAM	

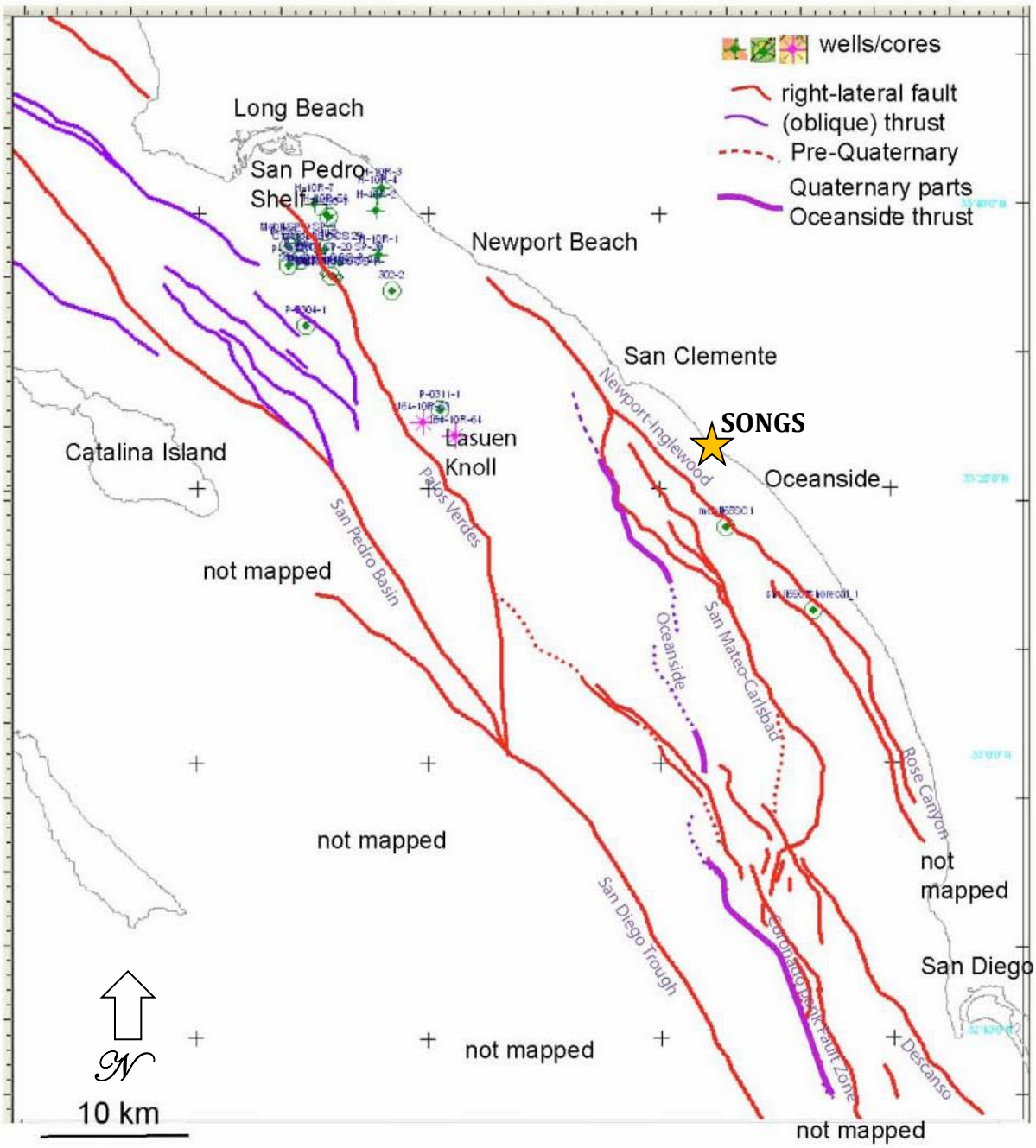

GeoPentech Geotechnical & Geoscience Consultants	**OFFSHORE FAULT MAP BY SORLIEN ET AL. (2009b)**	FIGURE A-7d
	SAN ONOFRE NUCLEAR GENERATING STATION SEISMIC HAZARD ASSESSMENT PROGRAM	

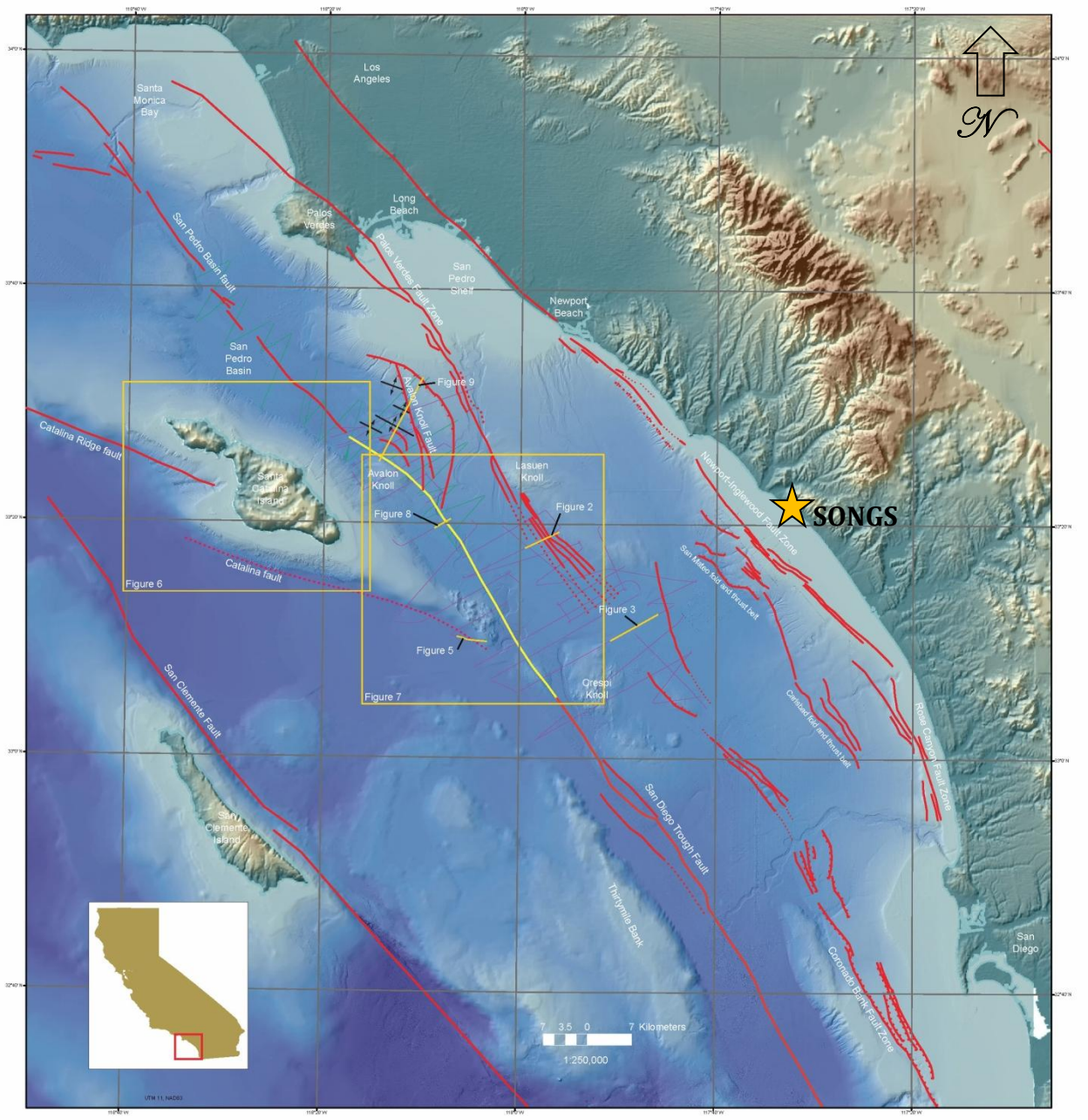

GeoPentech
Geotechnical & Geoscience Consultants

OFFSHORE FAULT MAP BY CONRAD ET AL. (2010)

FIGURE
A-7e

SAN ONOFRE NUCLEAR GENERATING STATION

SEISMIC HAZARD ASSESSMENT PROGRAM

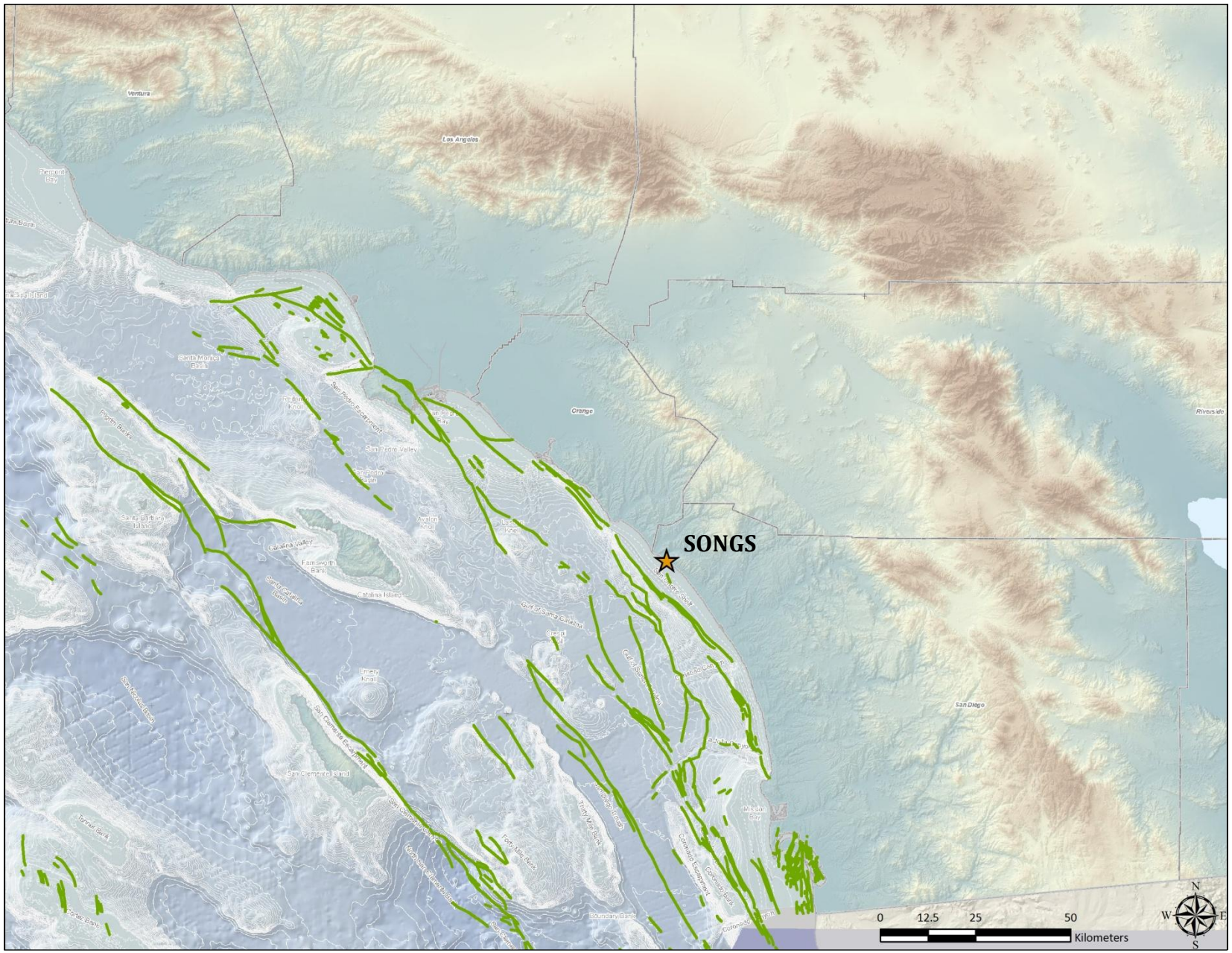

GeoPentech
Geotechnical & Geoscience Consultants

SAN ONOFRE NUCLEAR GENERATING STATION
SEISMIC HAZARD ASSESSMENT PROGRAM

QUATERNARY FAULT AND FOLD DATABASE OFFSHORE FAULT MAP FROM USGS (2009)

FIGURE
A-7f